An Old Story with New Twists: Lactate Dehydrogenase 5 (LDH-V) in Tumor Development

Investigation of the relationship between LDH-V and hypoxia/tumor characteristics by functional analysis of LDH-deficient tumor cells *in vitro* and in experimental tumor models

D i s s e r t a t i o n

Zur Erlangung des akademischen Grades

d o c t o r r e r u m n a t u r a l i u m

(Dr. rer. nat.)

Im Fach Biologie

eingereicht an der

Mathematisch-Naturwissenschaftlische Fakultät I

Der Humboldt-Universität zu Berlin

von

Dipl. Ing. Maher Najjar, 15.02.1980, Berlin

Präsident der Humboldt-Universität zu Berlin
Prof. Dr. Dr. h.c. Christoph Markschies

Dekan der Mathematisch-Naturwissenschaftlische Fakultät I
Prof. Dr. Lutz-Helmut Schön

Gutachter/innen:
1. Prof. Dr. Alf Hamann
2. PD Dr. Sanna Käkönen
3. PD Dr. Bernard Händler

Tag der mündlichen Prüfung: **4. Dezember 2009**

To Sema, the most wonderful woman in my life for the past 11 years.

With all my love, this book is dedicated to you.

Die Arbeit wurde im Zeitraum von November 2006 bis September 2009 unter der Leitung von Dr. Sanna-Maria Käkönen, Dr. Ningshu Liu und Dr. Holger Hess-Stumpp in der Therapeutic Research Group (TRG) Oncology, Bayer Schering Pharma AG, Berlin, angefertigt.

ZUSAMMENFASSUNG

Seit ungefähr einem halben Jahrhundert ist bereits bekannt, dass sich Tumorzellen durch die Fähigkeit auszeichnen, Glukose verstärkt zu nutzen und in hohen Raten umzusetzen. Die von Tumorzellen exzessiv exprimierte Laktat-Dehydrogenase Typ A (*LDH-A*) ist hierbei das Schlüssel-Enzym für den katalytischen Stoffwechsel um Pyruvat in Laktat unter Gewinnung von Energie umzuwandeln. Dieser „glykolytische Phänotyp“ scheint entstehenden malignen Tumorzellen einen Selektionsvorteil zu vermitteln. Hierbei handelt es sich wohl um eine metabolische Strategie des Tumors, Proliferation auch unter hypoxischen Bedingung zu gewährleisten. Bei LDH handelt es sich um einen wichtigen prognostischen Marker für die Einstufung der Aggressivität und die Behandlung von Tumoren. Hierbei ist ein hohes Level an LDH im Serum mit einer schlechten Prognose für Patienten mit unterschiedlichen Krebsformen korreliert. Für *LDH-A* wurde auch gezeigt, dass es an der Entstehung von Malignität beteiligt ist, auch wenn gerade erst begonnen wurde, den zugrunde liegenden molekularen Mechanismus zu verstehen.

Ziel dieser Arbeit war es daher, das Wissen um die Funktion des Genproduktes von *LDH-A* (LDH-V) in Bezug auf die Proliferation von Tumorzellen, die Expression Angiogenese-fördernder Gene, maligne Konversion von Tumoren und die Metastasierung zu vertiefen. Zusätzlich sollte die Rolle von LDH auf die Genexpression HIF-regulierter Proteine, die das Überleben von Tumorzellen und vor allem der Glykolyse fördern, untersucht werden. Hierfür wurden *LDH-A knockdown*-Klone von dem murinen B16F10 Melanom und Lewis Lung Karzinom sowie dem humanem HT29 Kolonkarzinom generiert. Mit diesen sollte aufgedeckt werden, wie sich die reduzierte Fähigkeit Pyruvat in Laktat zu metabolisieren auf Tumorzellwachstum *in vitro* und *in vivo* molekular auswirkt. Als erstes wurde der auf shRNA-Technologie basierende stabile knockdown des *LDH-A* Genprodukts in allen verwendeten Zelllininen erfolgreich durchgeführt. Anschließend wurden die unterschiedlichen Auswirkungen dieser LDH-V Unterdrückung bezüglich Tumorigenität *in vitro* und *in vivo* in den drei verschiedenen Tumormodellen beobachtet.

In dieser Arbeit konnte eine Signifikante Korrelation zwischen Tumorgewicht und LDH Spiegeln im Serum gefunden werden, wobei dieses zusätzlich mit der LDH Sekretion der Tumorzellen *in vitro* assoziiert war. Der *knockdown* von *LDH-A* führte *in vitro* zu

einer Hemmung der Proliferation in Lewis Lung und B16F10, während bei HT29 Tumorzellen kein solcher Effekt beobachtet werden konnte. Interessanterweise ließen sich nicht bei allen drei Zelllinien die durch limitierte LDH Aktivität ausgelösten Effekte auf die *in vitro* Proliferation auf das Tumorwachstum *in vivo* übertragen: Das Wachstum der Lewis Lung als auch der HT29 Tumoren *in vivo* war durch die Reduktion von *LDH-A* drastisch vermindert, während die Größe der B16F10 Tumoren davon nicht beeinflusst war. Eine Reihe von Untersuchungen zu den zugrunde liegenden molekularen Mechanismen implizierten, dass diese unterschiedlichen Effekte *in vitro* bzw. *in vivo*, höchstwahrscheinlich auf Unterschiede in der Mikroumgebung der Tumoren zurückzuführen ist. Es konnte hier gezeigt werden, dass B16F10 Tumoren unter LDH Suppression verstärkt VEGF exprimieren. Dadurch waren diese Zellen *in vivo* in der Lage, durch verstärkte Vaskularisierung des Tumors der durch *LDH-A knockdown* ausgelösten Hemmung des Tumorwachstums zu entkommen. Bei Lewis Lung Tumorzellen hingegen, führte die Unterdrückung von LDH-V zu einer beeinträchtigten Glukoseaufnahme unter normoxischen sowie hypoxischen Bedingungen. Die reduzierte Aufnahme von Glukose hatte *in vivo*, in einer vielschichtigen komplexen Struktur, deutlich größere Auswirkungen als auf einer eindimensionalen Zellkulturschale. Des Weiteren wurde im Rahmen dieser Arbeit mittels einer Genom-weiten Genexpressionsanalyse, gefolgt von funktionalen Analysen, in HT29 Zellen gezeigt, dass der knockdown von *LDH-A* zu Bildung einer potentiell pro-metastatischen Genexpressionssignatur führte und zusätzlich die Expression von Hif-1α durch Ausbildung eines *Feedback-Loops* verstärkte. Die Ergebnisse der vorliegenden Arbeit liefern neue Erkenntnisse zur Rolle von LDH-V während der Tumorprogression und können als Grundlage für zukünftige, neue Therapiestrategien bei Krebspatienten dienen.

ABSTRACT

For more than two thirds of last century it has been known that one of the most consistent hallmarks of cancer cells is their propensity to utilize and catabolize glucose at high rates. Lactate dehydrogenase type A (*LDH-A*) is a metabolic key enzyme catalyzing pyruvate into lactate and is excessively expressed by tumor cells. This 'glycolytic phenotype' appears to confer emerging malignant cells with a selective advantage and is considered as a metabolic strategy for tumors to proliferate under hypoxia. LDH is an important prognostic marker in cancer staging and therapy. High serum LDH activity is associated with poor patient prognosis in different tumor types. *LDH-A* has been shown to play a major role in tumor malignancy, but the molecular mechanism behind this role is only starting to be understood.

The objective of this work was to broaden our knowledge about the role of *LDH-A* gene product (LDH-V) in tumor cell proliferation, angiogenesis-related gene expression, tumor malignancy and metastasis. Additionally, the involvement of LDH in the gene expression of HIF-regulated proteins important in tumor survival and especially in glycolysis was further investigated. Herein, *LDH-A* shRNA knockdown clones of murine B16F10 melanoma, Lewis Lung carcinoma and human HT29 colon carcinoma were generated to uncover the molecular mechanisms between diminished ability of metabolizing pyruvate to lactate and tumor cell growth *in vitro* and *in vivo*. First, the *LDH-A* gene product and the LDH activity were successfully and stably knocked down in all cell lines using shRNA technology. Second, differential impacts of LDH-V ablation on the tumorigenicity *in vitro* and *in vivo* in the three tumor models were observed.

In this study, a significant correlation between tumor weight and serum LDH in *in vivo* tumor models was found, which additionally correlated with the *in vitro* LDH secretion. *In vitro,* suppression of *LDH-A* led to anti-proliferative effects in Lewis Lung and B16F10 tumor cells, while having no effect on HT29 cells. Interestingly, the consequence of limiting LDH activity *in vitro* did not show a direct correlation to the *in vivo* anti-tumor effects in LDH-deficient tumors: B16F10 tumor growth was unaffected by silencing *LDH-A*, while Lewis Lung and HT29 demonstrated a drastic reduction in tumor growth *in vivo*. A series of studies exploring the underlying molecular mechanisms suggested that the differential anti-tumor effects observed *in vitro* and *in*

vivo might be due to the differential tumor microenvironment. Thus, B16F10 tumors were found to have increased VEGF expression upon LDH knockdown, and therefore were able to compensate the tumor growth inhibition-driven by LDH deficiency through increased tumor vascularization *in vivo*. In contrast, LDH-V suppressed Lewis Lung cells demonstrated an impeded glucose uptake ability under normoxic and hypoxic conditions. This effect has stronger impact and becomes more effective when tumors grow as 3-dimension *in vivo*. Subsequently, a genome-wide gene expression analysis and functional assays of *LDH-A* deficient and control HT29 clones revealed potential new oncogenic features of *LDH-A* in tumor migration and invasion as well as a feedback loop to HIF1α. In summary, the collective data presented in this thesis provide new insights of LDH-V in tumor progression and therapeutic strategies for the treatment of cancer.

ACKNOWLEDGEMENTS

During the last years, when I was a PhD student at Bayer Schering Pharma AG, I received many help from various people around me. Without their kind help I would not have been able to write this thesis, and I am very happy to express my gratitude towards them in this section.

First, I would like to sincerely thank Dr. Holger Hess-Stumpp for giving me the opportunity to work in his group and for providing a very interesting project that was technically challenging and one in which I quickly became thoroughly absorbed into the experiments. I also would like to express my deepest gratitude towards my supervisors: Dr. Ningshu Liu and Dr. Sanna Käkönen. Both supervisors taught me how to reason and argument scientifically. I very much enjoyed all our discussions. They have always been available to help me out with all different kinds of questions. Under their supervision I learned how to work independently and became an independent researcher.

In this respect, I would also like to thank the following people: Bianka Timpner and Karola Henschel for there excellent technical advise and help in all *in vivo* experiments. Eva Geenen for being a great intern and for all her support. Dr. Tatjana Gust and Dr. Charlotte Kopitz for sincere friendship, for ongoing discussions and for critical reading of this manuscript.

I was very lucky to be able to participate in several conferences and presentations, which all proved to be very stimulating surroundings. Posters and presentations of this work have been presented at various internal and external meetings. I would like to thank the respective audiences for their valuable comments.

Finally, I would like to thank my family, for having supported me over the last 29 years and having made things possible for me.

TABLE OF CONTENTS

ABBREVIATIONS

µg	Microgram
µl	Microliter
18F-FDG-PET	18-fluorine 2-deoxyglucose positron emission tomography
AMPK	Adenosine mono-phosphate kinase
ATP	Adenosintriphosphate
BSA	Bovine serum albumin
Ca	Calcium
CDK	Cyclin-dependent kinases
CK2	Casein kinase 2
c-myc	Myelocytomatosis-oncogene
CO_2	Carbon dioxide
CRC	Colonrectal carcinoma
C-TAD	C-terminal transactivation domain
DMEM	Dulbecco's Modified Eagle Medium
ECL	Enhanced chemoluminescence
EDTA	Ethylenediaminetetraacetic acid
FACS	Fluorescence-activated cell sorting
FBS	Fetal bovine serum
FIH	Factor inhibiting HIF1
FITC	Fluorescein isothiocyanate
GFP	Green Fluorescence Protein
Glut-1	Glucose-transporter 1
GLUT4	Glucose transporter 4
h	Hours
H2B	Histone 2B
HIF1	Hypoxia-inducible factor 1
HIF-1α	hypoxia-inducible factor 1, alpha subunit
HRE	Hypoxia response elements
hTPO	Human thyroid peroxidase
HUVEC	Human Umbilical Vein Endothelial Cells
KD	Knockdown

LDH	Lactate Dehydrogenase
LDH-A	Lactate Dehydrogenase A gene
LDH-B	Lactate Dehydrogenase B gene
LDH-H	Lactate Dehydrogenase H monomere subunit
LDH-M	Lactate Dehydrogenase M monomere subunit
LDH-V	Lactate Dehydrogenase 5 tetramere protein
LL	Lewis Lung
Mg	Magnesium
min	Minutes
ml	Milliliter
MMP	matrix metalloproteinase
n	quantity
NADH	Nicotinamide adenine dinucleotide
NC	Non-silencing control
ng	Nanogram
NSCLC	Non-small cell lung cancer
N-TAD	N-terminal transactivation domain
OCA-S	the transcription complex Oct-1 coactivater S
OD	Optical density
PAGE	Polyacrylamide gel electrophoresis
PBS	Phosphate-buffered saline
PFK-1	6-phosphofructo-1-kinase
PFKFB1-4	Kinase/phosphatase family
PHD	Prolyl hydroxylase domain
PKB	protein kinases B
PTK/ZK	Vatalanib
r	correlation factor
RT	Room temperature
SD	Standard deviation
SDS	Sodium dodecyl sulfate
sh	Short hairpin RNA
TGFß-1	Transforming growth factor beta-1

TGFßR3	Transforming growth factor beta receptor III
TRG	Therapeutic research group
v/v	Volume per volume
VEGF-A	Vascular endothelial growth factor-A
VEGFR	Vascular endothelial growth factor receptor
w/v	Weight per volume
x g	Multiple of gravity
µg	Microgram

1 INTRODUCTION

1.1 Cancer

Cancer represent a substantial problem for both the affected individual and the society, and accounts for over 560,000 deaths (more than 1.4 million cancer cases) per year in the United States and is the No. 2 cause of the overall death. The cost of cancer therapy is estimated at $210 billion for 2009 (ASC 2009).

Cancerous diseases are characterized by uncontrolled proliferation and propagation of abnormal cells which invade and destroy other tissues and finally kill the organism by spreading to other regions of the body. Both exogenous, e.g. chemicals, radiation and viruses and endogenous factors, e.g. immunodeficiency and genetic predisposition can be involved in the development of cancer through introducing dynamic changes in the genome. These changes are based on mutations that produce oncogenes with dominant gain of function and tumor suppressor genes with recessive loss of functions. Tumorigenesis is considered to be a multistep process with four to seven stochastic events occurring until the transformation of normal human cells into highly malignant derivatives is completed. Thus, tumor cell pass through a kind of evolution by gathering single genetic changes, each conferring one or another type of growth advantage. These advantages are attributed to defects in regulatory circuits that control cell proliferation and homeostasis (Hanahan and Weinberg 2000).

1.2 Tumor growth and metabolism

All tissues, including tumors, need to follow a simple plan to survive and grow. They need to: (1) take up energy substrates, (2) metabolize these substrates to produce adenosintriphosphate (ATP) (cellular energy currency), and (3) remove metabolic waste. The way how different tissues accomplish these tasks varies, especially in tumors. Most tumor cells divide rapidly and consequently need a constant supply of substrates for energy production. Different tumors use different energy substrates including: fatty acids/ketone bodies, amino acids (e.g. glutamine), carbohydrates (e.g. glucose), and lactate. Although tumors have been shown to use all these substrates

for energy production, the two preferential substrates for tumors appear to be glutamine and glucose. Which substrate or substrates are used depends on the specific tumor and its microenvironment.

Tumors follow the same basic metabolic pathways as normal tissues, but changes in the microenvironment and the tumor cells themselves can have profound effects on their metabolism. There are two main factors that are thought to influence tumor metabolism: oxygen concentration and altered metabolic pathways/enzymes (Kim et al. 2007; Kroemer and Pouyssegur 2008).

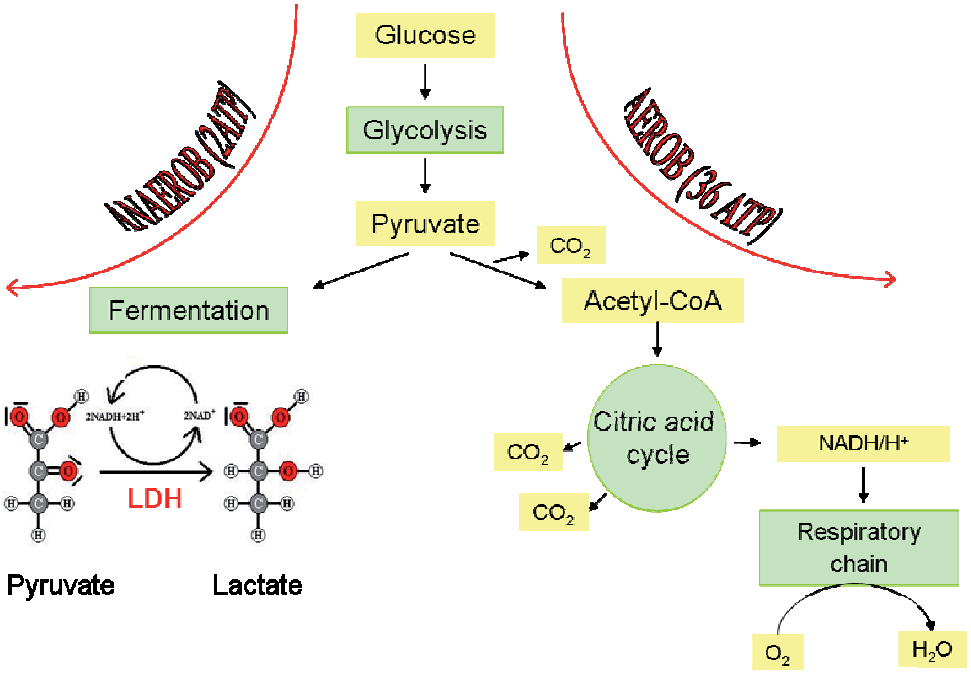

Figure 1. Possible pathways for ATP production. Ultimately, the product of glycolysis, pyruvic acid, must be metabolized aerobically. Aerobic metabolism is performed exclusively in the mitochondria. Pyruvic acid is converted to a acetylCoA and put into a pathway known as the Krebs cycle or citric acid cycle. Energy is released in form of ATP and, especially, as high energy electrons. The waste products of aerobic metabolism are CO_2 and H_2O. The anaerobic pathway, glycolysis produces less ATP in comparison to the aerobic metabolism, but has the advantage that it does not require oxygen. In addition, glycolysis occurs in the cytoplasm, not in the mitochondria. Pyruvic acid is converted to lactate through lactate dehydrogenase (LDH) in a process known as fermentation.

Oxygen concentration, or lack thereof (hypoxia, pO_2<10mm Hg) is an important factor in energy production because metabolism of most substrates is oxygen dependent. All substrates require oxygen for adenosine triphosphate (ATP) production except glucose. Glucose can be metabolized in the presence (oxidative phosphorylation) or in the absence of oxygen (glycolysis). The main difference between these two

glucose pathways is the number of ATP molecules produced for each molecule of glucose metabolized, 36 versus 2 respectively (Figure 1). The oxygen dependence of energy production becomes important in tumors because many tumors are hypoxic.

1.3 Hypoxia

The presence of hypoxic i.e. oxygen lacking conditions in tumors was first described in lung tumors more than 50 years ago (Thomlinson and Gray 1955) and it is nowadays well known that regions with very low level of O_2 are characteristic to many solid cancers. The most recognized reasons for altered tumor metabolism are the unique physiological stresses, such as hypoxia, acidosis and increased interstitial fluid pressure (Milosevic et al. 2004), that exist within the tumor. These microenvironmental stresses are largely the result of poorly formed tumor vasculature (Brown and Giaccia 1998). Significant regions of the tumor are at a great distance from the supporting blood vessels, and this distance causes a gradient of diffusion-limited hypoxia, low levels of nutrients and increased levels of waste products (Dasu et al. 2003). Hypoxia is perhaps the most pervasive of these stresses and variably exists when oxygen delivery does not meet the demand within the tumor tissue. Tumor cells respond to these conditions, and adapt their metabolism to adjust the oxygen demand and need to counteract the limited supply (Hockel and Vaupel 2001; Denko et al. 2003).

1.4 Aerobic glycolysis and its clinical importance

In 1931, Otto Heinrich Warburg (1883–1970) was awarded a Nobel prize for his studies on respiratory enzymes. Otto Warburg's classic treatise on the reprogramming of tumor metabolism from oxidative to glycolytic metabolism was published in London in 1930. Already decades ago, Otto Warburg noted that in tumors pyruvate is metabolized to lactate also under normoxic conditions and he reckoned that this has some advantages for tumor growth (Warburg 1930). This behavior of cancer is called aerobic glycolysis or the Warburg effect. Although the Warburg effect is one of the most universal characteristics of solid tumors, the molecular basis for this phenomenon has only recently been elucidated by studies indicating that increased expression of genes encoding glucose transporters and glycolytic enzymes in tumor cells is mediated by the transcription factors cellular-

myelocytomatosis-oncogene (c-myc) and the hypoxia-inducible factor 1, alpha subunit (HIF-1α) (Denko 2008; Brahimi-Horn and Pouyssegur 2009; Morrish et al. 2009). C-myc is a direct target for oncogenic mutations. In contrast, expression of hypoxia-inducible factor 1 is indirectly up-regulated via gain-of-function mutations in oncogenes and loss-of-function mutations in tumor suppressor genes that result in increased HIF-1α protein expression and/or increased HIF-1α transcriptional activity in a cell-type-specific manner (Semenza et al. 2001). As a result of genetic alterations and intratumoral hypoxia, HIF-1α is overexpressed in the majority of common human cancers (Zhong et al. 1999). In human breast cancer and brain tumors, HIF-1α overexpression strongly correlates with tumor grade and vascularity (Schindl et al. 2002).

1.4.1 Hypoxia Inducing factor-1α

HIF-1 is a dimeric protein consisting of a constitutively expressed ß-subunit and a strongly regulated α subunit. The α subunit contains an N-terminal and a C-terminal transactivation domain (N-TAD and C-TAD, respectively). The transcription of the alpha subunit is regulated by cytokines and additionally, post-translational by a regulated degradation of the protein (Pouyssegur et al. 2006). HIF-1α is hydroxylated at two proline residues located in N-TAD and at the asparagine residue located in C-TAD (Jiang et al. 1997; Pugh et al. 1997). This renders the molecule prone to degradation via the proteasomal pathway as it becomes a substrate of VHL, an E3 ubiquitin ligase, or impairs the interaction with another transcription cofactor, p300. In the absence of oxygen or under severe hypoxic conditions these control mechanisms are overcome and cellular HIF-1α levels rise dramatically. The diminished level of oxygen leads to the stabilization and activation of the hypoxia-inducible factor. The transcription factor HIF-1α regulates the expression of many genes that are involved in the development of the Warburg phenomenon (Gillies and Gatenby 2007; Denko 2008) such as the vascular endothelial growth factor-A (VEGF-A). The product of this gene, together with a number of other proteins such as angiopoietin-2, stimulate the formation of new vessels that migrate into the tumor mass, a process termed angiogenesis, and thereby reestablish oxygen and nutritional homeostasis (Carmeliet 2003). Among several effects, HIF-1α is related to the down-regulation of mitochondrial activity in cancer (Lopez-Rios et al. 2007), and thus the ability of

cancer cells to fully oxidize fuels. It even has been proposed to classify the severity of cancer on the basis of tumor lactate content (Walenta and Mueller-Klieser 2004). Presently, the Warburg effect derives its clinical importance from its role in the diagnosis and staging of cancer. The commonly used 18-fluorine 2-deoxyglucose positron emission tomography (18F-FDG-PET) technique images the Warburg effect. These scans detect the avid uptake of glucose in tumors with increased aerobic glycolysis (Gillies and Gatenby 2007).

1.4.2 HIF-1α-mediated regulation of glucose metabolism

The obvious importance of HIF1-α as transcriptional master regulator is underscored by the fact that more than 100 genes are regulated by the transcription factor HIF-1α via so-called hypoxia response elements (HRE) in their promoter regions.

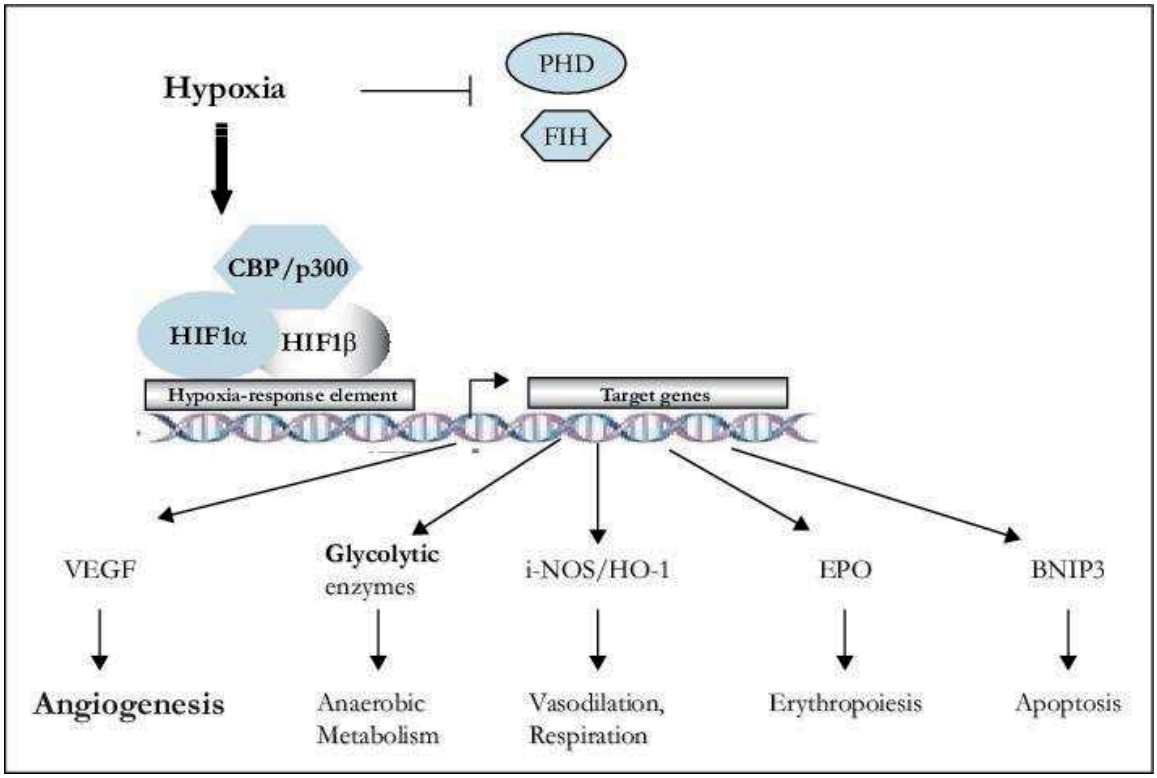

Figure 2. Hypoxia-induced pathways. Under hypoxic conditions the oxygen-dependent prolyl hydroxylase domain (PHD) and factor inhibiting HIF1 (FIH) hydroxylases are inactive. The alpha subunit of HIF is stable and translocates into the cell nucleus where it heterodimerizes with the beta subunit inducing the binding to DNA regions of target genes carrying a hypoxia-response element (HRE). Interaction with the co-activator CBP/p300 initiates the induction or repression of a large number of genes involved in angiogenesis, anaerobic glycolysis, vasodilation and respiration, erythropoiesis, and apoptosis (Brahimi-Horn and Pouyssegur 2006).

Hypoxia-inducible genes regulate several biological processes, including cell proliferation, angiogenesis, metabolism, apoptosis, immortalization and migration (Figure 2). The largest functional group of genes consistently regulated by HIF1 are associated with glucose metabolism (Vengellur et al. 2003; Allen et al. 2006; Chi et al. 2006). Glycolysis relies on linear processing of metabolites and thus, many of the enzymes in this pathway are induced together. HIF1 increases the expression of transporters necessary for glucose entry of into the cell, genes involved in the enzymatic breakdown of glucose to pyruvate as well as enzymes involved in the clearance of pyruvate. Pyruvate is not used by mitochondria in the hypoxic cell but instead is converted to lactate by lactate dehydrogenase (LDH) and released into the extracellular space. Recent data suggest that HIF1α can coordinate this process under aerobic as well as anaerobic conditions (Lum et al. 2007).

1.4.3 Lactate dehydrogenase

One HIF induced proteins is the M-subunit of LDH (Semenza et al. 1996a). LDH is a tetrameric protein composed of different combinations of either LDH-M or LDH-H, which represent 5 isoforms of the tetramer (Figure 3). LDH is universally present in all mammalian cells, but the specific LDH isoenzymes may predominate in different tissues according to their metabolic demand. The LDH-M tetramer protein is called LDH-5 or LDH-V (Li et al. 1983). LDH-M subunit is encoded by the *LDH-A* gene, LDH-H subunit by the *LDH-B* gene which is not regulated by HIF (Figure 3). Pan et al. demonstrated that both the H and M tetramers of LDH are present in normal tissue, but that the expression of the LDH-M tetramer i.e. LDH-5 is strongly increased in malignant tissue (Pan et al. 1991). Lactate acid is build through the transformation of pyruvate with LDH-5. For a long time the major role of lactate in glycolysis was considered as a sink of electrons from Nicotinamide adenine dinucleotide (NADH). In the clinical setting, high LDH activity in serum or plasma is used as a surrogate parameter and suggests a bad prognosis in several cancer indications (Koukourakis et al. 2006).

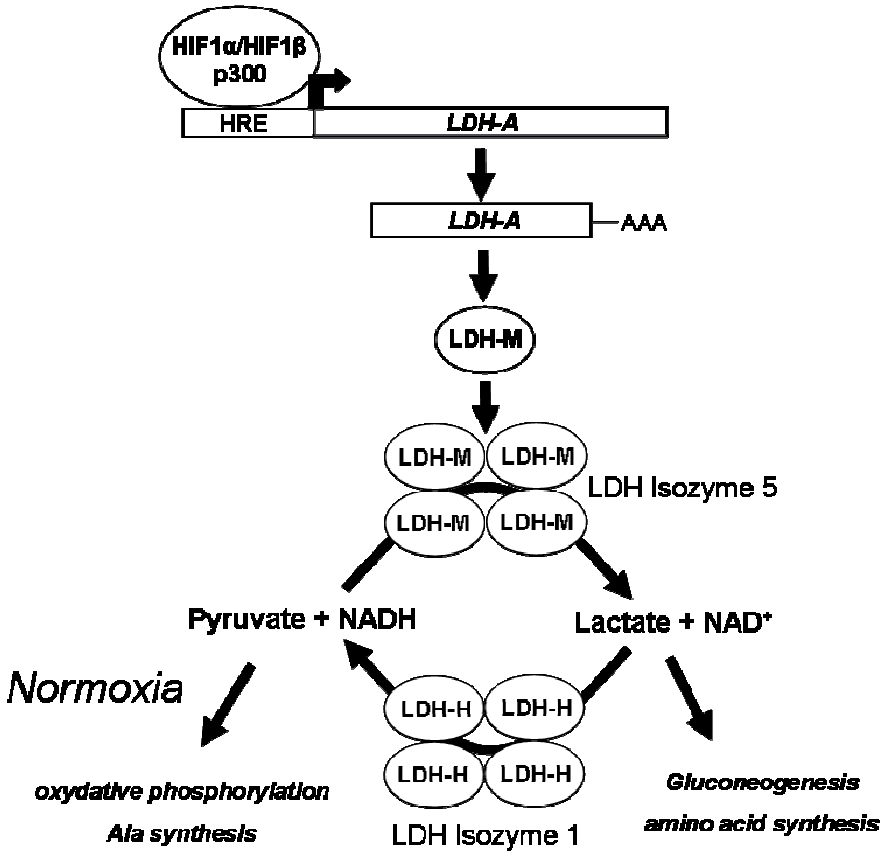

Figure 3. Scheme of the canonical role of LDH-5. Under low oxygen pressure HIF1α is no longer degraded and thus, hypoxia responsive genes such as LDH-A are transcribed. Simultaneously, glucose degradation mostly stops at the level of pyruvate as the Krebs cycle is not functional anymore. For a continued glycolysis the accumulation of NADH must be avoided by the reduction of pyruvate to lactate via LDH-5 (M4), which is the major enzyme supporting this process. In contrast LDH-1 (H4) rather fosters the opposite direction .

In non-small cell lung cancer (NSCLC), LDH-V has been shown to be preferentially expressed in tumor cells, but not in normal cells (Koukourakis et al. 2003). Normally, the enzyme is localized in the cytoplasm. However, in many tumors LDH was also found to be enriched in the nucleus (Cattaneo et al. 1985). Besides hypoxia and HIF, estrogen (Burke et al. 1978), cAMP (Miles et al. 1981; Firth et al. 1995) and c-myc (Shim et al. 1997) also influence *LDH-A* gene expression. Lewis et al. reported that the expression of *LDH-A* is required for the c-myc and Rcl induced transformation of rat fibroblasts (Lewis et al. 2000). The LDH-M tetramer provides NAD^+ for ongoing glycolysis under anaerobic conditions by reversible transformation of pyruvate to lactate (Figure 1) (Holbrook and Gutfreund 1973). According to Jovanovic et al. LDH forms complexes with adenosine mono-phosphate kinase (AMPK) or with casein kinase 2 (CK2 alias PK2) (Jovanovic et al. 2007). The activity of AMPK and CK2 is regulated by the redox state of the cell, here the NADH or NADPH levels: a highly

reduced state inhibits the activity of both, AMPK and CK2. This couples the availability of oxygen with the energy supply of the cells by a direct interaction of LDH with other enzymes. All these outcomes indicate the importance of this glycolytic enzyme.. Furthermore, LDH is a biomarker of cellular turn over. This important glycolytic enzyme was identified in serum as a surrogate marker of tumor burden and site of metastatic disease in cancer patients (Naik et al. 2008). Serum LDH and especially LDH-5 isoenzyme is used for diagnosis, staging, monitoring of therapy, detection of relapse, and as an important prognostic factor (Dalley et al. 2001; von Eyben 2001; Suh and Ahn 2007).

1.5 Angiogenesis

Angiogenesis is a physiological process involving the growth of new blood vessels from pre-existing vessels. It is a normal process in growth and development, as well as in wound healing. Tumor angiogenesis is the proliferation of a network of blood vessels that penetrates into cancerous growths, supplying nutrients and oxygen and removing waste products. Tumor angiogenesis actually starts with cancerous tumor cells releasing molecules that send signals to surrounding normal host tissue. This signaling activates certain genes in the host tissue that, in turn, make proteins to encourage growth of new blood vessels. However, it is also a fundamental step in the transition of tumors from a dormant state to a malignant one. HIF-1α is mainly responsible for the "angiogenic switch". HIF-1 functions as a master regulator of angiogenesis by controlling the expression of multiple angiogenic growth factors such as VEGF (Figure 4).

Krogh’s classical morphometric studies, performed 90 years ago, gave the first experimental evidence that angiogenesis must be involved in metabolic regulation. In these studies, a striking correlation between muscle capillary density and the metabolic rate of different species was found (Krogh 1919). Among the various endothelial markers used to assess to tumor angiogenesis, CD31, corresponding to the intercellular adhesion molecule PECAM-1, has been largely used for immunohistochemical analysis on formalin-fixed, paraffin-embedded tissue sections.

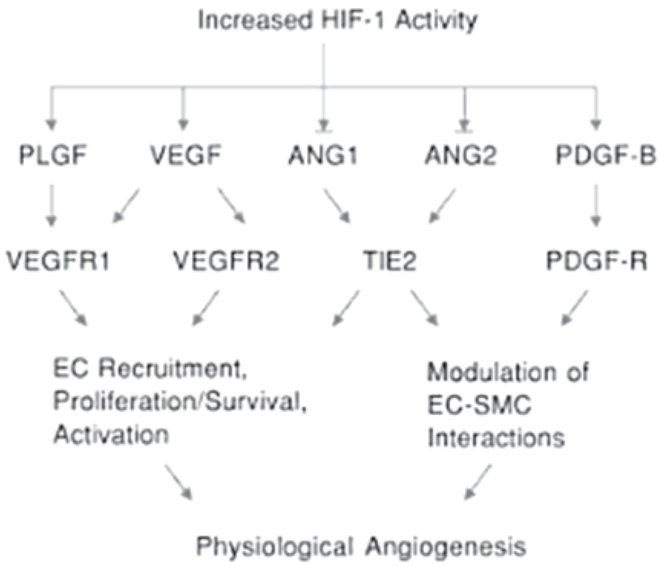

Figure 4. Regulation of angiogenic growth factor expression by HIF-1. Hypoxic conditions lead to increased HIF-1 activity and induce cell-type-specific changes in the expression of genes encoding angiogenic growth factors (Aird 2007).

A significant correlation between CD31 and serum baseline LDH levels in human gastric cancer patients was observed by Kolev et al., Further analysis indicated that intratumoral gene expression of *VEGFA* and *VEGFR1* are significantly associated with serum LDH levels. In addition, a strong correlation between gene expression of angiogenesis-related genes (*VEGF* and *VEGFR1*) and glycolysis (*LDHA* and *Glut-1*) was observed (Kolev et al. 2008). These findings suggest the strong correlation of LDH and angiogenesis and are in agreement with Koukourakis' reports of IHC analysis in colorectal carcinoma (CRC) and non-small cell lung cancer (NSCLC) (Koukourakis et al. 2003). This analysis demonstrated a link between LDH-5 overexpression and transcriptional gene regulation by HIF1α including genes responsible for hypoxia, angiogenic factor production and poor prognosis.

1.6 Metastasis

Hanahan and Weinberg describe six hallmarks of cancer cells: 1) immortality 2) abnormal growth regulation 3) self-sufficient growth 4) evasion of apoptosis 5) sustained angiogenesis 6) invasion and metastasis (Hanahan and Weinberg 2000). Metastasis is the transfer of malignant tumors from one organ to a distant organ (Figure 5). It is the most lethal attribute of cancer cells and clinical decisions

regarding treatment are based largely upon the likelihood of developing metastases (Fidler 2002b, a).

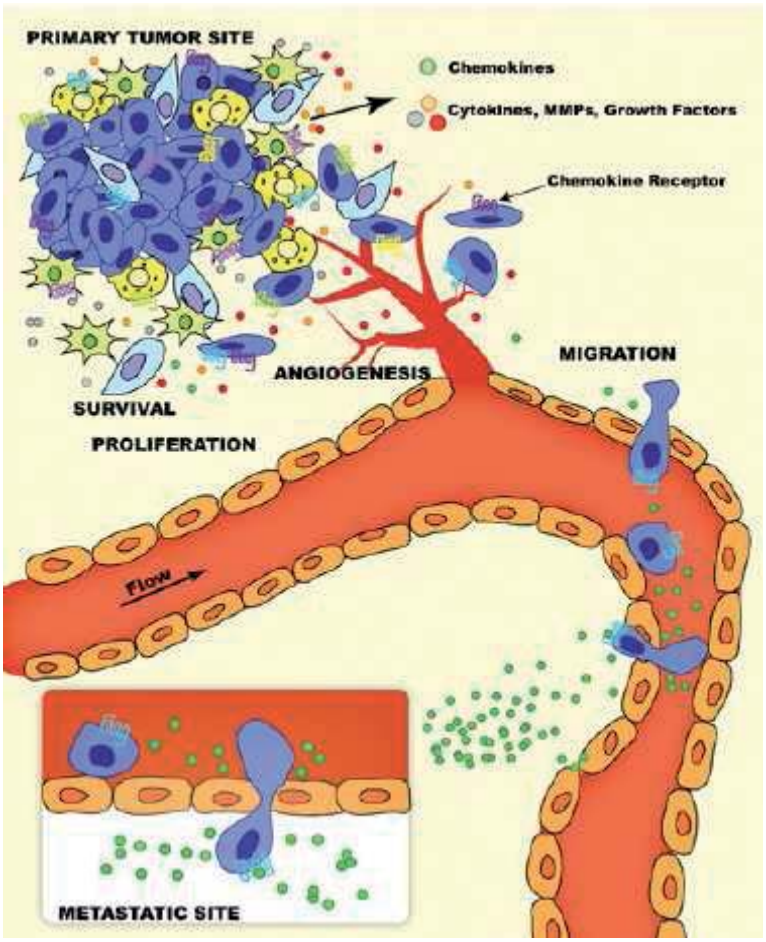

Figure 5. Illustration of the various steps in cancer growth and metastasis. This figure illustrates many aspects of cancer progression where chemokines/receptors and matrix metalloproteinase (MMPs) may play a role: growth of the primary tumor, angiogenesis (cell migration of endothelial precursors), metastasis, and growth survival of the metastasized cells which is probably the least efficient step in the metastatic process. (O'Hayre et al. 2008)

A number of groups have examined hypoxia-related factors that influence survival in patients with metastatic cancers (Sirott et al. 1993; Falkson and Falkson 1998; Kunisaki et al. 2009; Wu et al. 2009). One important finding is that intratumoral hypoxia correlates with an increased risk of invasion probably by the selection of mutations that promote invasion and by expression of genes that promote HIF-1 mediated invasion (Young et al. 1988; Cairns et al. 2001; Postovit et al. 2002).

Walenta et al. reported high molar concentrations of lactate in various tumors and this correlated with a high incidence of distant metastasis already in an early stage of the disease (Walenta et al. 2004). The aggressive tumor behavior has been reported to be associated with high LDH activity (Koukourakis et al. 2009) and this phenomenon may have several reasons. One of the suggested reasons is that increased LDH activity leads to lactic acid production and acidification of the extracellular matrix (Vaupel et al. 1989; Stubbs et al. 2000). Subsequently, the low extracellular pH triggers cathepsin D and gelatinase activity, amplifying the invasive ability of cancer cells (Rozhin et al. 1994; Martinez-Zaguilan et al. 1996). Moreover, under hypoxic conditions or in high concentrations of lactate macrophages are stimulated to release angiogenic factors contributing to the overall tumor angiogenicity and facilitating the development of metastases (Jensen et al. 1986; Zabel et al. 1996; Murray and Wilson 2001).

1.7 Fundamental findings

LDH activity in serum was used during the CONFIRM clinical trials as a criterion for patient stratification (Tyagi 2005). In these trials, colon cancer patients in first (CONFIRM 1) and second line therapy (CONFIRM 2) were treated with the standard triple regimen of oxaliplatin, leucovorin and 5-fluorouracil (5-FU). About half of the patients received in addition PTK/ZK (Vatalanib). Vatalanib is an orally active small-molecule inhibitor that targets the receptor TK domain of all 3 members of the VEGFR family. Preclinical studies in mice bearing human renal tumors showed that Vatalanib was able to inhibit growth of the primary tumor by 67%, and it was able to prevent the formation of lung and lymph node metastases (Drevs et al. 2000). It was found that patients with high serum LDH activity (>1.5 x normal) and therefore, considered having poor prognosis, responded much better to Vatalanib therapy than patients with a normal LDH activity (reflecting better prognosis). However, the molecular mechanism behind this finding was unclear and therefore, we wanted to clarify if LDH has a functional role in tumorigenesis. Shortly after the PTK/ZK story it was published by Fantin et al., that cells obtained from mammary gland tumors and dissected from *neu*-transgenic mice with a gene suppression of *LDH-A* showed a diminished proliferation *in vitro* and more importantly *in vivo*. (Fantin et al. 2006).

1.8 Aim of this work

LDH-V is necessary for the fermentation of pyruvate to lactate. In former times, it only played a key role in anaerobic glycolysis to obtain energy in the absence of oxygen. Although the basic mechanisms of LDH as a glycolytic enzyme has been known for a long time, new aspects of its function especially in tumor metabolism have become apparent in the last years. LDH is an important prognostic marker in cancer staging and therapy. LDH has been shown to play a major role in tumor malignancy, but the molecular mechanism behind this role is only starting to be understood.

The objective of this work was to broaden our knowledge about the role of LDH-V in tumor cell proliferation, angiogenesis-related gene expression and tumor malignancy and metastasis. Additionally, the involvement of LDH in the gene expression of HIF-regulated proteins important in tumor survival and specially in glycolysis was further investigated. The high glycolytic activity of Lung cancer, the strong correlation of serum LDH in patients with malignant melanomas (Rady et al. 1979; Shivers et al. 1998; Koukourakis et al. 2003) and the published correlation of LDH and malignancy in colon carcinomas (Koukourakis et al. 2006) lead us to believe that LDH play a key role in the mentioned tumors.

To determine LDH-V-dependent effects on these different tumor types, stable LDH-V knockdown clones of a human colon carcinoma (HT29), a murine melanoma (B16F10) and a lung carcinoma (Lewis Lung) were generated. The cell lines were then characterized *in vitro*, *in vivo* and *ex vivo*. The effect of LDH-V on apoptosis, angiogenesis and tumor growth was evaluated. Additionally, we analyzed a possible involvement of LDH in expression of other genes and specially on HIF-regulated proteins. Furthermore, tumor cell behavior on glucose uptake, migration and invasion after LDH-V suppression was determined.

1.9 Thesis structure

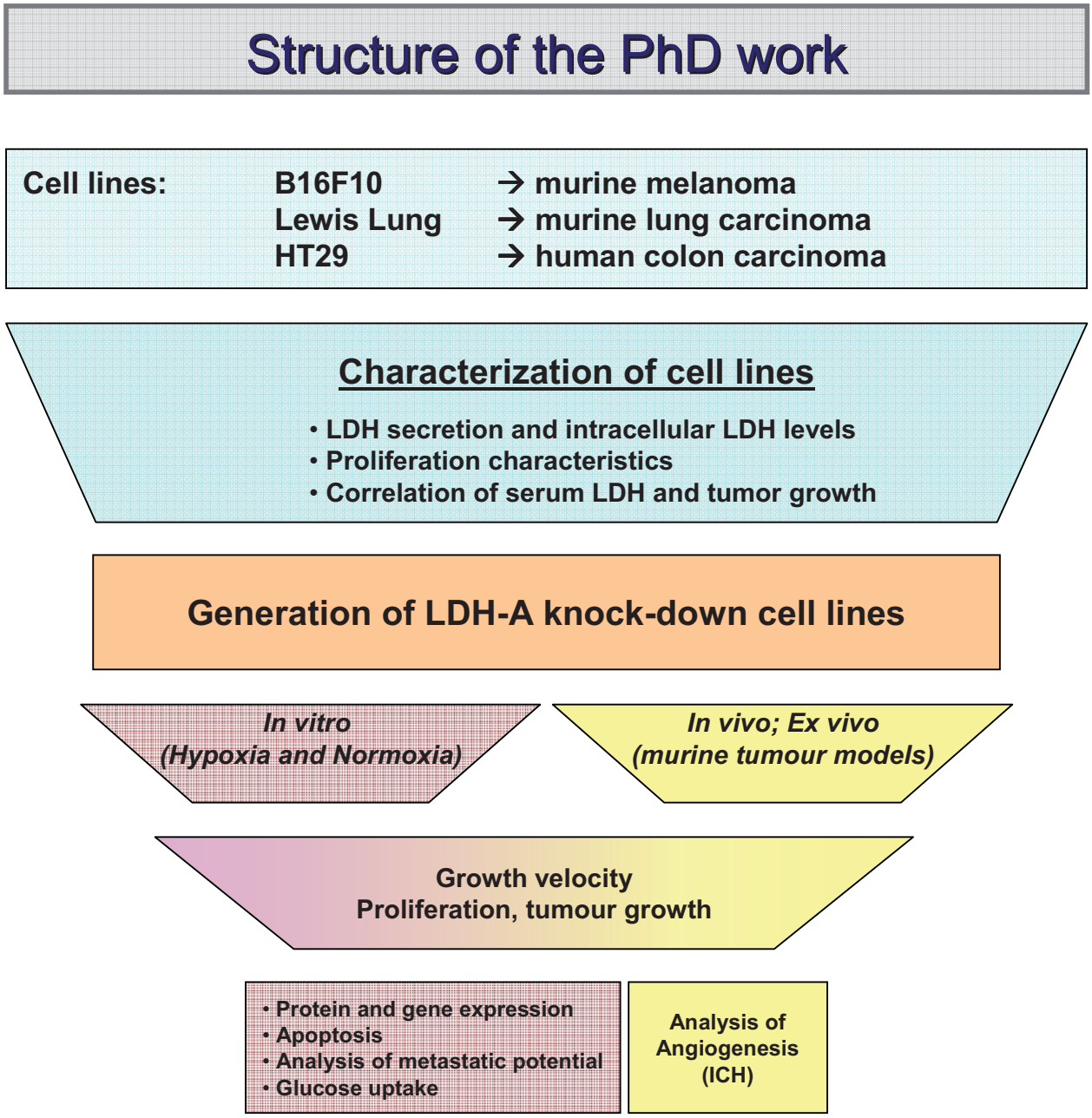

Figure 6. Scheme to study the effect of LDH-V on different tumor cells *in vitro* and *in vivo*.

2 MATERIALS AND METHODS

2.1 *In vitro* experiments

2.1.1 Cell lines and culture

Lewis Lung carcinoma cells were cultured in Dulbecco's Modified Eagle Medium (DMEM[a]) supplemented with 10% (v/v) fetal bovine serum (FBS), 2 mM L-alanyl-L-glutamine and 1% (v/v) sodium-pyruvate. B16F10 melanoma cells were maintained in DMEM/HAM's F10 (1:1) medium supplemented with 5% FBS and 2 mM L-alanyl-L-glutamine. HT29 human colon carcinoma cells were grown in DMEM/HAM's F10 (1:1) supplemented with 10% FBS, 2 mM L-alanyl-L-glutamine and 1% (v/v) nonessential amino acids.

Table 1. Cell lines used in this work

Name	Description	Supplier
Lewis Lung	Murine C57BL lung carcinoma	ATCC[b]
B16F10	Murine C57BL melanoma	ATCC
HT29	Human colon adenocarcinoma	ATCC

Cells were grown in their corresponding cell culture media as adherent monolayers at 37℃ and in 5% CO_2 atmosphere. Culturing the cells in 1% O_2 was considered as a hypoxic condition. For subculturing, cells were washed with PBS, detached by incubation with 0.05% trypsin/ 0.02% EDTA in PBS for two to five minutes and resuspended in serum-containing growth medium. Subsequently, the required number of cells was transferred to a new tissue culture flask (Corning, Wiesbaden, Germany).

[a] If not stated otherwise all cell culture media and reagents were purchased from Biochrome, Berlin, Germany.

[b] American type culture collection, Manassas, USA

2.1.2 Analysis of cell proliferation and cell cycle

2.1.2.1 Proliferation assay

Alarma Blue™ assay was used to examine the proliferation status and the effect of LDH-V gene silencing on the proliferation of the cell lines. AlamarBlue™ (Biotium, Inc., Hayward, CA, USA) detects cell viability via the conversion of the blue and nonfluorescent dye, resazurin, into the pink and fluorescent dye, resorufin during cell growth. Continued cell growth maintains a reduced environment while inhibition of growth maintains an oxidized environment. Reduction related to growth causes the REDOX indicator to change from the oxidized (nonfluorescent, blue) form to the reduced (fluorescent, red) form. The fluorescent signal is monitored using 530-560 nm excitation wavelength and 590 nm emission wavelength. The absorbance is monitored at 570 nm and 600 nm. For optimal result, background OD at 600 nm is subtracted from OD at 570 nm. The fluorescent and colorimetric signal generated from the assay is proportional to the number of living cells in the sample. 1 x 10^4 cells were seeded in 100 µl per well of a 96-well plate in 12 replicates and cultured for 24, 48, 72 and 96 hours under normoxic or hypoxic conditions. At each time point 10 µl AlarmaBlue™ were added to a three wells and cells incubated for another 2-3 hours at 37℃. The emission was measured at 570nm. Medium containing AlarmaBlue™ only was used as blank value.

2.1.2.2 Cell cycle analysis

For cell cycle analysis, 1 x 10^6 cells were plated in 10cm-diameter tissue culture dishes and cultivated at 37℃. After 48 hours, medium containing floating cells was transferred from the dish to separate 5 ml round-bottom tubes (BD Biosciences, Heidelberg, Germany). Adherent cells were washed with PBS (without Mg^{2+}, Ca^{2+}), trypsinized and transferred to the tubes containing the previously collected medium. After centrifugation for 10 min at 250 x g the supernatant was removed and the cell pellet was resuspended in 70% (v/v) ethanol (Merck, Darmstadt, Germany). The cell suspension was stored at -20℃ for at least 24 hours.

To examine the cell cycle cells were washed with PBS and centrifuged for 10 min at 250 x g. Supernatant was removed, cells resuspended in 200 µl PBS, 10 µl 5% (w/v) RNAse A (Sigma-Aldrich Chemie GmbH, Taufkirchen, Germany) in PBS and 200 µl

(100 µg/ml) propidium iodide (Sigma-Aldrich Chemie GmbH, Taufkirchen, Germany). Upon incubation at 4℃ for at least 30 minutes, pro pidium iodide fluorescence was measured using a FACSCalibur flow cytometer (BD Biosciences) and CellQuest Pro analysis software (BD Biosciences, Heidelberg, Germany). Forward scatter, orthogonal scatter and emitted fluorescence data were acquired on 10.000 events for each sample. A two-dimensional dot plot displaying cellular DNA content versus cell size was used to exclude cell aggregations from cell counting and cell cycle analysis.

2.1.3 Measurement of LDH activity

LDH activity was determined in cell lysates by using the Cytotoxicity Detection Kit from Roche Applied Science (Germany). The Cytotoxicity Detection Kit is designed as a precise, fast and simple colorimetric alternative assay (Figure 7) to quantify LDH activity released upon cytotoxicity/cytolysis damaged cells.

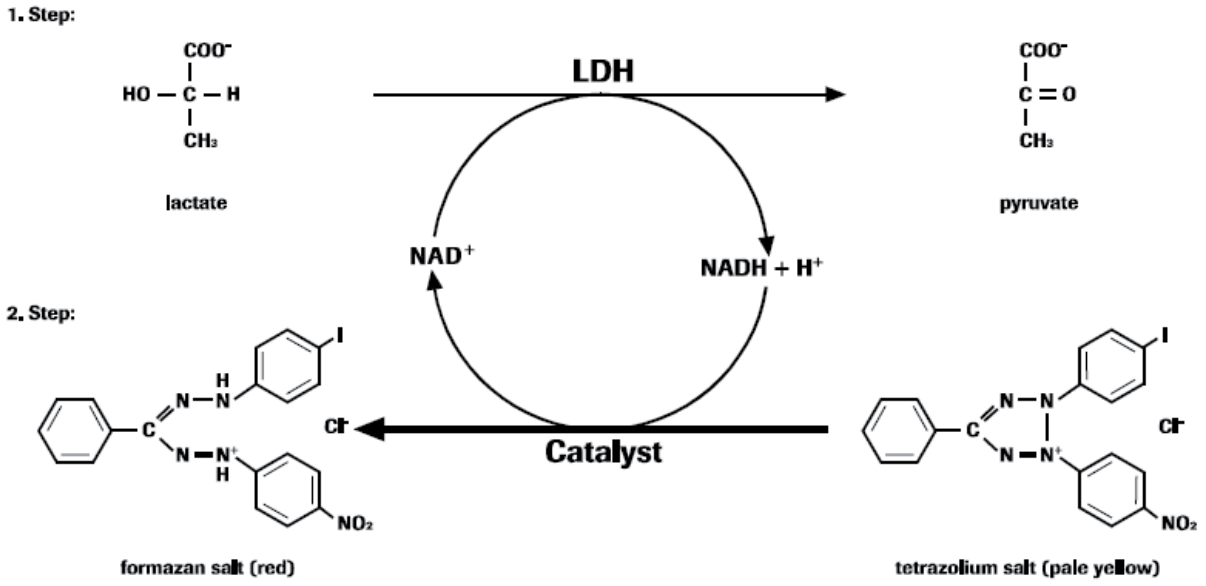

Figure 7.Functioning of the Cytotoxicity Detection Kit . In the first step, released lactate dehydrogenase (LDH) reduces NAD+ to NADH+ H+ by oxidation of lactate to pyruvate. In the second enzymatic reaction 2 H are transferred from NADH+ H+ to the yellow tetrazolium salt INT (2-[4-iodophenyl]-3-[4-nitrophenyl]-5-phenyltetrazolium chloride) by a catalyst. [source: Cytotoxicity Detection Kit (LDH) data sheet, version July 2005, Roche Applied Science].

1 x 10^5 cells were lysed in 500 µl 1% Triton x 100 in PBS and diluted 1:10 in PBS. 100 µl of this solution were added to 100 µl assay buffer and incubated at room temperature for 3 min. LDH activity was determined by the reduction of tetrazolium salt INT to formazan (spectrophotometric read out: 492/620 nm). Results from three experiments were normalized to mean average protein content, and in some cases expressed as relative LDH activity.

2.1.4 LDH-A knockdown

2.1.4.1 Selection of transfection method

The use of cationic liposome/DNA complexes (lipofection) for gene transfer into somatic cells has become a popular method of delivering genes. Interaction between cationic lipids and DNA through ionic interaction leads to the formation of cationic lipoplexes (Blaese et al. 1993; Guenzburg and Salmons 1997). The resulting complexes fuse with the anionic cell surfaces and DNA is delivered into the cells via endocytosis. However, the final transport of DNA into the nucleus is still not fully understood. Transfection using lipofection offers several advantages over viral vectors, such as simplicity of production, low toxicity and low immunogenicity.

Additionally, another transfection method, electroporation, also termed electrotransfer or electropermeabilization was tested. In this method, brief electric pulses are applied to cells or tissues in order to increase cellular permeability to macromolecules. This method has been reported to increase naked DNA expression by 60-fold or more. Finding the balance between the highest transfection efficiency and survival rate is very important, therefore we investigated the most suitable transfection method in all cell lines (Iversen et al. 2005; Han et al. 2008).

2.1.4.1.1 Electroporation / Nucleofection

Cell pellets of each cell line were resuspended in 100 µl Nucleofector Solution V (AMAXA) to a final concentration of 1 x 10^7 cells/ ml. 100 µl of the cell suspension and 2 µg GFP (Green Fluorescence Protein) vector were added to the electroporation cuvette. Cuvette was processed with AMAXA's electroporation device using the appropriate program for all cell line (P-20). Cells were transferred with a

plastic pipette into a 6-well plate containing 2 ml of pre-warmed medium at 37℃. After 24 hours, cells were analyzed using fluorescence microscopy (see 2.1.6).

2.1.4.1.2 Lipofection

2 x 10^5 cells were seeded in 24-well tissue culture plate in 500 µl. 2.5 µl Lipofectamine™ 2000 (Invitrogen, Karlsruhe, Germany) were diluted in 2.5 µl Opti-MEM® I Medium and incubated for 5 min. 2 µg GFP vector were diluted in serum-free 250 µl Opti-MEM® I Medium and was added to the diluted Lipofectamine. Suspension was mixed gently and incubated for 15 minutes at room temperature to allow complex formation. After incubation, diluted Lipofectamine™ 2000 - GFP mix was added to the wells of the 24-well tissue culture plate and mixed gently. After 5 min incubation, 1 ml complete growth medium without antibiotics was added to each well. Cells were gently mixed and incubated under culturing conditions. After 24 hours post-transfection, cells were analyzed using fluorescence microscopy.

2.1.4.2 Stable shRNA-mediated knockdown of LDH-A

Three SureSilencing™ shRNA Plasmids (Promotor: U1, Vector: pGeneClip-Neo [Promega, Mannheim, Germany], selective marker: Neomycin), containing a 21-base stem structure complementary to the LDH-A gene (Gene-bank NM_010699 murine LDHA and NM_005566 human LDHA) was designed by SuperArray (Biomol, Hamburg, Germany). B16F10, Lewis Lung and HT29 cancer cells were transfected using electroporation method as described in 2.1.4.1.1, with murine sh2-sh4 vectors for Lewis Lung and B16F10 (Table 2) and human sh2-sh4 vectors for HT29 (Table 3) cells. Non-silencing control (NC) shRNA (sh5) was used as control.

Table 2. Sequences of SureSilencing™ shRNA plasmid for human LDH-A

Clone ID	Insert Sequence (5' – 3')
sh2	CCACCATGATTAAGGGTCTTT
sh3	GCAGAGAGTATAATGAAGAAT
sh4	CCAGCGTAACGTGAACATATT
sh5 (NC)	ggaatctcattcgatgcatac

Table 3. Sequences of SureSilencing™ shRNA plasmid for mouse LDH_A

Clone ID	Insert Sequence (5' – 3')
sh2	GTACGTCCATGATGCATATCT
sh3	TGCCAACTGCAGGCTTCGATT
sh4	GGGCAGCTTTCTAACCATAT
sh5 (NC)	ggaatctcattcgatgcatac

2.1.5 Protein extraction, SDS-PAGE and Western blot

Cytoplasmic and nuclear protein was extracted from cultured Lewis Lung, B16F10, HT29 cells and LDH-A knockdown clones by using M-PER Mammalian Protein Extraction Reagent (Pierce, Perbio Science, Bonn, Germany) supplemented with protease inhibitor mix (Sigma-Aldrich Chemie GmbH, Taufkirchen, Germany) and benzonase (Merck, Darmstadt, Germany). With the exception of using only 200 µl extraction reagent for subconfluent cells protein extraction was performed without scraping according to the manufacturer's instructions. Protein yield was determined by employing BCA Protein Assay Kit (Pierce) according to the manufacturer's instructions.

Table 4. Primary and secondary antibodies used for Western blot analysis .

Primary antibodies	Company
anti-LDH-V	Abcam, Cambridge, UK
anti-ß-actin	ICN, Frankfurt am Main, Germany
anti-HIF1alpha	Cell Signaling, Danvers, USA
anti-carbonic anhydrase IX	Abcam, Cambridge, UK
anti-PHD2	US Biological, Massachusetts, USA
anti-LDH-B	Abcam, Cambridge, UK
anti-AKT	Cell Signaling, Danvers, USA
anti-pAKT473	Cell Signaling, Danvers, USA
anti-GLUT-4	Santa Cruz Biotechnology, Heidelberg, Germany
Secondary antibodies	
rabbit anti-sheep IgG	Abcam, Cambridge, UK
goat anti-mouse IgG	Jackson ImmunoResearch, Suffolk, UK
goat anti-rabbit IgG	Jackson ImmunoResearch, Suffolk, UK

For Western blot analysis, equal amounts of protein extracts prepared from cultured cells were denaturated in lithium dodecyl sulphate sample buffer[c] and separated on a 4-12% Bis-Tris gel in an XCell SureLock electrophoresis chamber filled with MOPS-SDS running buffer for 1 hour at 140 Voltages. The protein was electro-transferred to a polyvinylidene difluoride membrane for 1 hour at 35 Voltages. Unspecific binding was blocked with 5% (w/v) non-fat milk in PBS/ Tween 20 for one hour. The membrane was then incubated over night at 4℃ with the specific antibodies in 5% (w/v) non-fat milk in PBS/ Tween 20 (Table 4). Following three washes with PBS/ Tween 20, the membrane was incubated with the corresponding horseradish peroxidase-labeled secondary antibody for 1 hour at room temperature (Table 4), washed again with PBS/ Tween 20 and subjected to enhanced chemiluminescence reaction using ECL Plus Western Blotting Detection Reagents (GE, Munich, Germany). Chemiluminescence was detected on Hyperfilm ECL (GE Healthcare). If required, re-probing the membrane with an additional set of antibodies was performed upon 30-minute membrane stripping using Restore Western Blot Stripping Buffer (Pierce) according to the manufacturer's instructions.

2.1.6 Fluorescent microscopy

HT29 colon carcinoma cells were seeded in chamber slides at a concentration of 50,000 cells/ 500µl/ well and transfected or cultured as described. The culture medium was aspirated and cells were fixed with 3.7% formaldehyde in PBS for 10 min and permeabilized with 0.5% Triton X-100 in PBS for 2 min. After washing, unspecific binding was blocked with 1% BSA for 30 min. Cells were incubated for another 1 h with specific antibodies against tubulin (Sigma-Aldrich Chemie GmbH, Taufkirchen, Germany), LDH-V (Cell Signaling) and GLUT-4 (Santa Cruz Biotechnology) diluted in 1% BSA, and then incubated with FITC-conjugated secondary antibodies in 1% BSA solution for 1 h in the dark. Nuclei were stained by treating the cells with Hoechst 33342 dye at 0.1 µg/ ml in PBS for 2 min in the dark. Between the incubations cells were washed three times with PBS for 5 min. Slides were then mounted, sealed and imaged using a Zeiss Axiophot microscope coupled

[c] If not stated otherwise all reagents and devices used for gel electrophoresis and Western blot were purchased from Invitrogen.

to an AxioCam MRc CCD camera. Images were acquired with Axio Vision LE 4.5 software.

2.1.7 Apoptosis detection

Apoptosis is a genetically determined, biochemically-ordered process in which cells are induced to initiate a cellular suicide program in response to physiological signals, cellular damage or viral infection. In normal cells, the pathway is very tightly controlled, but deregulation of the apoptotic pathway contributes to the pathogenesis of many human diseases including cancer. Meso Scale Discovery's MULTI-SPOT^{TM} is a multiplex assay which can simultaneously measure the protein levels of three important members of the apoptotic pathway. Caspase-3, cleaved PARP and total Bcl-2 proteins are quantified in a single well from a single whole cell lysate.

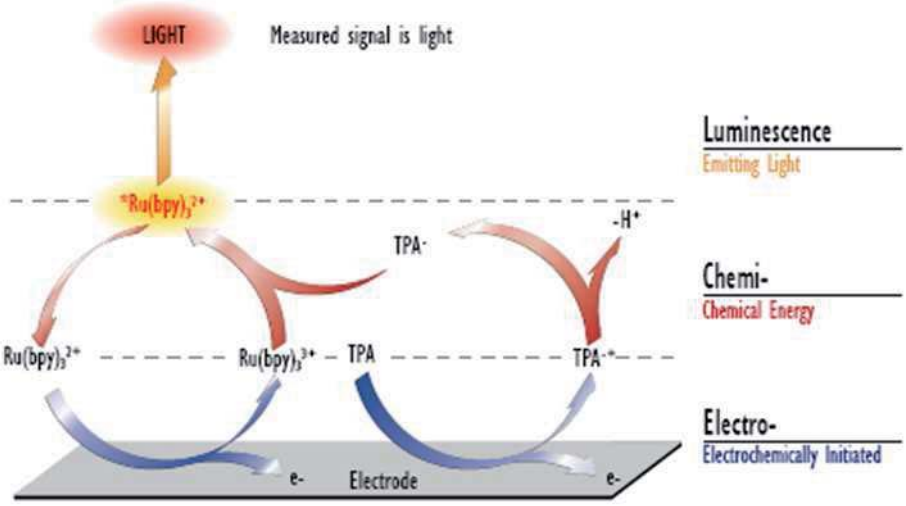

Figure 8. Electrochemiluminescence (ECL). [source: MSD data sheet, A New Way To Measure Classic Markers Of Apoptosis]

The sandwich immunoassay uses capture antibodies that have been immobilized on the surface of 96-well plates. Whole cell lysates are then incubated with the plates, followed by detection of the captured protein with an antibody labeled with an electrochemiluminescent tag. The results of this assay closely mimic those seen in Western blot analysis.

2.1.8 VEGF ELISA

The quantity of VEGF in each cell line was determined by using the human and mouse Quantikine kit (R&D systems, Germany). This assay employs the quantitative sandwich enzyme immunoassay technique. A microplate is pre-coated with a monoclonal antibody specific for VEGF. 1 x 10^5 cells/ 200 µl of each cell line were cultured in 96 well plates under the indicated hypoxic or normoxic conditions (2.1.1). After 48 hours, 100 µl of supernatant was removed, transferred to the pre-coated wells and incubated for 2 hours. Any VEGF present was bound by the immobilized antibody. Unbound substances were removed with washing-buffer, an enzyme-linked polyclonal antibody specific for VEGF was added to the wells and incubated for 2 hours. Unbound antibody-enzyme reagent was removed by washing, a substrate solution (protected from light) was added to the wells and incubated for 20 min. Color development was stopped by adding stop solution and color intensity was measured at 450 nm using a TECAN Sunrise™ multichannel absorbance plate reader.

2.1.9 Microarray analysis

Illumina BioArray® technology is based on optically wired 3-micron beads that self assemble in micro-wells etched on a silica slide, referred to as a BeadChip (Figure 9). Each bead is covered with a specific oligonucleotide, often a 50-mer, and multiple copies of each bead type are present on one microarray. Illumina products are designed for high-throughput testing of multiple specimens in parallel. BeadChips contain up to 12 microarrays per slide and the Illumina Array Matrix format attaches beads to fiber optic bundles that are compatible with 96-well plates. The actual chip analysis was processed by Bayer Schering Pharma's Target Discovery – Global Technology department under the direction of Dr. Annette Sommer. Statistical analyses and normalization of the obtained raw data was done by MicroDiscovery, Berlin, Germany.

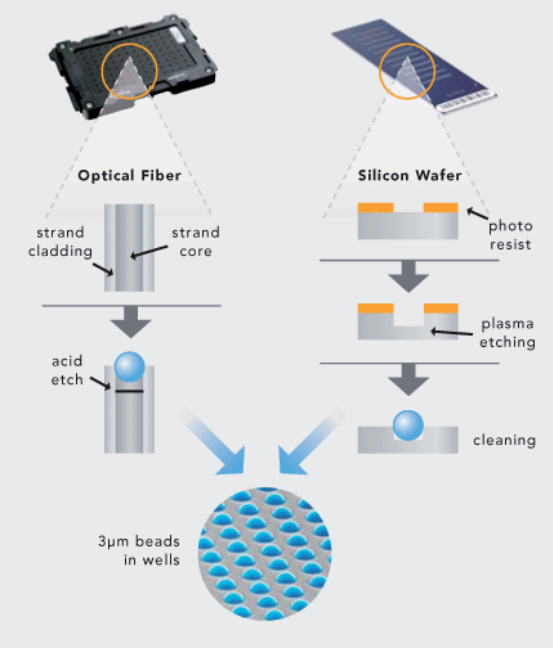

Figure 9. Illumina multi-array format. BeadArray technology is deployed on either of two multi-sample array formats for DNA or RNA-analysis applications. With both the 96-sample Array Matrix and the multi-sample BeadChip formats, uniform pits are etched into the surface of each substrate to a depth of approximately 3 microns prior to assembly. Beads are then randomly assembled and held in these microwells by Van der Waals forces and hydrostatic interactions with the walls of the well. [source: Illumina product sheet]

2.1.9.1 Sample preparation

HT29 colon carcinoma cells were harvested and counted. As indicated in Figure 10, 5 x 10^5 cells/ 2ml/ well were seeded in 6 well plates and first incubated for 24 h under normoxic conditions. Then half of the plates were cultured under hypoxic conditions. After 6 hours (for short-term hypoxia effect) the first part of the plates (~ 60% confluent) was washed twice with PBS and lysed with 350 µl RLT buffer (QIAGEN, Germany) and frozen at -20℃. The maximum duration for this step was 2 min. After 24 hours (for long-term hypoxia effect), the remaining plates (~ 75% confluent) were washed twice with PBS and lysed with 350 µl RLT buffer and frozen at -20℃. The maximum duration for this steps was also 2 min. RNA isolation of all cells was performed after 3 days storage in the freezer at -20℃.

.

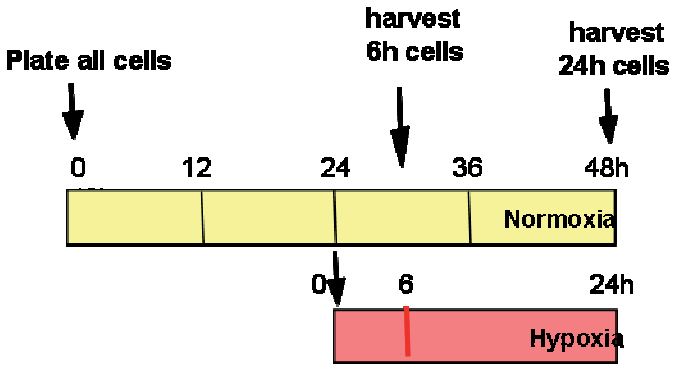

Figure 10. Timelines for Illumina sample preparation of HT29 cells. HT29 colon carcinoma cells were seeded and cultured for 24 h under normoxic conditions. After the culturing time half of the plates were then cultured under hypoxic conditions. Cells of both hypoxic and normoxic conditions were harvested after 6 and 24 hours.

2.1.9.2 RNA isolation

RNA isolation was performed with the QIAGEN RNeasy kit (QIAGEN, Germany). 70% ethanol (v/v) (1 ml) was added to the lysate and mixed by pipetting. The lysate was transferred to an RNeasy spin column placed in a 2 ml collection tube. Tube was centrifuged for 15 s at 10,000 rpm (10,400 x g). Flow-through was discarded. 350 µl RW1 buffer was added to the spin column and centrifuged for 15 s at 10,000 rpm to wash the spin column membrane. Flow-through was discarded. 10 µl DNase I stock solution was added to 70 µl RDD buffer, mixed by gently inverting the tube, and centrifuged briefly to collect residual liquid from the sides of the tube. DNase I incubation mix (80 µl) was added to the RNeasy spin column membrane, and place on the bench top (20 – 30℃) for 15 min. RW1 buffer (350 µl) was added to the spin column and centrifuged for 15 s at 10,000 rpm. Flow-through was discarded. Another 700 µl RW1 buffer was added to the spin column and centrifuged for 15 s at 10,000 rpm. Flow-through was discarded. RPE buffer (500 µl) was added to the RNeasy spin column and centrifuged for 15 s at 10,000 rpm. Flow-through was discarded. Another 500 µl RPE buffer was added to the RNeasy spin column and centrifuged for 2 min at 10.000 rpm. Spin column was placed in a new 2 ml collection tube and centrifuge at full speed for 1 min. Spin column was placed in a new 1.5 ml collection tube and 30 µl RNAse free water was added directly to the spin column membrane. Tube was centrifuged for 1 min at 10,000 rpm to elute the RNA. RNA analysis was performed with the RNA 6000 Nano kit (Agilent, Waldbronn, Germany) according to the

manufacturer's protocol and measured with the Agilent 2100 Bioanalyzer (Agilent, Waldbronn, Germany).

2.1.10 *In vitro* analysis of metastatic potential of the cancer cell lines

2.1.10.1 2D scratch assay

1 x 10^6 cells of each cell type were seeded onto a 24-well plate and cultured for 48 h. Medium was aspirated and a cell-scratch established by using a 100 µl pipette-tip. Wells were washed 3 times with 1 ml PBS and fresh medium with 10 ng/ ml Mitomycin C (Sigma-Aldrich Chemie GmbH, Taufkirchen, Germany), an inhibitor of DNA synthesis, was added to each well to avoid cell proliferation. Pictures were taken after 0 h, 6 h and 24 h of incubation with the Nikon Digital Sight DS-5M camera. All pictures were normalized with Photoshop and the distance of migration was measured with Photoshop's calculator. The results are given in pixel points, which allows a sensitive distance measurement.

2.1.10.2 Transendothelial migration assay

The CytoSelect™ Tumor Transendothelial Migration Assay (Cell Biolabs, San Diego, USA) was used to analyze the invasion behavior of LDH-V deficient HT29 cells. 100,000 endothelial HDMVEC cells were suspended in 300 µl medium and added to each insert of a 24-well plate containing 500 µl of culture medium. Endothelial cells were cultured for 48 h until a monolayer was formed. Cells were treated with 2 µL TNFα stock solution. Cancer cells were harvested and a cell suspension at 5 x 10^5 cells/ml in serum-free medium was prepared. CytoTracker™ (10x) was added to a final concentration of 1x. Cell suspension was incubated for 60 min at 37ºC in a cell culture incubator. Cells were centrifuged at 1000 rpm for 2 min, medium was aspirated and cells were washed twice with serum-free medium. Cell pellet was resuspended at 5 x 10^5 cells/ml in serum-free medium. Endothelial culture medium was carefully removed from migration insert without disturbing the endothelial monolayer and the insert was transferred to another well containing 500 µl of tumor cell culture medium including 10% FBS. 300 µl of the cell suspension was added to the inside of each insert and cells were incubated for 20 h in a cell culture incubator.

The medium from the inside of the insert was carefully aspirated. Cotton-tipped swabs were used to gently remove non-migratory cells from the interior of the inserts. Insert was transferred to a clean well containing 200 µl of 1x Lysis Buffer. After an incubation of 5 min at room temperature with shaking, 100 µl of the mixture were transferred to a 96-well plate suitable for fluorescence detection (Costar). Fluorescence was measured with the VICTOR fluorescence plate reader at 485 nm/ 535 nm.

2.2 *In vivo* experiments

Animal studies were conducted in accordance to the German Animal Welfare Act of 1998 and with approval from the responsible authorities. All mice were maintained under pathogen-free, controlled conditions.

2.2.1 Tumor growth experiments

1 x 10^6 HT29 cells in 100 µl Matrigel/ serum-free RPMI medium (1:1), 5 x 10^5 Lewis Lung cells in 100 µl serum-free RPMI medium, 5 x 10^5 B16F10 tumor cells in 100 µl serum-free RPMI medium and the corresponding derived LDH-A knockdown clones also in 100 µl serum-free RPMI medium were subcutaneously injected into the left side of mice (n=8/group/cell line). For human HT29 cells, a xenotransplantation model with immuno-suppressed nude mice (Charles River, Sulzfeld, Germany) was used, and for murine Lewis Lung and B16F10 cells a syngenic model with C57BL/6 female mice (Charles River, Sulzfeld, Germany) was used. Tumor size was measured twice a week with a caliper and tumor surface was calculated (width x length). The mean tumor area at the beginning of the measurements was around 20 mm² in all models. Tumors were measured at different time points of the experiment. For animal welfare reasons, mice were sacrificed and tumor biopsies were isolated for further *ex vivo* analysis at a maximum mean tumor area of 140 mm².

2.3 Ex vivo experiments

2.3.1 Determination of serum LDH

At the endpoint of the *in vivo* experiments mice were decapitated and around 300 µl hole blood were collected in a prepared serum gel micro tube for blood samples (Sarsted, Nümbrecht, Germany). Blood samples were carefully and thoroughly mixed and incubated for 30 min at room temperature. Samples were centrifuged at 10,000 rpm for 3 min at room temperature. 100 µl of the serum was transferred into a new tube and frozen a -80℃. Serum samples were analyze d for LDH levels with the ADIVA 1650 chemistry system (ADIVA machine, Bayer UK) as described in the manufacturer's protocol.

Lactate dehydrogenase catalyzes the reversible reaction:

$$\textbf{L-lactate + NAD + H}^{+} \xrightarrow{LDH} \textbf{pyruvate + NADH}^{+}$$

The bidirectional reaction is monitored spectrophotometrically by measuring the increase in NADH at 340 nm produced in the lactate-to-pyruvate reaction.

2.3.2 Histological analysis of microvessel density

CD31 immunostaining was performed on 5-µm-thick formalin-fixed paraffin sections using the Dako Autostainer (Universal Staining System, model LV-1). Proteolytic enzymes were blocked with proteinase K ready-to-use solution (15 min, RT) (Dako, Hamburg, Germany) and endogenous peroxidase activity was blocked with 0.5% H_2O_2 for 15 min at room temperature. To inhibit non-specific staining during immunohistochemistry, sections were incubated for 10 min at room temperature in protein block (serum-free, ready-to-use (Dako)) followed by incubation with biotinylated primary anti-CD31 antibody (1:100, PECAM-1, monoclonal, rat anti-mouse, BD Biosciences Pharmingen, San Jose, CA, USA) for 15 min and extravidin-

peroxidase (1:300, Sigma-Aldrich Chemie GmbH, Taufkirchen, Germany) for 15 min. Antibodies were diluted in antibody diluent (DAKO). The immunostaining was performed using the liquid DAB + substrate chromogen system according to the manufacturer's instructions (Dako). The slides were counterstained for 1 min with hematoxylin (Dako) and washed with water for 10 min. Slides were then imaged using a Zeiss Axiophot microscope coupled to an AxioCam MRc CCD camera. Images were taken with the help of Axio Vision LE 4.5 software.

3 RESULTS

3.1 Cell lines have similar intracellular LDH levels but differ in LDH secretion

3.1.1 Intracellular levels of LDH

Intracellular LDH activity and amount / levels of LDH-V protein were analyzed *in vitro* in wild type (w/t) B16F10 melanoma, Lewis Lung carcinoma and HT29 colon carcinoma cells under normoxic conditions. Western blot analysis showed a very similar amount of intracellular LDH-V protein in the murine cell lines B16F10 and LL cells, whereas higher levels of LDH-V protein were detected in the human HT29 cells. This difference may be due to the fact that the LDH-V antibody is human specific and only cross-reacts with murine LDH-V. Thus, LDH activity was measured by using cytotoxicity detection and normalized to total protein amount (Figure 1). All three cell lines produced similar amounts of active LDH.

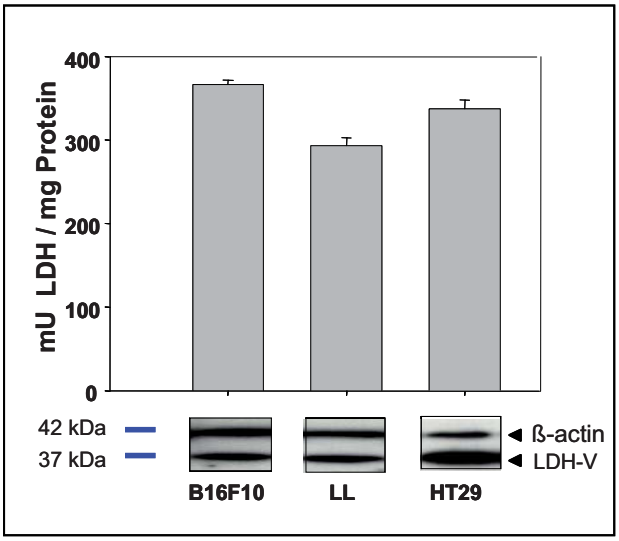

Figure 11. Similar LDH activity and the amount of LDH-V protein in three cell lines. B16F10, Lewis Lung and HT29 tumor cells were cultured for 48 hours and subjected to protein extraction. For Western blot analysis, isolated protein was separated using SDS polyacrylamide gel electrophoresis, transferred to a PVDF membrane and incubated with anti-human LDH-V and anti-ß-actin antibody as loading control. LDH activity was measured using cytotoxicity detection. Mean values and standard deviation of triplicates are shown in mU/mg total protein. (mean ± SD; n = 3)

3.1.2 Proliferation and LDH secretion

Metabolic pathways such as glycolysis are designed for the maintenance of energy and cell growth. In addition to the similar intracellular LDH activity, all tree cell lines showed likewise proliferation profiles (Figure 2). Subsequently, LDH secretion was analyzed in the supernatants from different time-points of the proliferation experiment and revealed a different secretion pattern between the cell lines. While LL cells did not secret LDH until they were confluent (40 h), B16F10 cells continuously secreted LDH. In contrast, HT29 cells did not show any LDH secretion even after reaching confluency (Figure 2).

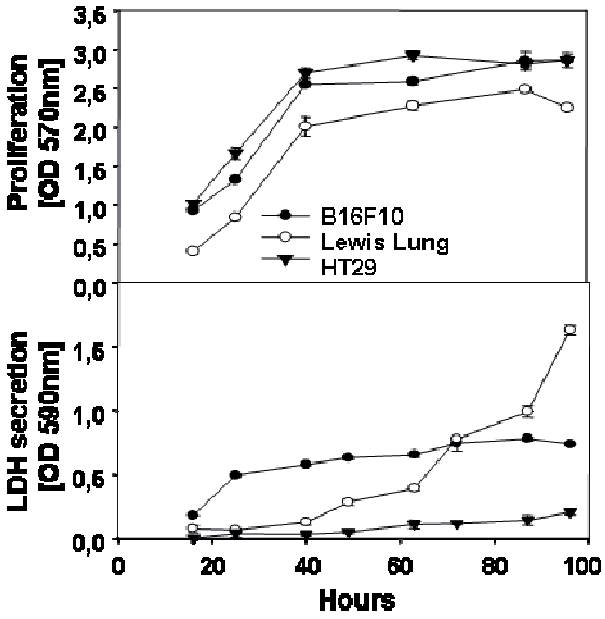

Figure 12. Different **LDH secretion patterns of tumor cell lines.** Cell lines were cultured in triplicates in a 96-well plate for indicated times (hours). At each time point 100 µl supernatant were analyzed with the LDH cytotoxicity kit and LDH activity was detected at 590 nm. Proliferation was determined by Alarma Blue as indicated in materials and methods. (mean ± SD; n = 3)

3.1.3 Correlation between tumor weight and serum LDH levels

Serum LDH is a prognostic tumor marker used in clinical practice (Culine 2009). We questioned if LDH plays a role in proliferation and tumor growth. To investigate the LDH levels of our selected cell lines *in vivo*, LDH activity was determined in the serum of several previous tumor growth experiments as indicated in materials and methods For all three cell lines a significant correlation between tumor growth and levels of serum LDH was found (Figure 3, $p<0.001$). B16F10 syngenic models

showed the strongest correlation (r=0.956) between tumor growth and levels of serum LDH compared to Lewis Lung syngenic models (r=0.747) and HT29 xenografts (r=0.674).

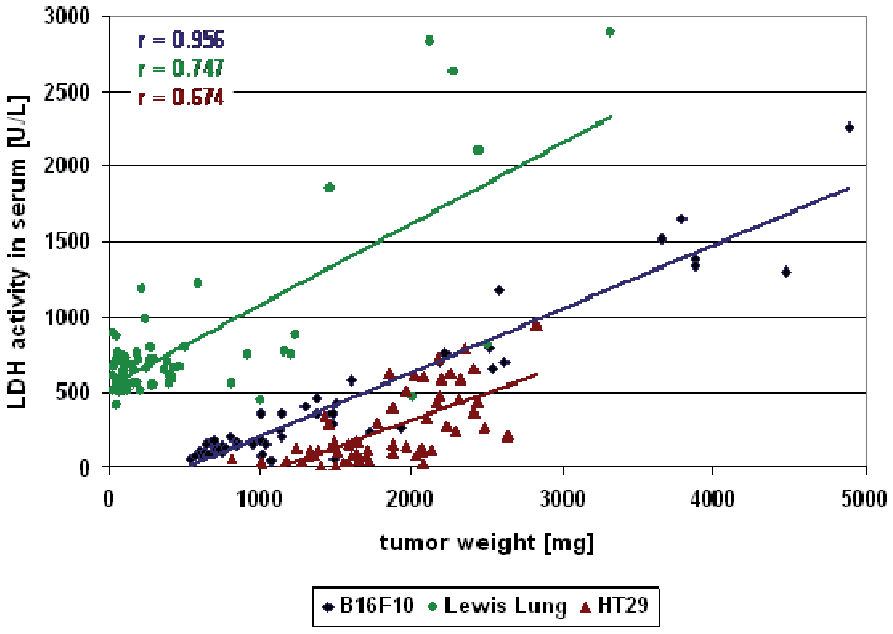

Figure 13. Tumor weight correlates with serum LDH level. Mice were inoculated subcutaneously with $1x10^6$ cells of each cell line. At different endpoints tumor specimen and serum were collected. Tumor weight of B16F10 (n=56), Lewis Lung (n=63) and HT 29 (n=60) tumors was measured and serum LDH levels were determined. Linear regression analysis of LDH activity and tumor weight are shown. Pearson linear correlation coefficient and p-value were calculated using SigmaStat and are shown as r- and p-values, respectively. $p<0.001$

3.2 Electroporation yields higher transfection efficiency than lipofection

To further investigate the role of LDH on tumor growth and malignancy, the impact of LDH gene silencing was analyzed in subsequent experiments. First, the most efficient transfection method was determined for all three cell lines by comparing the nucleofection method from AMAXA (electroporation) and lipofection.

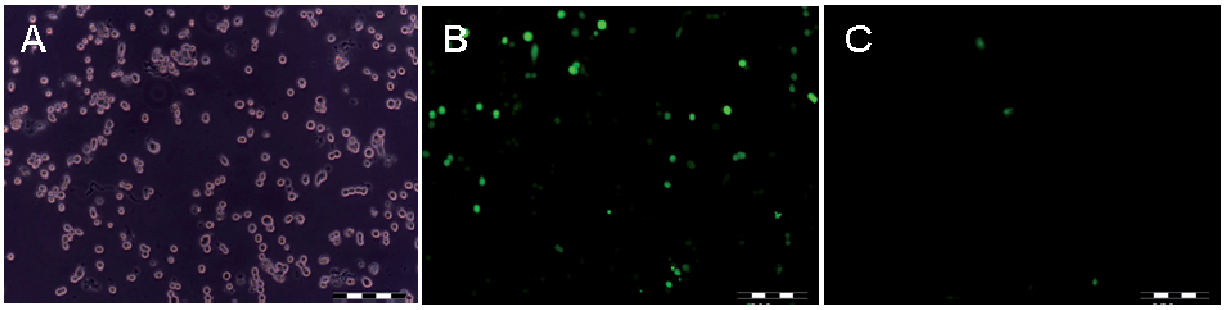

Figure 14. Electroporation yields better transfection efficiency than lipofection with Lipofectamine™2000. (A) Murine B16F10 cells were transfected with 2 µg of pmaxGFP using (B) electroporation or (C) Lipofectamine™2000. After 24 hours GFP expressing cells were visualized by fluorescence microscopy. Scale bar, 200 µm.

B16F10 cells were transfected with a GFP-expressing control vector using either electroporation (Figure 14 B) or lipofection (Figure 14 C). As shown in Figure 14 a higher transfection efficiency was achieved in B16F10 cells by electroporation. Additionally, similar results were obtained for Lewis Lung and HT29 cells (data not shown). Thus, nucleofection is the most suitable transfection method for all cell lines used in this study yielding high transfection efficiency and cell viability.

3.3 Stable shRNA-mediated *LDH-A* silencing in LL, B16F10 and HT29 tumor cells

3.3.1 *LDH-A* knockdown in murine cell lines

The impact of inhibiting glucose to lactate conversion was evaluated to investigate the relation between tumor growth and the glycolysis phenotype of tumor cell. Short hairpin RNAs (shRNAs) complementary to murine LDH-V were used to stably suppress LDH expression. B16F10 and LL tumor cells were transfected via nucleofection with recombinant vectors expressing three LDH-specific shRNAs (sh2, sh3 and sh4) and one non-silencing control sequence (sh5) under the U1 promotor and a neomycin resistance gene. Efficiency of LDH gene silencing was identified by Western blot analysis and LDH activity of lysed cells.

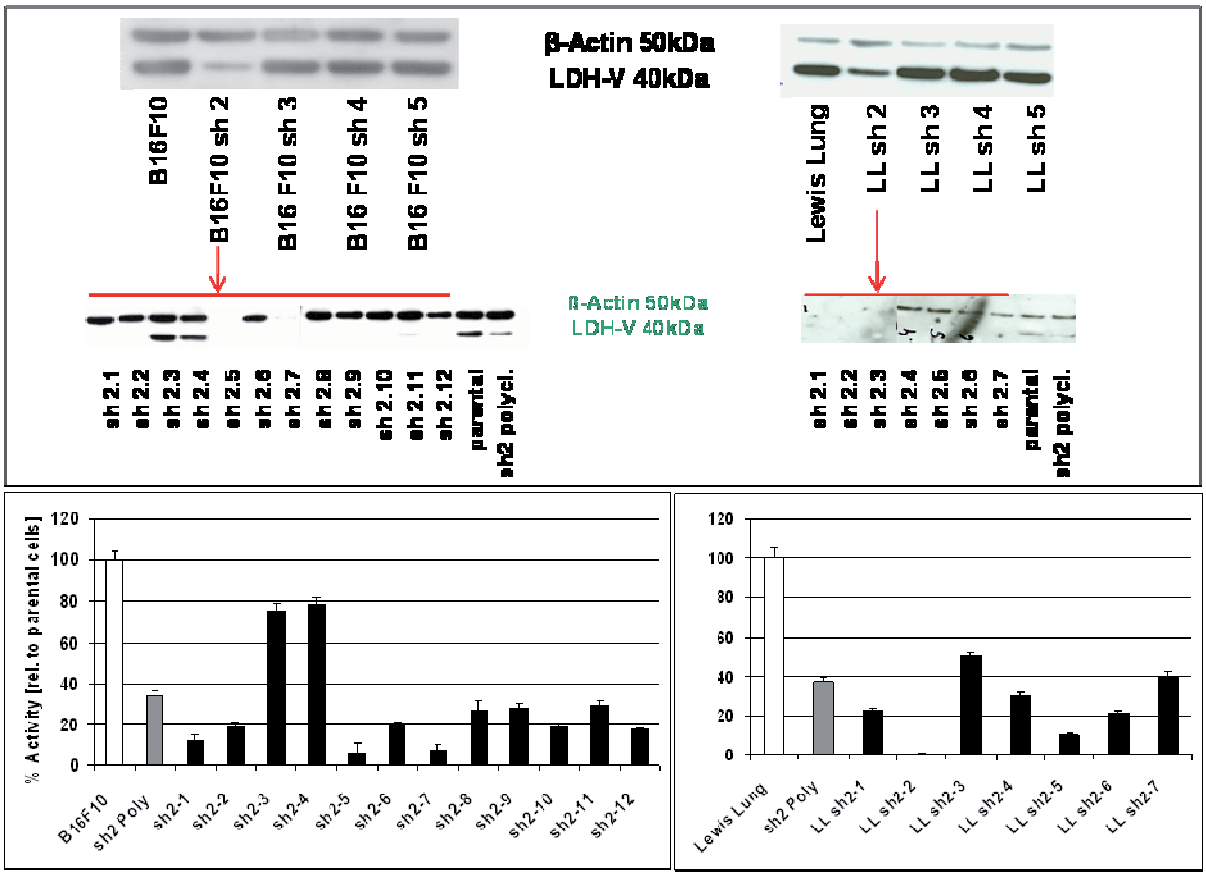

Figure 15. Transfection with shRNA2 construct results in strongest LDH-V gene silencing. Murine Lewis Lung and B16F10 cells were transfected either with 2 µg of LDH-specific shRNAs or a non silencing control (sh5) by nucleofection. The strongest LDH silencing was achieved by the shRNA2 construct. Single cell clones were isolated and LDH-V expression detected by Western blot analysis and activity measurement. (mean ± SD; n = 3)

The highest level of *LDH-A* protein suppression (LDH-V) was achieved by shRNA2 in both murine cell lines (Figure 5). Single cell clones of both cell lines transfected with shRNA2 were selected by culturing with 1200 mg/ml Neomycin. A series of stable clones expressing varying degrees of *LDH-A* protein were isolated by the limiting-dilution method and tested for LDH-V expression. LDH silencing was also assessed by enzymatic assay (Figure 5). The silencing efficiency was very high in most of the selected clones. LDH-V protein was strongly suppressed (≥75%) in B16F10 clones 2.1, 2.2, 2.6 - 2.12 and in LL clones 2.1, 2.2, 2.4 – 2.6 compared to the non-silencing shRNA (sh5) and the parental cell line.

3.3.2 *LDH-A* knockdown in human HT29 cells

Human HT29 cells were stably transfected with four different *LDH-A*-specific shRNAs to decrease protein expression. A non-silencing vector was used as control (sh5). The human specific shRNA 4 (sh4) generated the best LDH-V suppression. Single clones were isolated and selected with the limiting- dilution method.

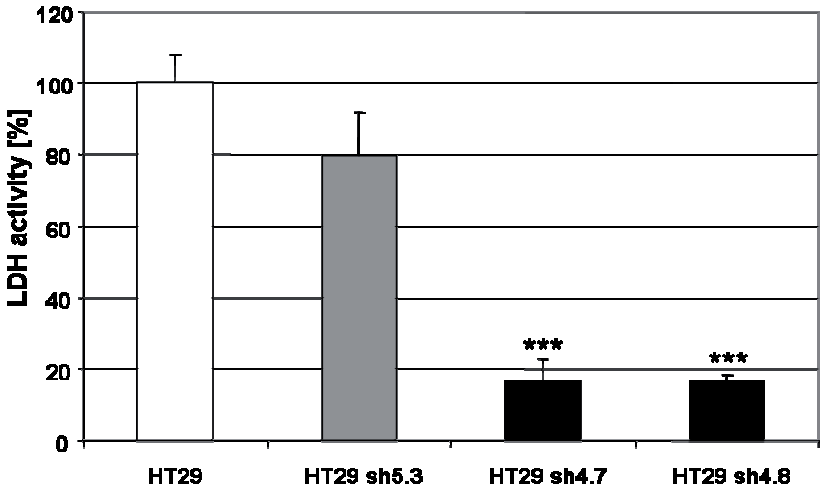

Figure 16. Transfection with shRNA4 construct yields the best LDH-V knockdown in HT29 cells. Human HT29 cells were transfected with either 2 µg of *LDH-A*-specific shRNA or a non silencing control (sh5) using nucleofection. The strongest *LDH-A* knockdown was achieved by the shRNA4 construct. Single clones were selected and LDH-V was detected by activity measurement. Mean values and standard deviations of three independent experiments are shown (***p<0.001 vs. parental cell line).

LDH silencing was assessed by enzymatic assay. Strongest suppression of LDH activity was obtained in clones 4.7 and 4.8 (Figure 16). In subsequent experiments two clones of each cell line with the strongest LDH knockdown were tested and compared to the parental cell lines and clones transfected with control shRNA5 (sh5) as controls.

3.4 LDH-V deficiency impedes growth of murine LL and B16F10 cells *in vitro*

As the previous experiments indicate silencing of LDH-V does not result in complete cell death. Even strongly reduced *LDH-A* protein levels do not lead to any morphological changes in the cell clones (data not shown).

To test the influence of *LDH-A* silencing on growth properties of LL, B16F10 and HT29 cells and its clones, proliferation assays were performed under normoxic or hypoxic culture conditions (Fig. 7 and 8).

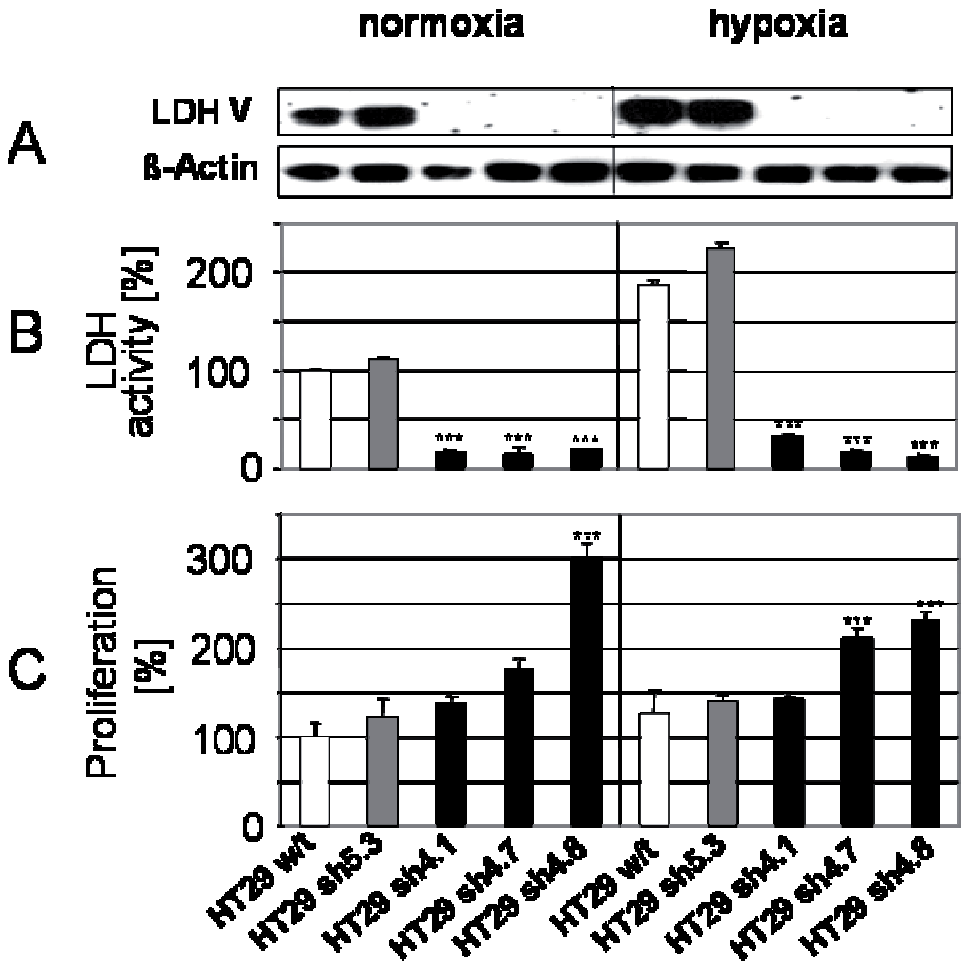

Figure 17. Effect of *LDH-A* knockdown on growth of tumor cells under normoxic and hypoxic conditions *in vitro*. (A) Western blot analysis was performed on whole cell lysates of parental HT29 (w/t), control (sh5.3) and *LDH-A*-deficient HT29 clones 4.1, 4.7 and 4.8 under normoxic or hypoxic conditions. Sheep polyclonal anti-*LDH-A* antibody and anti-ß-actin antibody as loading control were used on the same membrane. (B) *LDH-A* activity expressed as percentage of enzyme activity in parental HT29 cells of controls and *LDH-A*-deficient cells, grown under normoxic or hypoxic conditions. (C) Percentage of proliferation of selected clones stably expressing *LDH-A*-specific shRNAs relative to w/t cells. Mean values and standard deviations of four independent experiments are shown (***p<0.001 vs. parental cell line).

Protein expression of LDH-V shows a strong correlation with total LDH activity (Figure 17 A and B; Figure 18 A and B) in all tumor cells. The in vitro growth rate of HT29 did not correlate with the amount of LDH-V suppression in either normoxic or hypoxic conditions (Figure 7 C). None of the clones showed a reduced proliferation.

In comparison to the control clone sh5.3 and the parental cell line LDH-silenced HT29 clones grew similar or faster. *LDH-A* protein and activity were significantly reduced in all *LDH-A* shRNA-knockdown clones compared to controls.

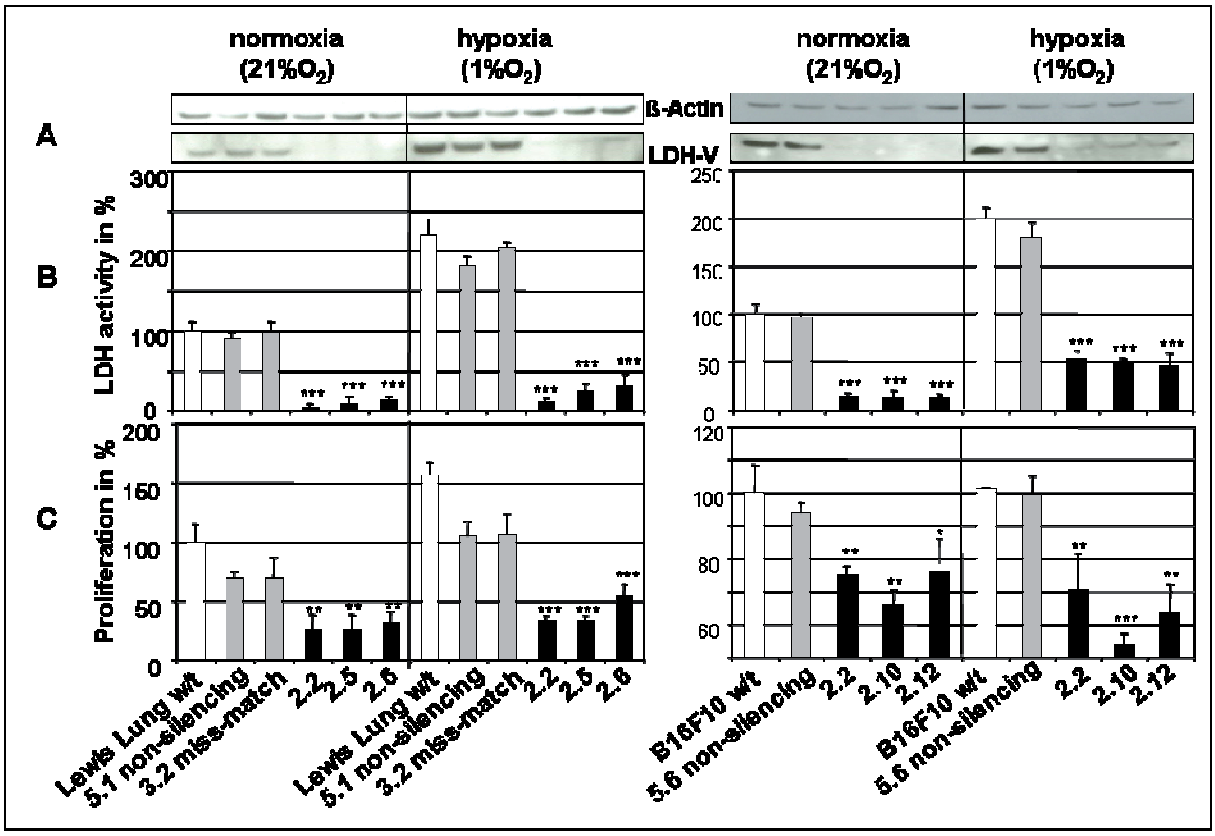

Figure 18. Effect of *LDH-A* knockdown on growth of tumor cells under normoxic and hypoxic conditions *in vitro*. Parental Lewis Lung cells (w/t), control cells and *LDH-A*-deficient Lewis Lung clones 2.2, 2.5 and 2.6 as well as parental B16F10 cells (w/t), non-silencing control cells and *LDH-A*-deficient B16F10 clones 2.2, 2.10, 2.12 were grown under normoxic or hypoxic culture conditions. (A) Western blot analysis was performed on whole cell lysates and LDH and ß-actin protein as loading control detected by sheep polyclonal anti-LDH-V antibody and anti-ß-actin antibody. (B) LDH-V activity expressed as percentage of enzyme activity in parental Lewis Lung and B16F10 (cells of controls and *LDH-A*-deficient cells, grown under normoxic and hypoxic conditions. (C) Percentage of proliferation of stably expressing *LDH-A*-specific shRNA clones relative to w/t cells and control cells. Mean values and standard deviations of four independent wells are shown (*p<0.05; **p<0.01; ***p<0.001 vs. parental cell line).

Comparable to the results obtained with LDH-silenced HT29 clones, Lewis Lung knockdown clones showed enhanced LDH-V protein expression under hypoxic versus normoxic conditions (Figure 17 A and Figure 18 A). In contrast, hypoxic culture conditions did not induce LDH expression in B16F10 control cells. However, LDH activity increased up to two-fold in all three cell lines under hypoxic conditions

(Figure 7 B and 8 B). The knockdown cells showed baseline LDH activity under normal conditions and also increased activity under hypoxic conditions. Unlike the human HT29 cells, downregulation of LDH-V activity interfered with proliferation of both B16F10 and Lewis Lung cells *in vitro*. Knockdown clones grew slower than control or parental cell lines. Contrary to *LDH-A* deficient Lewis Lung and HT29 cells, w/t cells grew faster under hypoxic conditions (Figure 7 C and 8 C). B16F10 cells did not show any differences in growth under hypoxic or normoxic condition (Figure 8 C).

3.5 LDH-V suppression affects cell cycle distribution

As *in vitro* proliferation was inhibited in *LDH-A* deficient B16F10 and Lewis Lung tumor cells the effect of *LDH-A* suppression on cell cycle distribution was examined. Cell cycle distribution of all cell lines was determined after 24-hour culture under normoxic or hypoxic conditions using the fluorescent dye propidium iodide and flow cytometry. Propidium iodide intercalates in DNA molecules and thereby allows the detection of DNA content and further the assessment of the cell cycle stage for single cells.

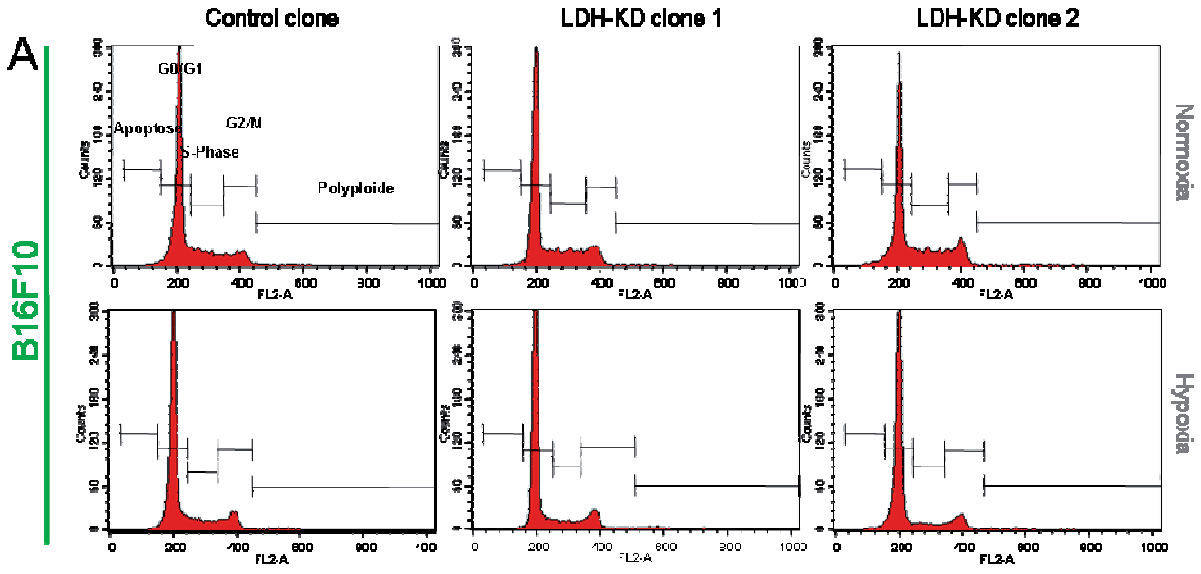

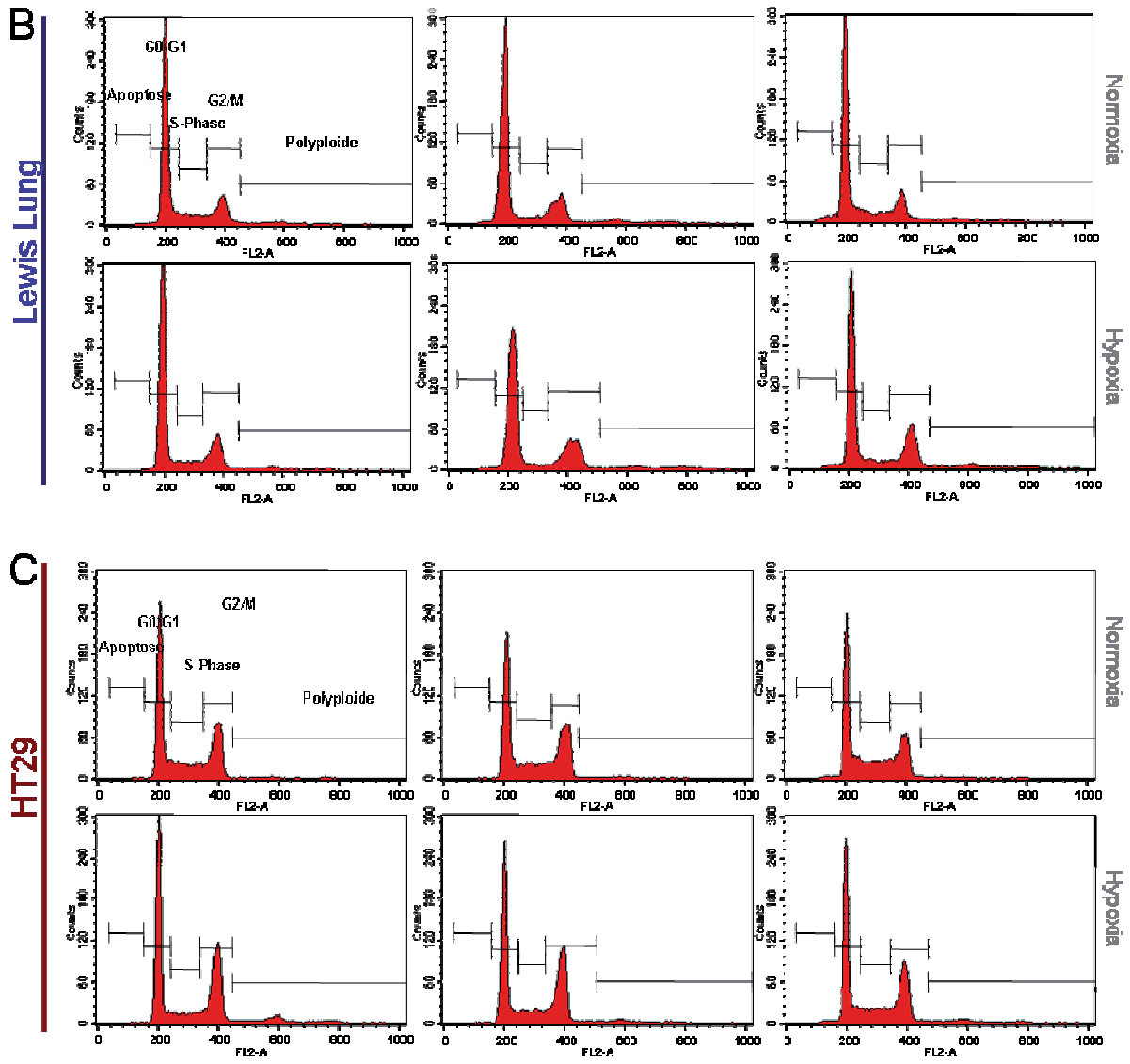

Figure 19. Cell cycle distribution after *LDH-A* knockdown. Cells were cultured for 24 hours under normoxic or hypoxic conditions. Cell cycle analysis of (A) B16F10, (B) Lewis Lung and (C) HT29 control (control clone) and *LDH-A* suppressed (LDH-KD clones) cells were performed using propidium iodide and flow cytometry as described.

Figure 9 shows representative graphs obtained from the cell cycle analysis of B16F10 (A), Lewis Lung (B) and HT29 (C) cells. For all cell lines the highest peak consists of cells with a relative DNA content of 2N (unreplicated complement of DNA), indicating that most of the cells are in G1 phase, i.e. early interphase after cell division. No major change in cell cycle distribution was observed after *LDH-A* suppression in any cell line. For more precise information, percentages of cell cycle distribution (G1, S and G2/M phase) were analyzed as ratio of percentage of total cells (Table 5).

Table 5. Cell cycle analysis of *LDH-A* knockdown cell lines under normoxic or hypoxic conditions.

		G1 Phase		S Phase		G2/M	
		Normoxia	*Hypoxia*	*Normoxia*	*Hypoxia*	*Normoxia*	*Hypoxia*
B16F10	control clone	70.51	76.43	16.58	11.09	11.22	10.86
	LDH-KD clone 1	68.08	80.31	20.05	7.59	10.66	10.79
	LDH-KD clone 2	61.4	80.23	21.3	7.21	14.32	9.49
Lewis Lung	control clone	65.95	64.46	11.47	9.1	18.02	21.21
	LDH-KD clone 1	67.42	59.97	7.54	5.22	17.93	27.17
	LDH-KD clone 2	65.79	56.62	11.2	8.16	16.25	25.96
HT29	control clone	48.66	47.3	19.97	10	29.73	34.93
	LDH-KD clone 1	43.59	44.99	20.98	13.15	33.1	37.72
	LDH-KD clone 2	46.52	45.3	23.33	17.77	27.51	31.31

increase	change	*decrease*
	10%	
	30%	
	50%	

Distribution of the cell cycle stage between the cell lines and the culturing conditions differed. Under normoxic conditions all LDH-V knockdown clones showed similar cell cycle distribution as the control clones and no major changes were observed. While most of the B16F10 and Lewis Lung cells were in G1 phase (60% - 70%), only ~ 45% of the human HT29 cells were in this cell cycle stage.

Hypoxic conditions affected the *LDH-A* deficient clones of B16F10 and Lewis Lung differently. While the amount of G1 cells in both B16F10 knockdown clones increased, the amount of Lewis Lung cells with *LDH-A* knockdown in G1 phase declined. Due to the fact that this effect occurs exclusively in LDH-knockdown clones, the amount of G1 cells might be LDH-related. In all cell lines and clones a varying intense remission of cells in S phase was detectable. Notable was the very strong drop-off (>50%) in both B16F10 LDH-V deficient clones. In all Lewis Lung (from 17.4% ± 1.0% to 24.8% ± 3.2%, mean ± SD), and HT29 (from 30.1% ± 2.8% to 34.7% ± 3.2%, mean ± SD) cell lines, the G2/M phase increased under hypoxia. Noticeable is the strong induction of G2/M cells in both Lewis Lung *LDH-A* knockdown clones. In contrast, G2/M status of B16F10 cells was not affected or was even reduced in one knockdown clone.

3.6 *In vivo* tumor growth reduction after LDH-V suppression

In several cancer histologies *LDH-A* overexpression is a negative prognostic marker (Koukourakis et al. 2006). My previous experiments demonstrated that downregulation of *LDH-A* activity interferes with proliferation of Lewis Lung and B16F10 cells i*n vitro*. In HT29 cells proliferation even increased after *LDH-A* suppression. Therefore, further experiments concentrated to find out whether LDH-V suppression affects tumor growth also *in vivo*.

HT29, Lewis Lung and B16F10 tumor cells and *LDH-A* knockdown clones derived from these cell lines were injected subcutaneously into the left side of mice (n = 8 mice/ cell line). For human HT29 cells, a xenotransplantation model in immunosuppressed nude mice was used and for murine Lewis Lung and B16F10 cells a syngenic model in C57BL/6 mice was used. The mean tumor area at the beginning of the experiments was around 20mm² and was measured at different time points of the experiment. Mice were scarified and tumor biopsies were isolated for further *ex vivo* analysis at a maximum mean tumor area of 140mm² for animal welfare reasons.

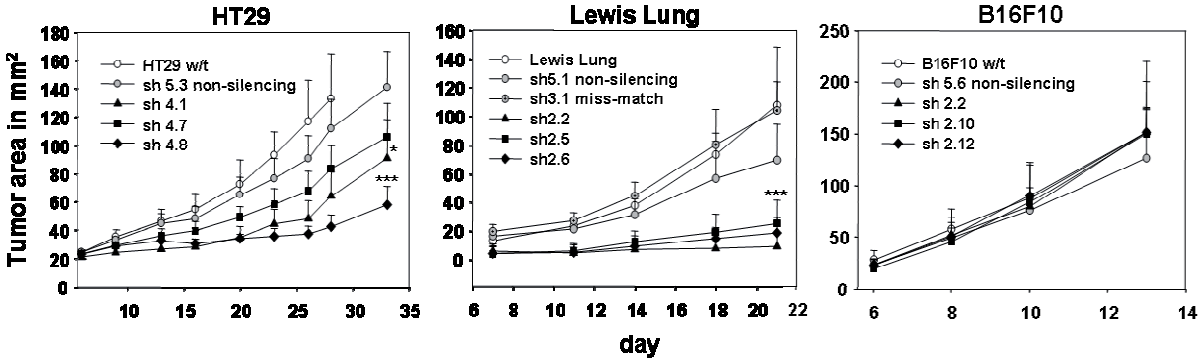

Figure 20. Growth characteristics of LDH-V suppressed tumors in HT29 xenografts, B16F10 and Lewis Lung syngenic models. Cells were implanted subcutaneously in nude mice or C57BL/6 mice as described in materials and methods. Tumor area was measured at different time points using a caliper. LHD-A suppressed HT29 and Lewis Lung cell lines showed a statistically significant slower growth behavior than the control cell lines. All B16F10 LDH knockdown and control tumors demonstrated very similar growth behavior. Error bars: n = 8, mean ±SEM, *p<0.05; ***p<0.001 vs. non-silencing control cell-line (sh5).

Growth rate of colon carcinoma, lung carcinoma and melanoma vary due to cell origin and mutation status. HT29, Lewis Lung and B16F10 tumors needed approximately 24, 21 and 11 days, respectively, to reach a tumor area of 100mm². In all cases, parental cell lines and control cells with the non-silencing plasmid (sh5) grew very similarly indicating that transfection and vector insertion did not change the growth behavior. In contrast to the *in vitro* experiments (Figure 17), *LDH-A* suppression interfered with HT29 tumor growth *in vivo*. As shown in Figure 20, tumor growth was significantly reduced in HT29 and Lewis Lung tumors derived from *LDH-A* silenced clones. No growth inhibition due to *LDH-A* suppression was observed in B16F10 tumors. Although the mean of B16F10 tumor growth among all the clones was very similar, the standard deviation within a group is very high (SD ± 50 mm²). Visual observation showed differences among the tumor specimens. The melanin producing B16F10 melanoma tumors were black, soft and bloody. HT29 and Lewis Lung tumors were white, round to oval and smooth shaped. Furthermore, the tumors were dense and solid and some of them were necrotic. However, within the tumor types no morphological differences between *LDH-A* knockdown and control tumors were visible (data not shown).

3.7 LDH-V suppression does not induce apoptosis

Tumor cells are protected against apoptosis through different possible mutations and mechanisms. Apoptosis induction is a common therapeutic effect of various clinical compounds. As previous experiments demonstrated LDH-V silencing leads to reduced proliferation. Thus, following experiments analyzed whether LDH-V silencing induces apoptosis in the tumor cells.

HT29, Lewis Lung and B16F10 tumor cells and *LDH-A* knockdown clones derived from these cell lines were cultured under normoxic or hypoxic conditions for 48 hours, lysed and supernatants were analyzed. Apoptotic markers such as ratio of p53/t53, Caspase 3 and 7 were measured and revealed that apoptosis of all three cell lines, control and LDH-V knockdown clones was not changed (data not shown). Thus, apoptosis may not be the reason for the reduced proliferation rate and tumor growth rate *in vitro* and tumor *in vivo*.

3.8 Increased VEGF expression was observed in B16F10 *LDH-A* knockdown clones

Vascular endothelial growth factor (VEGF) is an important signaling protein involved in both vasculogenesis and angiogenesis. VEGF has been implicated with poor prognosis in various cancers and is a successful therapeutic target. Inhibition of this growth factor leads to a reduced angiogenesis and results in tumor growth inhibition. Previous studies have demonstrated that especially B16F10 is highly sensitive to VEGF-receptor tyrosine kinase inhibition, which results in decreased angiogenesis. Thus, the effect of LDH-V suppression on VEGF expression was investigated *in vitro*.

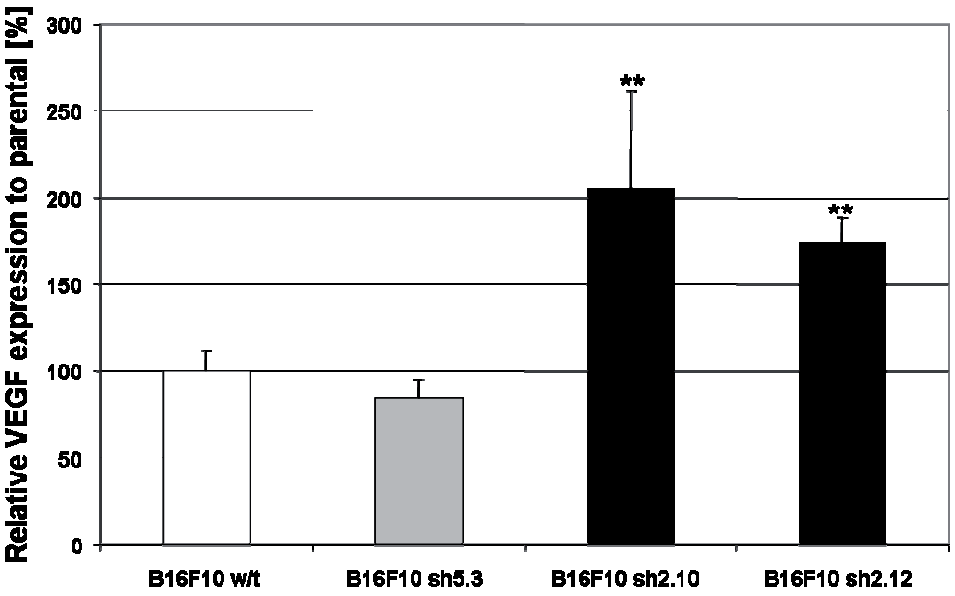

Figure 21. Increased VEGF expression in B16F10 LDH-V suppressed cones. Parental B16F10 (w/t), non-silencing control (sh5.3) cells and *LDH-A*-deficient B16F10 clones sh2.10 and sh2.12 were cultured under hypoxic conditions for 48 hours. VEGF in the supernatant was measured as indicated by ELISA. Results are given in percent VEGF expression relative to w/t cells. Mean values and standard deviations of three independent experiments are shown (**p<0.01; vs. parental cell-line).

Cells were cultured for 48 h under normoxic or hypoxic conditions, lysates were collected and VEGF concentrations were quantified by ELISA. In all cells the VEGF protein expression is increased by hypoxia (~50%). Only LDH-silenced clones of B16F10 expressed twofold more VEGF protein than compared parental and control cells under hypoxic conditions (Figure 21). VEGF expression of both HT29 and LL LDH-V silenced clones was equal to parental and control cells (data not shown).

3.9 Increased VEGF expression of LDH-silenced B16F10 tumors leads to high microvessel density

The *in vitro* findings might explain how B16F10 tumors overcome growth suppression by LDH-V knockdown. An increased vascularization of tumors by providing enough nutrition could compensate the lack of LDH-V. To further evaluate this hypothesis microvessel density was analyzed. Tumors of the growth experiment (Figure 20) were analyzed *ex vivo*. Microvessel density was measured by immunohistochemical staining with CD 31 monoclonal antibody as described in materials and methods.

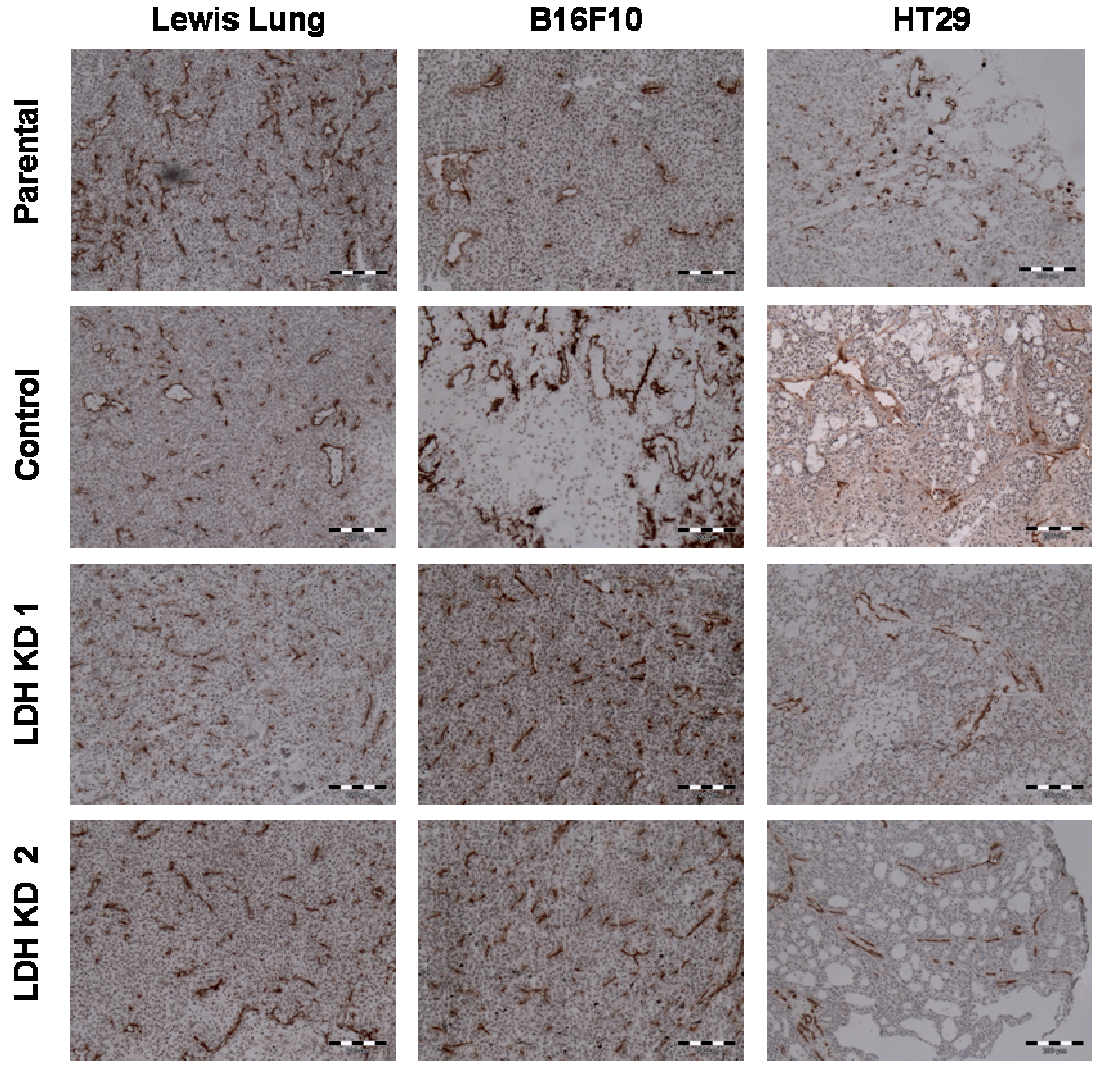

Figure 22. Strong vascularization of B16F10 LDH-V suppressed tumors. Lewis Lung, B16F10 and HT29 tumors derived from parental, control and LDH-knockdown cell transplants were removed, fixed, and subjected to CD31 staining and the number of the blood vessels were counted (n=3 sections). LDH-V suppression in Lewis Lung and HT29 cells did not affect microvessel density and formation. However, microvessel density in B16F10 was increased after downregulation of LDH-V. Scale bars, 200µm.

Like VEGF expression *in vitro*, microvessel density was also higher in all LDH-knockdown clones of B16F10 tumors (LDH KD 1 and LDH KD 2) (Figure 21). In contrast, HT29 and Lewis Lung and their respective clones showed no differences in VEGF production and microvessel density. Vascularization of HT29 tumors was even significantly lower than in Lewis Lung and B16F10 tumors.

3.10 Silencing of LDH-V interferes with glucose uptake in Lewis Lung cells

Tumors with higher glucose uptake are associated with lower survival rates and lower disease-free survival rates (Hanin et al. 2008). Glucose uptake correlates with tumor aggressiveness and metastasis. Subsequent experiments tested whether the lack of the glycolytic enzyme LDH-V might affect glucose uptake. Cells were cultured under normoxic or hypoxic conditions for 48 hours and he positron-emitting glucose analogue 18F-2-fluoro-2-deoxy-d-glucose (FDG) was used to identify glucose uptake *in vitro*. As mentioned earlier, hypoxia alters energy production by increasing glycolysis through the hypoxia-inducible factor 1 (HIF1). The low-efficiency cancer cells must take up quantitatively much more glucose than normal tissue. Under hypoxic conditions, glucose uptake of parental and control cell lines increased up to twofold compared to normoxic conditions. This effect is due to HIF1-dependent transactivating genes involved in extracellular glucose import (Denko 2008). However, LDH-V suppression interfered with the glucose uptake of LDH-V-suppressed Lewis Lung clones. Uptake was significantly decreased under both normoxic and hypoxic conditions (up to 70% and 90%, respectively). Unlike LDH-V-suppressed Lewis Lung clones none of the LDH-V suppressed HT29 or B16F10 clones showed a strong inhibition of glucose uptake. Thus, LDH-V-deficient HT29 B16F10 cells seem to have an ability to compensate the lack of LDH.

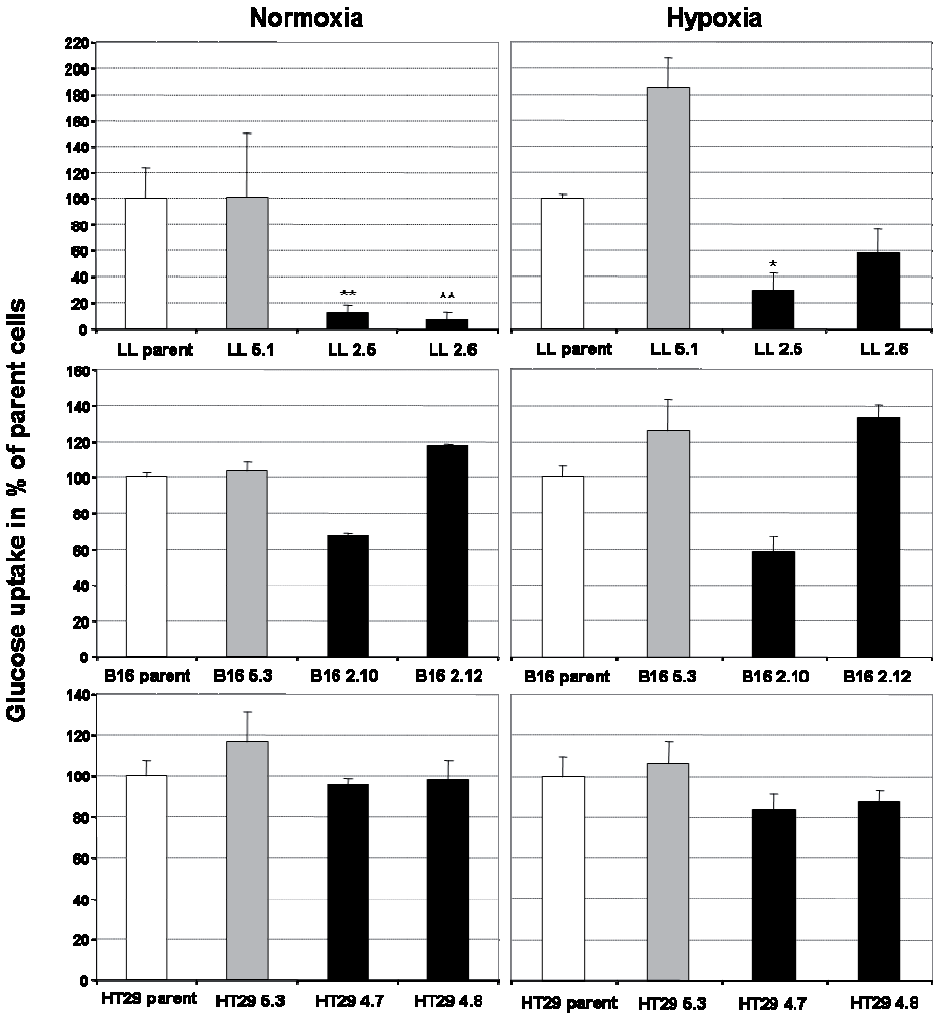

Figure 23. LDH-V suppression effects on glucose uptake in Lewis Lung cells. Parental cells, control cells and LDH-V deficient clones of Lewis Lung (LL), B16F10 and HT29 were cultured under normal oxygen pressure or hypoxic conditions for 48 hours. After washing with PBS, cells were incubated with ^{18}FDG for 10 min and, lysed with 1N NaOH. Radioactive supernatant was analyzed with a gamma counter. Results are shown as percent glucose uptake relative to parental cells. Glucose uptake of LDH-suppressed Lewis Lung clones 2.5 and 2.6 was significantly reduced under both conditions. B16F10 LDH-V knockdown clones 2.10 and HT29 clones 4.7 and 4.8 showed only a slightly reduced glucose uptake. Mean values and standard deviations of four independent experiments are shown (*p<0.05; **p<0.01; vs. parent cell line).

3.11 *LDH-A* knockdown influences expression of several genes in HT29 clones

As shown in chapter 3.6, LDH has an negative impact on tumor growth of LDH-V reduced HT29 derived tumors. To further investigate this phenomenon quantitative gene expression analysis of LDH-deficient HT29 cells was performed using the Illumina chip method as described in material and methods.

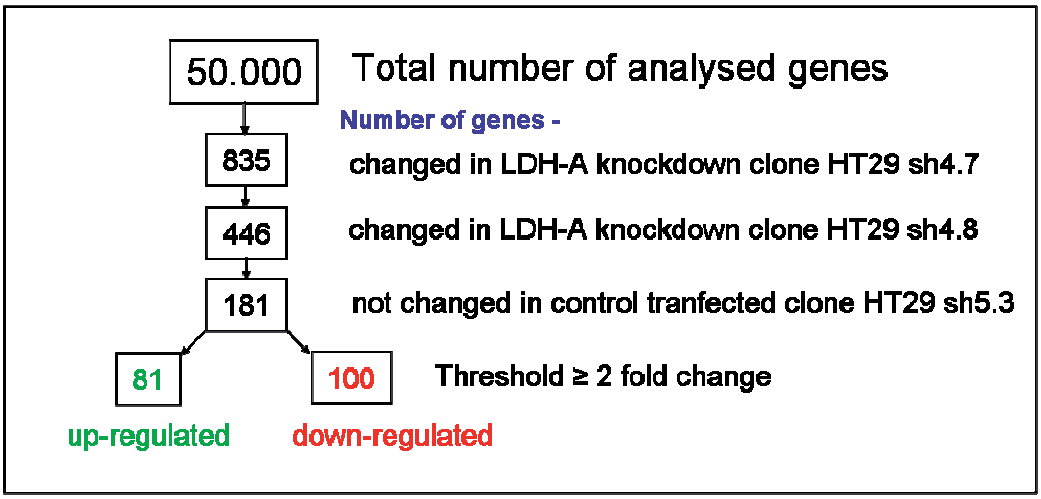

Figure 24. *LDH-A* knockdown influences expression of several genes. HT29 parental cells, control cells and *LDH-A* knockdown clones were cultured for 24 hours under normoxic and hypoxic conditions. Cells were processed and measured with the h-6 human Illumina chip. Figure shows the amount of genes up- and downregulated in both knockdown clones 4.7 and 4.8 compared to parental and 5.3 control cell line.

Figure 24 shows the amount of genes of LDH-V- suppressed cells whose expression differs from control cells. LDH depletion affects several genes. A great range of effected genes plays a role in tumor metabolism. Genes showing the most prominent changes in expression were analyzed in further experiments.

The microarray analysis showed among others increased PFKFB4 expression in LDH-reduced cells. PFKFB4 is involved in tumor metabolism and specially in the glycolysis pathway. Glycolysis is essential for tumor survival and spread. Most of these enzymes are induced by hypoxia through the activation of the HIF-1 complex, a transcriptional activator that controls the expression of most of hypoxia-regulated genes and therefore influence in HIF related gene expression (Denko 2008).

3.12 Lack of *LDH-A* has an effect on HIF1α expression and hypoxia regulated gene products *in vitro*

The influence of LDH-V deficiency on protein expression was further investigated by analyzing proteins related to cell metabolism, such as HIF1α and the HIF-related genes CAIX, PHD2, LDH-H and VEGFα in human HT29 cells (Figure 25). These genes play key roles in tumor survival. Supernantants of cell lysates were analyzed for protein expression after culturing the cells for three days under normoxic or hypoxic conditions. Part of the cultures were allowed to recover from hypoxia for an additional day under normoxia. HIF1α protein expression increased in all cells under hypoxic conditions and was most strongly increased in *LDH-A* deficient clones compared to the non-silencing clone sh5.3 and HT29 parental cell line insinuating an inverse relation of HIF1α and LDH-V protein content. After three days of incubation under hypoxia and one day recovery under normoxia no HIF1α protein was observed in the control cell lines, but was still detectable in two of three *LDH-A* deficient clones. HIF1α was only degraded. in clone sh4.1 having the highest residual LDH-V protein expression. The expression of the HIF degrading prolyl-hydroxylase PHD2 was induced under hypoxic conditions and remained present after recovery under normoxia. The CAIX protein expression was increased in all cells under hypoxia. As seen before, the expression level of CAIX was reduced in LDH-suppressed clones compared to control cells. Additionally, LDH-V suppression also affected the expression of LDH-H (*LDH-B* gene). Under hypoxic conditions LDH-H content was reduced in all cells and almost no LDH-H protein was observed disappeared for the silenced clones. This effect remained after recovery to normoxic conditions. The VEGF protein expression was increased by hypoxia (~50%) in all cells. Recovery for one day under normoxia resulted in the adjustment of cellular VEGF concentration to concentrations observed under normoxia (~20% above normoxic levels) (Figure 25).

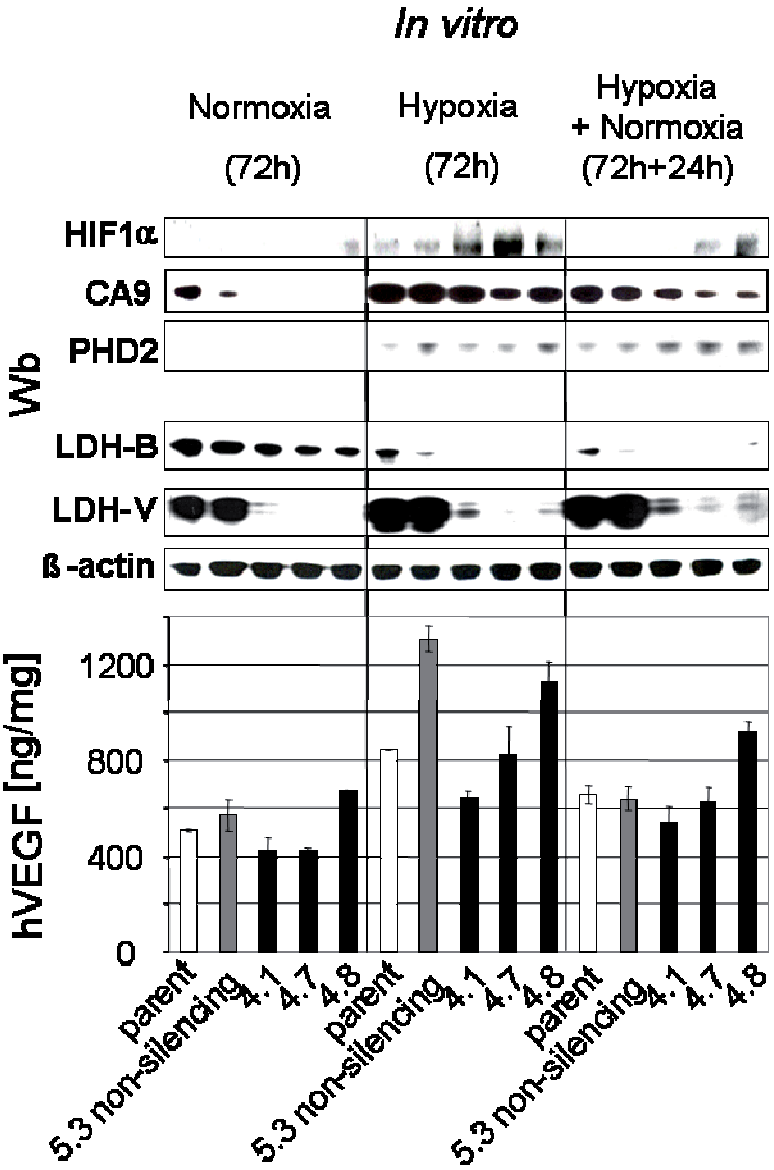

Figure 25. Expression of hypoxia related genes influenced by *LDH-A* silencing. HT29 cells were cultured for 72h under normoxic or hypoxic conditions. Part of the cultures were cultured another 24h under normoxic conditions. Cells were lysed and analyzed by immunoblotting with specific antibodies. A β-actin antibody was used as a loading control. hVEGF concentration was determined by ELISA. *LDH-A*-silenced cells showed increased amounts of HIF1α protein but lower amounts of CAIX, FIH and LDH-H. Hypoxia induced the expression of the proteins HIF1α, CAIX and PHD and VEGF. Error bars: n=3, mean ± SD

3.13 Reduced *LDH-A* expression interferes with AKT phosphorylation and GLUT-4 expression and localization

The AKT protein family, which members are also called protein kinases B (PKB) plays an important role in the cellular signaling of mammalian cells. It has an important functional role at, or in the vicinity of, GLUT4 (glucose transporter 4)

vesicles in the insulin-dependent translocation of those vesicles to the plasma membrane (Cong et al. 1997).

GLUT4 plays a pivotal role in insulin-induced glucose uptake to maintain normal blood glucose levels. Since we previously described an effect on glucose uptake in Lewis Lung cells and the mRNA analysis of HT29 cells indicated a LDH influence on tumor-metabolism and HIF1α related genes, we questioned whether the HIF related AKT pathway is affected in the absence of LDH-V activity.

3.13.1 Western blot analysis of HT29 clones and controls

In vitro cell lysates of HT29 cells with or without *LDH-A* silencing cultured under both normoxic and hypoxic conditions were generated and protein expression was analyzed using Western blot technology.

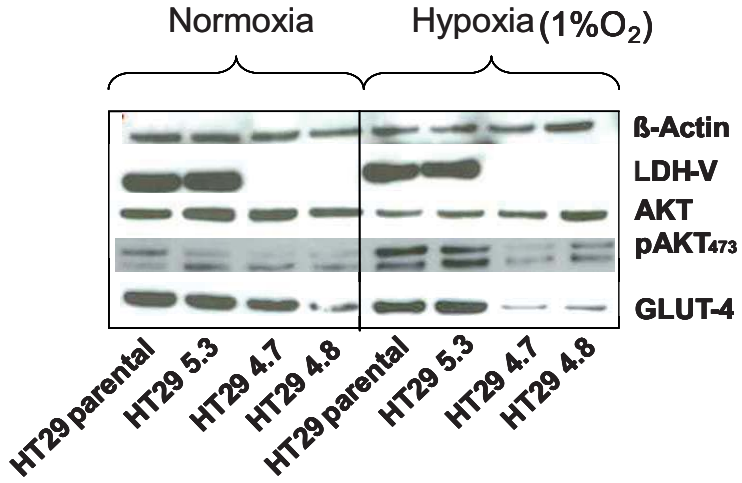

Figure 26. Decreased AKT_{473} phosphorylation and Glut-4 expression due to LDH-V suppression. Cells were cultured for 48 hours under normoxic and hypoxic conditions and subjected to protein extraction. For Western blot analysis, isolated protein was separated using SDS polyacrylamide gel electrophoresis, transferred to a PVDF membrane and incubated with anti-human LDH-V, AKT, $pAKT_{473}$ and GLUT-4 antibodies. ß-actin staining was used as loading control.

Figure 26 shows a hypoxia-related increase in phosphorylation of the serine-473 AKT site in HT29 parental cells and the control clone. This effect is disturbed in both LDH-V knockdown clones 4.7 and 4.8. The protein level of total AKT is in all clones comparable. GLUT-4 is strongly reduced in both LDH-V suppressed clones under hypoxic condition.

3.13.2 Fluorescence microscopy analysis of HT29 clones and controls

To analyse the functional meaning and to confirm the absence of GLUT-4, cells were first cultured under hypoxia and then stained with FITC-conjugated GLUT-4 antibody. An intact cytoskeleton was analyzed by staining with FITC-conjugated anti-α-tubulin. To validate the absence of LDH-V protein in the knockdown cells, all clones were marked with FITC-conjugated anti-LDH-V. All stainings were processed in combination with DAPI to highlight the nucleus. LDH-V reduction was confirmed in both knockdown clones which did not show a changed or deformed cytoskeleton (Figure 27 A). Additionally, the reduced GLUT-4 expression in both LDH-V deficient clones (Figure 26) was also verified via antibody staining (Figure 27 B). Furthermore, an internalization of remaining GLUT-4 was observed. Both the parental and control HT29 cell line showed a high amount of membrane-bound GLUT-4.

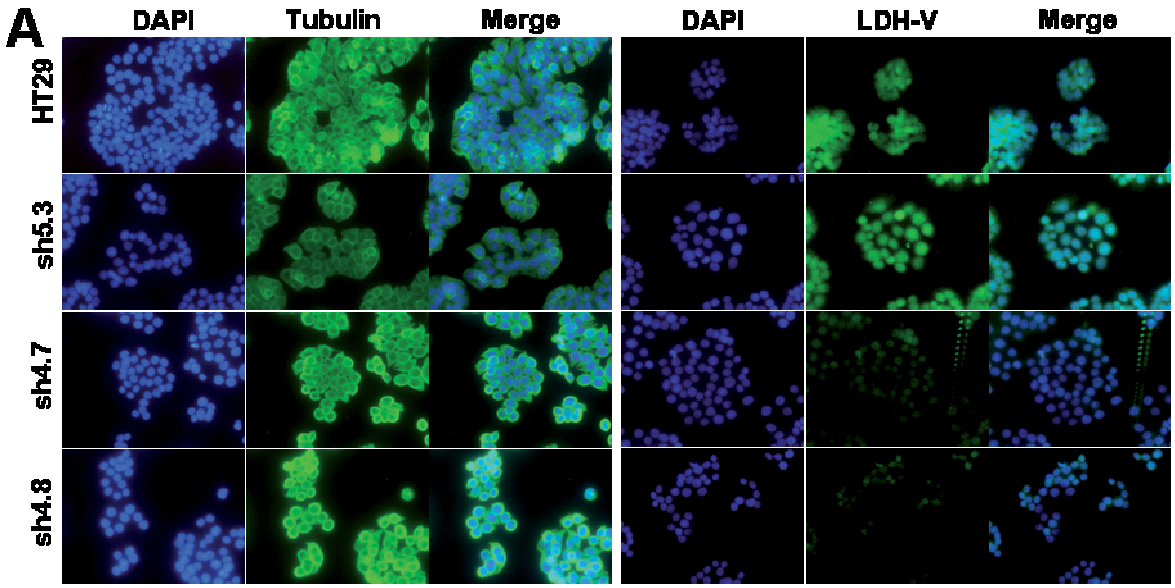

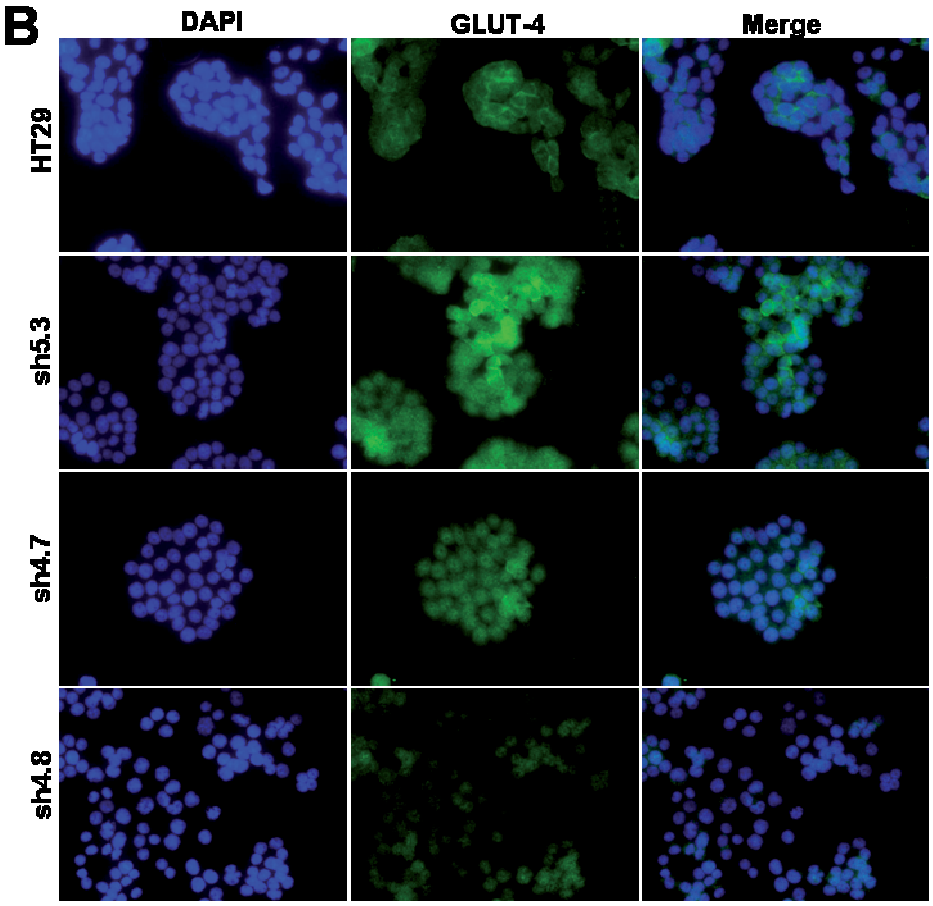

Figure 27. LDH-V knockdown of HT29 cells results in an internalization of GLUT4. HT29 parental, control (sh5.3) and LDH-knockdown clones (sh4.7 and sh4.8) were incubated with growth media for 48 hours under hypoxia, fixed with paraformaldehyde and stained for α-tubulin, LDH-V and GLUT-4. Fluorescence analysis was performed by confocal laser scanning microscopy. (A) The tubulin staining showed that HT29 cytoskeleton was not affected by LDH-V suppression. LDH-V expression was reduced in the LDH-knockdown clones sh4.7 and sh4.8. (B) GLUT-4 expression was reduced in both knockdown clones.

3.14 *LDH-A* suppression reduces migration and invasion of tumor cells

Crucial steps in the metastasis processes, including cell mobility and migration, tissue invasion and the ability to home to specific organs, are controlled by specific signaling pathways known to depend on HIF target genes.

As previously shown, LDH-V absence alters the expression of several HIF1α-related genes. Furthermore, significant changes in gene expression were observed for at least four genes that play a pivotal role in tumor metastasis and invasion (Table 6).

Table 6. *LDH-A* suppression induces changes in expression of several genes involved in metastasis

Symbol	Name	fold-change sh4.7 [log]	fold-change sh4.8 [log]	p-value
ATF3	activating transcription factor 3	-1.049	-1.145	7.00E-27
TIMP2	metallopeptidase inhibitor 2	1.385	1.72	1.03E-42
TGFBI	transforming growth factor, beta-induced	1.583	2.711	5.59E-75
TGFBR3	transforming growth factor, beta receptor III	1.069	2.762	2.49E-76

HT29 parental cells, control cells and *LDH-A* knockdown clones were cultured for 24 hours under normoxic and hypoxic conditions. Cells were processed and measured with the h-6 human Illumina chip. Table shows fold-change in relation to controls (log) and p-values of metastasis key genes. Red indicates down- and green upregulated genes.

Genes showing a different expression pattern in *LDH-A*-silenced HT29 cells as compared to control cells are listed in Table 6. ATF3, TIMP2, TGFBI and TGFBR3 are key genes known to affect metastasis and invasion of colorectal tumor cells (Ishiguro and Nagawa 2001; Guzinska-Ustymowicz and Kemona 2005; Mendes et al. 2007; Ma et al. 2008). While the expression of the metastasis supporter ATF3 was significantly downregulated, expression of the other indicated metastasis suppressor genes were upregulated (Table 6). Thus, LDH-V deficient cell appear to be affected in their metastatic potential. The influence of LDH-V on the metastatic and invasive potential of tumor cells was investigated in more detail by two different approaches .

3.14.1 2D scratch assay

The 2D migration assay is a well established and the most commonly used assay to study the migration potential of tumor cells. The assay has contributed to the fundamental understanding of cell migration processes.

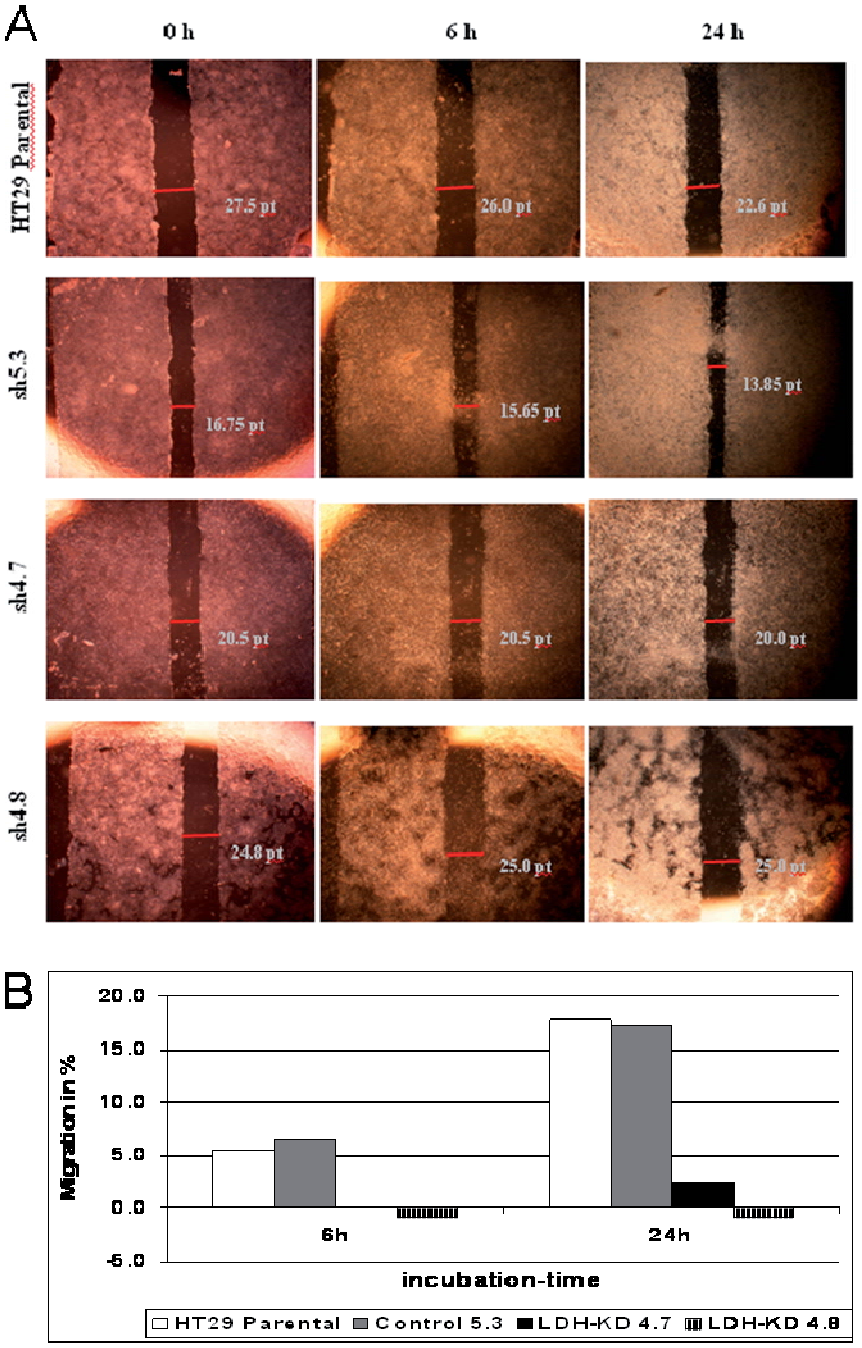

Figure 28. LDH-V suppression inhibits migration of HT29 cells. Parental cells, control cells and LDH-V knockdown clones of HT29 cells were cultured in 6 well plate until confluency. (A) Scratch assays were performed and representative photomicrographs taken at the indicated time points . To determine the relative closure of the gap, photomicrographs as shown in (A) were taken at different time points and measured. (B) The gap widths immediately after wounding were arbitrarily set as 0% migration. HT29 parental cells and control cells showed a time-dependent migration. Both LDH-V knockdown clones 4.7 and 4.8 showed strongly inhibited cell migration. Three experiments with comparable results were performed.

HT29 parental cells, control cells (sh5.3) and both LDH-V knockdown clones (4.7, 4.8) were analyzed for the ability to migrate into a denuded area using a 2D scratch assay a. A 0.5 - 1mm “scratch” was made in the cell-monolayer and the cells were

further cultured for 6 and 24 hours. At each time-point photomicrographs were taken and gap widths were measured in pixel points (Figure 28 A). The results of that experiment show a strongly reduced migration ability of both LDH-A reduced knockdown clones 4.7 and 4.8 (Figure 28 B). After 6 hours parental and control cell lines showed a migration rate of up to 7% after 6 hours and up to 18% after 24 hours of culture. In contrast, migration was strongly impaired in the knockdown clones.

3.14.2 Transendothelial migration assay

The initial arrest and attachment of tumor cells to vascular endothelium precedes their extravasation from the blood stream and is a crucial step in the tumor metastatic cascade of tumors. Since the migration was affected in the knockdown clones, we also expected a reduced invasion behavior of these cells.

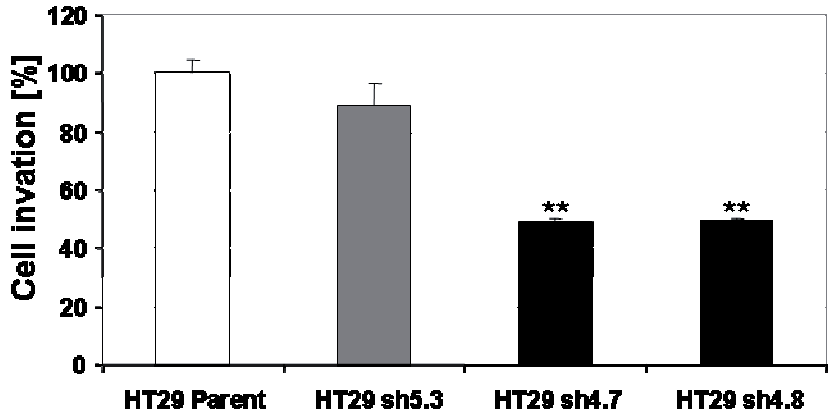

Figure 29. Reduced invasion rate of HT29 LDH-V knockdown clones. Tumor transendothelial migration assays were performed with all HT29 clones . Fluorescence was measured at 485nm/ 535nm. Results were shown as percentage of invasion relative to parental cells. HT29 w/t cells and control clone sh5.3 showed a high migration rate through the transendothelial well, whereas. migration of both knockdown clones was significantly reduced. Error bars: n = 3; mean ± SD, **p<0.01 vs. parental cell line.

CytoSelect™ Tumor Transendothelial Migration Assay from Cell Biolabs provides a robust system for the quantitative determination of tumor-endothelium interactions and transmigrations. The assay was performed with the HT29 clones as described using HUVEC cells (Human Umbilical Vein Endothelial Cells) as monolayer on the membrane (Figure 29).

Results of the migration assay confirmed the previously detected migration impairment of LDH knockdown clones. Migration rate of both LDH-V knockdown clones (sh4.7 and sh4.8) was reduced by up to 50% in comparison o both parental and control cells. Therefore, LDH-V seems to have a direct or indirect impact on tumor migration and invasion.

3.15 Summary of all LDH-V knockdown effects

Table 7. Summary of all *in vitro* and *in vivo* cell functions effected by LDH-V knockdown (+ effect, - no effect)

	B16F10	Lewis Lung	HT29
LDH activity	+	+	+
LDH-V protein	+	+	+
proliferation	+	+	-
tumor growth	-	+	+
VEGF expression	+	-	-
tumor vascularisation	+	-	-
cell cycle (hypoxia)	+ (G1)	+ (G2/M)	-
Apoptosis	-	-	-
Glucose uptake	-	+	-
migration/ invasion			+

4 Discussion

In various preclinical and clinical studies, a positive correlation between serum LDH and tumor mass (Dalley et al. 2001; Koukourakis et al. 2009), clinical staging of the tumor (Koukourakis et al. 2006; Suh and Ahn 2007; Naik et al. 2008) and malignancy (Rady et al. 1979; Lehtinen et al. 1988; Koukourakis et al. 2003; Walenta and Mueller-Klieser 2004) has been demonstrated. However it is not clear if LDH is a general prognostic marker for all tumor types, and if LDH could be a therapeutical target for the treatment of cancers. In this study, we were able to verify significant correlation between tumor weight and serum LDH levels in preclinical xenograft melanoma, colon carcinoma and lung carcinoma models. Using genetic knockdown of LDH expression in these three tumor models following with a series of molecular, celluar and pharmacological analysis, differential impacts of LDH-V ablation on the tumorigenicity *in vitro* and *in vivo* as well as the potential underlying mechanisms were elucidated.

4.1 Tumor type- and microenvironment-dependent impacts of LDH-V silencing on tumor cell proliferation and growth

Ablation of LDH-A in HT29 colon carcinoma cells had no effect on *in vitro* proliferation rate, while LDH-A-deficient B16F10 and Lewis Lung tumor cells demonstrated a strongly reduced proliferation rate *in vitro*. Such tumor type-dependent anti-proliferative effects are in lines with the previous publications. Fantin et al. observed reduced proliferation rates *in vitro* after *LDH-A* silencing in Neu4145 mammary gland tumor cells (Fantin et al. 2006). In contrast, *LDH-A* suppression had no effect on the proliferation rate of CHO cells (Kim and Lee 2007). These findings were corroborated by measurement of native human thyroid peroxidase (hTPO) levels in the cell cultures, which were not altered by *LDH-A* silencing. In accordance with our findings in HT29 cells increased proliferation rates after *LDH-A* silencing were also found by Jeong et al. (Jeong et al. 2006). We hypothesize that the effect of impaired LDH-V expression on proliferation *in vitro* might depend on if the tumor cells are addicted to LDH-V for metabolism, e.g. cells with constitutive glycolysis might be more sensitive to LDH-V knockdown even under normal culture conditions.

Interestingly, the consequence of LDH-V knockdown *in vivo* could be different from what observed in *vitro*. Thus, LDH-V deficiency could not lead to anti-proliferative effect in HT29 cells *in vitro*, while a significantly reduced tumor progression over time and reduced terminal tumor weight (data not shown) were clearly demonstrated *in vivo* in comparison to the controls. The grade of tumor growth retardation seems to correlate with the suppression of LDH-V protein levels in the various clones. This result suggested that tumor microenvironment plays an important role in LDH-V-regulated tumor metabolism. The fact that the pH of HT29 cells growing in vivo is considerably lower than that growing on culture dish as monolayer and buffered with neutral medium supports the above hypothesis. This observation is also consistent with findings of Fantin et al., who demonstrated a retarded growth of Neu4145 mammary gland tumor cells in mouse xenografts after silencing of *LDH-A* (Fantin et al. 2006).

Surprisingly, ablation of LDH-V in B16F10 melanoma tumors was incapable of suppressing tumor growth *in vivo,* though a dramatic decrease in proliferation demonstrated in *in vitro* studies and the strong correlation between tumor weight and serum LDH levels was observed in our study and described previously in patients with malignant melanomas (Rady et al. 1979; Shivers et al. 1998). One plausible explanation for the discrepancy between *in vitro* and *in vivo* could be that inhibition of LDH-V *in vivo* could activate a signalling pathway that supported tumor growth through tumor-microenvironment interaction and counteracted LDH-V-deficiency-mediated anti-tumor activities. We were then interested in identifying such molecules.

B16F10 tumors are strongly angiogenic, and thus commonly used as model to test angiogenesis inhibitors. Menon et al. demonstrated that inhibition of angiogenesis with theophylline, a methylxanthine drug used in therapy for respiratory diseases prevents neovascularization of B16F10 tumors (Menon et al. 2002) and thus prevents tumor growth. Furthermore, Chen et al. demonstrated in a B16F10 spontaneous metastasis model *in vivo* that ligustrazine, a constituent of an anti-angiogenic plant component, inhibited new vessel formation, decreased the expression of CD34 and VEGF in primary tumor tissue and reduced the number of metastasis nodi on the lung surface (Chen et al. 2009). As such we firstly attempted to compare the angiogenesis in B16F10 control and LDH-V-deficient tumors. We found that lack of LDH significantly increased the expression of VEGF and VEGF-dependent

angiogenesis in B16F10 but not in HT29 or Lewis Lung tumors. This result suggested that the increased VEGF expression after LDH-V suppression may stimulate the activation and growth of endothelial cells and provide an environment supporting the survival of LDH-V-deficient B16F10 melanoma. The mechanism, involved in this survival pathway, could be clarified by further investigations.

Cell cycle progression depends on the activation of cyclin-dependent kinases (CDK), which act consecutively in G1 to initiate S phase and in G2 to initiate mitosis (Loyer et al. 2005). In the experiments, we could demonstrate that impaired *in vitro* cell proliferation of B16F10 LDH-V knockdown cells, especially under hypoxic conditions is due to G1 arrest and in Lewis Lung cells an impaired proliferation occurs due to G2/M arrest. Consistent with the *in vitro* proliferation assay, knockdown of LDH-V in HT29 cells did not interfere the cell cycle. LDH levels have been shown being fluctuated during cell cycle progression and peaked at S-phase. Based on the previous publications, cells were arrested at G1/S upon the inhibition of LDH. Though at this stage, it is not understood why and how cell cycle was arrested at G2/M in Lewis Lung cells, it is certainly a considerable interest to further investigate the mechanism underlying this new finding.

Another important finding described in this study is the regulation of glucose uptake by LDH, which may directly contribute to the anti-tumor property observed in LDH-deficient Lewis Lung and B16F10 cells. LDH knockdown induced a strong decrease in glucose uptake in Lewis Lung and a slightly decrease in B16F10 tomor cells but not in HT29 cells. Since tumors, especially those with metabolic switch to glycolysis, requires more glucose, therefore changes in glucose uptake were generally found to correlate with tumor growth as determined by caliper measurements (Tian et al. 2004; Leyton et al. 2005). Clearly, the decreased glucose uptake could be one of the factor contribute to the growth inhibition of Lewis Lung and B16F10 after LDH suppression *in vitro*.

4.2 *LDH-A* dependent gene regulation

Another important aim of this work was encouraged by findings of Ronai (1993), who reported that LDH distributes to the nucleus and binds to DNA. Later LDH was demonstrated to be part of the transcription complex Oct-1 coactivater S (OCA-S). In this complex it participates in the regulation of histone 2B (H2B) transcription in a $NADH/NAD^+$ dependent way (Zheng et al. 2003). From our findings it appears to be likely, that other genes than H2B are also regulated by a complex of LDH with transcription factors.

4.2.1 Hypoxia related genes

The stabilization of the HIF1α subunit under low oxygen conditions and the subsequent formation of the HIF transcription factor complex binding to HRE´s of HIF1 regulated genes is well described (for review see (Wenger 2002). Indeed, we observed the induction of HIF1α and HIF-regulated proteins under hypoxic conditions. HIF1α as well as was CAIX, PHD2 and LDH-V were upregulated in HT29 cells. Most interestingly, the hypoxic induction of HIF1α was more prominent in cell lines with silenced *LDH-A*. One day recovery from hypoxia lead to complete degradation of HIF1α, whereas in two of three *LDH-A* silenced clones HIF1α was still present. The level of HIF1α protein inversely correlated with that of LDH-V protein under the investigated cell culture conditions. Thus, we anticipate that the expression of *LDH-A* in addition to hypoxia affects the HIF1α protein content. This regulation pathway of HIF-1α by LDH-V, which is reverse to the well described induction of LDH-V has not been reported so far.

Genes induced by HIF enable the switch from aerobic to hypoxic metabolism in tumor cells where glucose is converted to pyruvate and finally to lactic acid. This avoids degradation of potential building blocks, which are essential for cellular structures. The enzymatic activity of LDH isozyme 5 implies the generation of acid. To cope with this challenge CAIX is upregulated on the tumor cell surface. CO_2 decays from intracellular bicarbonate after uptake of a proton and permeates freely the cell membrane (Svastova et al. 2004). Extracellularly it is again hydrated by CAIX, liberating a proton. As net reaction this leads to a continuous titration of intracellular acid and to the acidification of the extracellular space. Thus CAIX contributes to the maintenance of a physiological pH within the tumor cell. In our

study we showed the induction of CAIX under hypoxic conditions as described previously (Wykoff et al. 2000), and a decrease of this enzyme in tumor cells with suppressed expression of LDH-V.

Under moderately hypoxic conditions, PHD2 the iso-enzyme reported to have the highest activity for HIF-1α hydroxylation (Huang et al. 2002), is inactive and therefore HIF1α protein levels are increased. This enables the transcription of genes highly sensitive for moderately reduced O_2 levels ("N-TAD genes"). Under these conditions FIH (Factor Inhibiting HIF) still hydroxylates a sequence with an asparagine residue at the C-terminus of HIF1α, which is responsible for the binding of the cofactor p300 to HIF1 in the transcription factor complex. If oxygen concentrations are further decreased, beyond the loss of activity of PHD2, FIH becomes inactivated and thus permits the transcription of an additional hypoxia regulated group of genes ("C-TAD genes"; Lando et al., 2002). We investigated the expression of HIF1 regulated genes. PHD2 was unchanged by *LDH-A* silencing. LDH-H is generally considered not to be regulated by low oxygen supply in cell culture (Ebert et al. 1996). Unexpectedly we observed a loss of LDH-H expression under hypoxic conditions. LDH-H protein expression was most strongly suppressed in *LDH-A* silenced clones. This observation may point to a secondary regulation of *LDH-B*, since HRE is not found in its promoter. In accordance with our results, a negative regulation of LDH-H in hypoxic tissues was reported in two *in vitro* studies previously (Buono and Lang 1999; Rossignol et al. 2003).

4.2.2 Genes involved in glycolysis

Elstrom and colleagues showed that activation of a single oncogene, namely Akt, is sufficient to stimulate aerobic glycolysis in tumors (Elstrom et al. 2004), while the same oncogene, Akt, activates HIF-1α (Mottet et al. 2003) which, in turn, up-regulates enzymes involved in anaerobic glycolysis and glucose absorption (Semenza et al. 1996b). We demonstrated a reduced phosphorylation of Akt in LDH-V deficient HT29 tumors. As the consequence, translocation of intracellular GLUT4 vesicles to the plasma membrane (Cong et al. 1997) was also found being inhibited. These results suggest a novel mechanism by which LDH-V activity regulates glucose transporter through phosphorylating and activating AKT.

Another key step in the control of the glycolytic rate is the conversion of fructose-6-P to fructose-1,6-P(2) by 6-phosphofructo-1-kinase (PFK-1). The activity of PFK-1 is allosterically controlled by fructose-2,6-P, the product of the enzymatic activity of a dual kinase/phosphatase family of enzymes (PFKFB1-4) that are increased in a significant number of tumor species (Yalcin et al. 2009). In turn, PFKFB1-4 enzymes are induced by hypoxia through the activation of the HIF-1 complex.. We observed a 3-fold increased PFKFB4 expression in LDH-V knockdown HT29 cells. Collectively, several HIF1α –target genes were found being upregulated upon the inhibition of LDH-V. It would be interesting to know which signal molecules involved in the feedback loop and how LDH-V deficient cells try to compensate the lack of LDH and increase the “survival” factor Hif1α.

4.3 Influence of LDH-V on Metastasis and Migration

Cancer metastasis comprises several steps. First, tumor cells are shed into the blood stream (intravasation), circulating in the blood, and finally transmigrating out of the vessels (extravasation) into a new location of the body (Fidler 1990). Recent studies discuss a possible molecular explanation for the clinical correlation between intratumoral hypoxia and tumor aggressiveness which is in particular characterized by tumor invasion and the ability to metastasize (Brahimi-Horn and Pouyssegur 2006). Since we observed a LDH-V dependent increase of HIF1α and some HIF1α regulated genes, we questioned whether HIF regulated metastasis- and migration-related genes are subsequently increased in these cells. Among others, four metastasis-related genes were regulated in HT29 *LDH-A* knockdown cells. ATF3, a 21-kDa leucine zipper containing a transcription factor belonging to the Jun/Fos family (Hsu et al. 1992) was downregulated in LDH-V deficient cells. ATF-3 is expressed at very low levels in normal, quiescent cells but can be rapidly and highly induced in different cell types by multiple extracellular signals (Wolfgang et al. 1997; Hai et al. 1999). Tatsuaki Ishiguro and Hirokazu Nagawa reported that the ATF3 gene regulates HT29 colon cell metastasis and migration through enhancing tumor cell adhesion and invasion. In these studies, TI-241 (mouse ATF3 homologue) was transfected into a low metastatic B16-BL6 cell line, which converted the parental cells to high-metastatic cells (Ishiguro and Nagawa 2001).

ATF-3 is a common target of transforming growth factor-1 (TGFB-1), a multipotent cytokine with a wide range of physiological and pathological effects (Piek et al. 1999; Massague and Wotton 2000). TGFB-1 is the most potent known growth inhibitor for epithelial cells (Piek and Roberts 2001). The role of TGFB and the TGFB receptor III (TGFBR3) in tumor progression is still not completely understood

Inhibition of ATF3 in LDH-V deficient HT29 cells has also impacts on the expression of ATF3-regulated gene TIMP2, a matrix metalloproteinase 2 (MMP2) inhibitor (Danilewicz et al. 2003), was found being upregulated . MMP2 belongs to a broad family of zinc-dependent proteases important in extracellular matrix degradation. It is involved in numerous pathogenic processes, including tumor invasion and metastasis (Leppa et al. 2004). Rigg and Lemoine demonstrated *in vitro* that TIMP-expressing pancreatic tumor cells are significantly less invasive than those cells transfected with a control vector. *In vivo*, adenoviral delivery of TIMP1 or TIMP2 to nude mice harboring intraperitoneal human pancreatic cancers resulted in prolonged survival compared with control mice if gene therapy was administered early (Rigg and Lemoine 2001).

The downregulation of ATF3 and the upregulation of TGFBI, TGFBR3 and TIMP2 in LDH-V deficient HT29 cells may have functional consequence of suppressing the metastasis and migration potential of tumor cells (Figure 30). Our *in vitro* experiments demonstrated a strongly reduced migration and invasion potential of all LDH-V deficient HT29 clones compared to the control cells. Based on the gene expression and in vitro cellular migration data, further investigation on the metastasis properties of LDH-V deficient tumor cells in vivo would be considerable interesting.

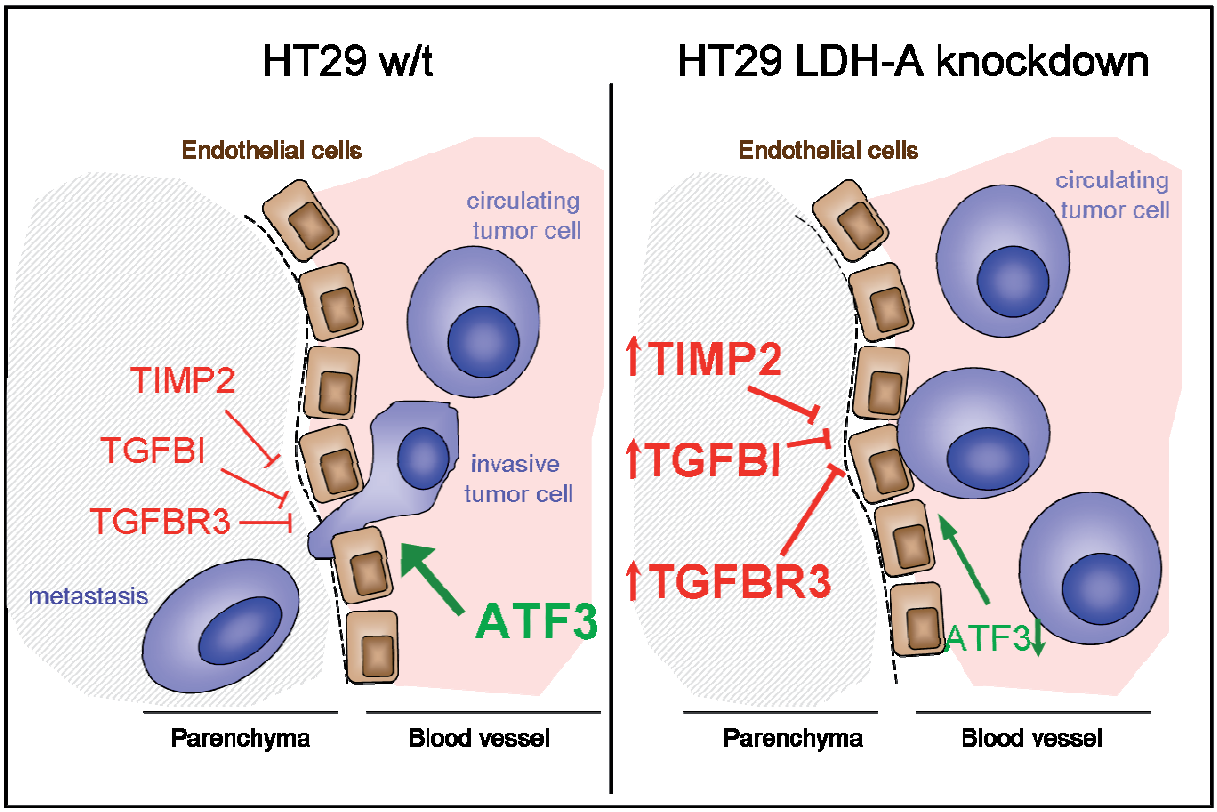

Figure 30. Comparison of genes involved in metastasis of HT29 after LDH-V suppression. Upregulation of TIMP2, TGFBI and TGFBR3 might inhibit invasion of circulating tumor cells through endothelial cells into tissue. LDH-V knockdown-dependent downregulation of ATF3 also correlated with reduced metastatic potential.

4.4 Conclusion and future studies

The results of this study primarily performed in human HT29 colon carcinoma, murine B16F10 melanoma and murine Lewis Lung carcinoma cells support previous experimental data and identify new findings. In summary, we demonstrate that in HT29 colon carcinoma the effect of *LDH-A* expression on tumor growth is not linked to cellular proliferation *in vitro*. Similar results were obtained for the B16F10 melanoma cells. However, both *in vitro* cell proliferation and *in vivo* tumor growth of Lewis Lung carcinoma are influenced by LDH-V knockdown. Lewis Lung and B16F10 differs in increased checkpoint stagnation of G1/M and G2 phase, respectively. Interestingly, glucose uptake of Lewis Lung cells is strongly LDH-V dependent. Clarification of that interesting and cell line specific mechanism might help to understand the correlation between LDH and glucose uptake. Furthermore, functional analysis of LDH-V silencing provided information about the direct link of LDH-V and migration/ invasion of HT29 cells. Further *in vivo* metastasis experiments will help to understand this effect. All together, the data underline a crucial role for LDH in tumor growth and metastasis. Most strikingly, we provide evidence that expression levels of HIF1α and some hypoxia regulated genes are influenced by the expression of *LDH-A* in HT29 cells. *LDH-A* seems to be capable of modulating tumor cells in a such way that tumors adapt their specific growth requirements under scarce conditions. HIF1α was strongly upregulated in *LDH-A* silenced cells, while the HIF1 regulated genes VEGF and CAIX showed no correlation with its altered expression levels.

With the obtained information about the role of LDH-V in cancer development, a big step in fundamental research was reached. The data obtained in this study may be suitable for therapeutic design in the future to reach a clinical approach. This study shows, that an impact on tumor metabolism might help preventing metastasis and decrease tumor malignancy. Additionally, the knowledge of LDH-dependency of different tumor types, that was gained in this study, might also help to narrow down the cancer types suitable for this type of therapy.

REFERENCES

Aird, W.C. (2007). Endothelium as a therapeutic target in sepsis. *Curr Drug Targets, 8*, 501-507.

Alberts, B. (2002). *Molecular Biology of the cell*.Garland Science.

Allen, J.W., Khetani, S.R., Johnson, R.S., Bhatia, S.N. (2006). In vitro liver tissue model established from transgenic mice: role of HIF-1alpha on hypoxic gene expression. *Tissue Eng, 12*, 3135-3147.

ASC (2009). Facts and Figures 2009. *American Cancer Society, Atlanta, 2009)*.

Blaese, R., Mullen, C., Ramsey, W. (1993). Strategies for gene therapy. *Pathol Biol., 41*, 672-676.

Brahimi-Horn, C., Pouyssegur, J. (2006). The role of the hypoxia-inducible factor in tumor metabolism growth and invasion. *Bull Cancer, 93*, E73-80.

Brahimi-Horn, M.C., Pouyssegur, J. (2009). HIF at a glance. *J Cell Sci, 122*, 1055-1057.

Brown, J.M., Giaccia, A.J. (1998). The unique physiology of solid tumors: opportunities (and problems) for cancer therapy. *Cancer Res, 58*, 1408-1416.

Buono, R.J., Lang, R.K. (1999). Hypoxic repression of lactate dehydrogenase-B in retina. *Exp Eye Res, 69*, 685-693.

Burke, R.E., Harris, S.C., McGuire, W.L. (1978). Lactate dehydrogenase in estrogen-responsive human breast cancer cells. *Cancer Res, 38*, 2773-2776.

Cairns, R.A., Kalliomaki, T., Hill, R.P. (2001). Acute (cyclic) hypoxia enhances spontaneous metastasis of KHT murine tumors. *Cancer Res, 61*, 8903-8908.

Carmeliet, P. (2003). Angiogenesis in health and disease. *Nat Med, 9*, 653-660.

Cattaneo, A., Biocca, S., Corvaja, N., Calissano, P. (1985). Nuclear localization of a lactic dehydrogenase with single-stranded DNA-binding properties. *Exp Cell Res, 161*, 130-140.

Chen, L., Lu, Y., Wu, J.M., Xu, B., Zhang, L.J., Gao, M., Zheng, S.Z., Wang, A.Y., Zhang, C.B., Zhang, W.W., Lei, N. (2009). Ligustrazine inhibits B16F10 melanoma metastasis and suppresses angiogenesis induced by Vascular Endothelial Growth Factor. *Biochem Biophys Res Commun, 386*, 374-379.

Chi, J.T., Wang, Z., Nuyten, D.S., Rodriguez, E.H., Schaner, M.E., Salim, A., Wang, Y., Kristensen, G.B., Helland, A., Borresen-Dale, A.L., Giaccia, A., Longaker, M.T., Hastie, T., Yang, G.P., van de Vijver, M.J., Brown, P.O. (2006). Gene expression programs in response to hypoxia: cell type specificity and prognostic significance in human cancers. *PLoS Med, 3*, e47.

Cong, L.N., Chen, H., Li, Y., Zhou, L., McGibbon, M.A., Taylor, S.I., Quon, M.J. (1997). Physiological role of Akt in insulin-stimulated translocation of GLUT4 in transfected rat adipose cells. *Mol Endocrinol, 11*, 1881-1890.

Culine, S. (2009). Prognostic factors in unknown primary cancer. *Semin Oncol, 36*, 60-64.

Dalley, C.D., Lister, T.A., Cavenagh, J.D., Rohatiner, A.Z. (2001). Serum LDH, a prognostic factor in elderly patients with acute myelogenous leukaemia. *Br J Cancer, 84*, 147.

Danilewicz, M., Sikorska, B., Wagrowska-Danilewicz, M. (2003). Prognostic significance of the immunoexpression of matrix metalloproteinase MMP2 and its inhibitor TIMP2 in laryngeal cancer. *Med Sci Monit, 9*, MT42-47.

Dasu, A., Toma-Dasu, I., Karlsson, M. (2003). Theoretical simulation of tumor oxygenation and results from acute and chronic hypoxia. *Phys Med Biol, 48*, 2829-2842.

Denko, N.C. (2008). Hypoxia, HIF1 and glucose metabolism in the solid tumor. *Nat Rev Cancer*.

Denko, N.C., Fontana, L.A., Hudson, K.M., Sutphin, P.D., Raychaudhuri, S., Altman, R., Giaccia, A.J. (2003). Investigating hypoxic tumor physiology through gene expression patterns. *Oncogene, 22*, 5907-5914.

Drevs, J., Hofmann, I., Hugenschmidt, H., Wittig, C., Madjar, H., Muller, M., Wood, J., Martiny-Baron, G., Unger, C., Marme, D. (2000). Effects of PTK787/ZK 222584, a specific inhibitor of vascular endothelial growth factor receptor tyrosine kinases, on primary tumor, metastasis, vessel density, and blood flow in a murine renal cell carcinoma model. *Cancer Res, 60*, 4819-4824.

Ebert, B.L., Gleadle, J.M., O'Rourke, J.F., Bartlett, S.M., Poulton, J., Ratcliffe, P.J. (1996). Isoenzyme-specific regulation of genes involved in energy metabolism by hypoxia: similarities with the regulation of erythropoietin. *Biochem J, 313 (Pt 3)*, 809-814.

Elstrom, R.L., Bauer, D.E., Buzzai, M., Karnauskas, R., Harris, M.H., Plas, D.R., Zhuang, H., Cinalli, R.M., Alavi, A., Rudin, C.M., Thompson, C.B. (2004). Akt stimulates aerobic glycolysis in cancer cells. *Cancer Res, 64*, 3892-3899.

Falkson, C.I., Falkson, H.C. (1998). Prognostic factors in metastatic malignant melanoma. An analysis of 236 patients treated on clinical research studies at the Department of Medical Oncology, University of Pretoria, South Africa from 1972-1992. *Oncology, 55*, 59-64.

Fantin, V.R., St-Pierre, J., Leder, P. (2006). Attenuation of LDH-A expression uncovers a link between glycolysis, mitochondrial physiology, and tumor maintenance. *Cancer Cell, 9*, 425-434.

Fidler, I.J. (1990). Critical factors in the biology of human cancer metastasis: twenty-eighth G.H.A. Clowes memorial award lecture. *Cancer Res, 50*, 6130-6138.

Fidler, I.J. (2002a). Critical determinants of metastasis. *Semin Cancer Biol, 12*, 89-96.

Fidler, I.J. (2002b). The organ microenvironment and cancer metastasis. *Differentiation, 70*, 498-505.

Firth, J.D., Ebert, B.L., Ratcliffe, P.J. (1995). Hypoxic regulation of lactate dehydrogenase A. Interaction between hypoxia-inducible factor 1 and cAMP response elements. *J Biol Chem, 270*, 21021-21027.

Gillies, R.J., Gatenby, R.A. (2007). Adaptive landscapes and emergent phenotypes: why do cancers have high glycolysis? *J Bioenerg Biomembr, 39*, 251-257.

Guenzburg, W., Salmons, B. (1997). Virus vector design in gene therapy. *Mol Med Today, 1*, 410-417.

Guzinska-Ustymowicz, K., Kemona, A. (2005). Transforming growth factor beta can be a parameter of aggressiveness of pT1 colorectal cancer. *World J Gastroenterol, 11*, 1193-1195.

Hai, T., Wolfgang, C.D., Marsee, D.K., Allen, A.E., Sivaprasad, U. (1999). ATF3 and stress responses. *Gene Expr, 7*, 321-335.

Han, S.Y., Gai, W., Yancovitz, M., Osman, I., Di Como, C.J., Polsky, D. (2008). Nucleofection is a highly effective gene transfer technique for human melanoma cell lines. *Exp Dermatol, 17*, 405-411.

Hanahan, D., Weinberg, R.A. (2000). The hallmarks of cancer. *Cell, 100*, 57-70.

Hanin, F.X., Lonneux, M., Cornet, J., Noirhomme, P., Coulon, C., Distexhe, J., Poncelet, A.J. (2008). Prognostic value of FDG uptake in early stage non-small cell lung cancer. *Eur J Cardiothorac Surg, 33*, 819-823.

Hockel, M., Vaupel, P. (2001). Tumor hypoxia: definitions and current clinical, biologic, and molecular aspects. *J Natl Cancer Inst, 93*, 266-276.

Holbrook, J.J., Gutfreund, H. (1973). Approaches to the study of enzyme mechanisms lactate dehydrogenase. *FEBS Lett, 31*, 157-169.

Hsu, J.C., Bravo, R., Taub, R. (1992). Interactions among LRF-1, JunB, c-Jun, and c-Fos define a regulatory program in the G1 phase of liver regeneration. *Mol Cell Biol, 12*, 4654-4665.

Huang, J., Zhao, Q., Mooney, S.M., Lee, F.S. (2002). Sequence determinants in hypoxia-inducible factor-1alpha for hydroxylation by the prolyl hydroxylases PHD1, PHD2, and PHD3. *J Biol Chem, 277*, 39792-39800.

Ishiguro, T., Nagawa, H. (2001). ATF3 gene regulates cell form and migration potential of HT29 colon cancer cells. *Oncol Res, 12*, 343-346.

Iversen, N., Birkenes, B., Torsdalen, K., Djurovic, S. (2005). Electroporation by nucleofector is the best nonviral transfection technique in human endothelial and smooth muscle cells. *Genet Vaccines Ther, 3*, 2.

Jensen, J.A., Hunt, T.K., Scheuenstuhl, H., Banda, M.J. (1986). Effect of lactate, pyruvate, and pH on secretion of angiogenesis and mitogenesis factors by macrophages. *Lab Invest, 54*, 574-578.

Jeong, D.W., Cho, I.T., Kim, T.S., Bae, G.W., Kim, I.H., Kim, I.Y. (2006). Effects of lactate dehydrogenase suppression and glycerol-3-phosphate dehydrogenase overexpression on cellular metabolism. *Mol Cell Biochem, 284*, 1-8.

Jiang, B.H., Zheng, J.Z., Leung, S.W., Roe, R., Semenza, G.L. (1997). Transactivation and inhibitory domains of hypoxia-inducible factor 1alpha. Modulation of transcriptional activity by oxygen tension. *J Biol Chem, 272*, 19253-19260.

Jovanovic, S., Jovanovic, A., Crawford, R.M. (2007). M-LDH serves as a regulatory subunit of the cytosolic substrate-channelling complex in vivo. *J Mol Biol, 371*, 349-361.

Kim, J.W., Gao, P., Dang, C.V. (2007). Effects of hypoxia on tumor metabolism. *Cancer Metastasis Rev, 26*, 291-298.

Kim, S.H., Lee, G.M. (2007). Down-regulation of lactate dehydrogenase-A by siRNAs for reduced lactic acid formation of Chinese hamster ovary cells producing thrombopoietin. *Appl Microbiol Biotechnol, 74*, 152-159.

Kolev, Y., Uetake, H., Takagi, Y., Sugihara, K. (2008). Lactate dehydrogenase-5 (LDH-5) expression in human gastric cancer: association with hypoxia-inducible

factor (HIF-1alpha) pathway, angiogenic factors production and poor prognosis. *Ann Surg Oncol, 15*, 2336-2344.

Koukourakis, M., Giatromanolaki, A., Sivridis, E. (2009). Colorectal Cancer: Lactate Dehydrogenase (LDH) Activity as a Prognostic Marker

In Netherlands, S. (Ed.) *Methods of Cancer Diagnosis, Therapy, and Prognosis* (pp. 241-253).

Koukourakis, M.I., Giatromanolaki, A., Sivridis, E., Bougioukas, G., Didilis, V., Gatter, K.C., Harris, A.L. (2003). Lactate dehydrogenase-5 (LDH-5) overexpression in non-small-cell lung cancer tissues is linked to tumor hypoxia, angiogenic factor production and poor prognosis. *Br J Cancer, 89*, 877-885.

Koukourakis, M.I., Giatromanolaki, A., Sivridis, E., Gatter, K.C., Harris, A.L. (2006). Lactate dehydrogenase 5 expression in operable colorectal cancer: strong association with survival and activated vascular endothelial growth factor pathway--a report of the Tumor Angiogenesis Research Group. *J Clin Oncol, 24*, 4301-4308.

Kroemer, G., Pouyssegur, J. (2008). Tumor cell metabolism: cancer's Achilles' heel. *Cancer Cell, 13*, 472-482.

Krogh, A. (1919). The number and distribution of capillaries in muscles with calculations of the oxygen pressure head necessary for supplying the tissue. *J Physiol, 52*, 409-415.

Kunisaki, C., Takahashi, M., Nagahori, Y., Fukushima, T., Makino, H., Takagawa, R., Kosaka, T., Ono, H.A., Akiyama, H., Moriwaki, Y., Nakano, A. (2009). Risk factors for lymph node metastasis in histologically poorly differentiated type early gastric cancer. *Endoscopy, 41*, 498-503.

Lehtinen, M., Wigren, T., Lehtinen, T., Kallioniemi, O.P., Aine, R., Aaran, R.K., Ojala, A. (1988). Correlation between serum tumor marker levels and tumor proliferation in small cell lung cancer. *Tumor Biol, 9*, 287-292.

Leppa, S., Saarto, T., Vehmanen, L., Blomqvist, C., Elomaa, I. (2004). A high serum matrix metalloproteinase-2 level is associated with an adverse prognosis in node-positive breast carcinoma. *Clin Cancer Res, 10*, 1057-1063.

Lewis, B.C., Prescott, J.E., Campbell, S.E., Shim, H., Orlowski, R.Z., Dang, C.V. (2000). Tumor induction by the c-Myc target genes rcl and lactate dehydrogenase A. *Cancer Res, 60*, 6178-6183.

Leyton, J., Latigo, J.R., Perumal, M., Dhaliwal, H., He, Q., Aboagye, E.O. (2005). Early detection of tumor response to chemotherapy by 3'-deoxy-3'-

[18F]fluorothymidine positron emission tomography: the effect of cisplatin on a fibrosarcoma tumor model in vivo. *Cancer Res, 65*, 4202-4210.

Li, S.S., Fitch, W.M., Pan, Y.C., Sharief, F.S. (1983). Evolutionary relationships of vertebrate lactate dehydrogenase isozymes A4 (muscle), B4 (heart), and C4 (testis). *J Biol Chem, 258*, 7029-7032.

Lopez-Rios, F., Sanchez-Arago, M., Garcia-Garcia, E., Ortega, A.D., Berrendero, J.R., Pozo-Rodriguez, F., Lopez-Encuentra, A., Ballestin, C., Cuezva, J.M. (2007). Loss of the mitochondrial bioenergetic capacity underlies the glucose avidity of carcinomas. *Cancer Res, 67*, 9013-9017.

Loyer, P., Trembley, J.H., Katona, R., Kidd, V.J., Lahti, J.M. (2005). Role of CDK/cyclin complexes in transcription and RNA splicing. *Cell Signal, 17*, 1033-1051.

Lum, J.J., Bui, T., Gruber, M., Gordan, J.D., DeBerardinis, R.J., Covello, K.L., Simon, M.C., Thompson, C.B. (2007). The transcription factor HIF-1alpha plays a critical role in the growth factor-dependent regulation of both aerobic and anaerobic glycolysis. *Genes Dev, 21*, 1037-1049.

Ma, C., Rong, Y., Radiloff, D.R., Datto, M.B., Centeno, B., Bao, S., Cheng, A.W., Lin, F., Jiang, S., Yeatman, T.J., Wang, X.F. (2008). Extracellular matrix protein betaig-h3/TGFBI promotes metastasis of colon cancer by enhancing cell extravasation. *Genes Dev, 22*, 308-321.

Martinez-Zaguilan, R., Seftor, E.A., Seftor, R.E., Chu, Y.W., Gillies, R.J., Hendrix, M.J. (1996). Acidic pH enhances the invasive behavior of human melanoma cells. *Clin Exp Metastasis, 14*, 176-186.

Massague, J., Wotton, D. (2000). Transcriptional control by the TGF-beta/Smad signaling system. *Embo J, 19*, 1745-1754.

Mendes, O., Kim, H.T., Lungu, G., Stoica, G. (2007). MMP2 role in breast cancer brain metastasis development and its regulation by TIMP2 and ERK1/2. *Clin Exp Metastasis, 24*, 341-351.

Menon, L.G., Ingle, A.D., Gude, R.P. (2002). Tumor regression of B16F10 melanoma in vivo by prevention of neovascularization: study on theophylline. *Cancer Biother Radiopharm, 17*, 213-217.

Miles, M.F., Hung, P., Jungmann, R.A. (1981). Cyclic AMP regulation of lactate dehydrogenase. Quantitation of lactate dehydrogenase M-subunit messenger RNA in isoproterenol-and N6,O2'-dibutyryl cyclic AMP-stimulated rat C6 glioma cells by hybridization analysis using a cloned cDNA probe. *J Biol Chem, 256*, 12545-12552.

Milosevic, M., Fyles, A., Hedley, D., Hill, R. (2004). The human tumor microenvironment: invasive (needle) measurement of oxygen and interstitial fluid pressure. *Semin Radiat Oncol, 14*, 249-258.

Morrish, F., Isern, N., Sadilek, M., Jeffrey, M., Hockenbery, D.M. (2009). c-Myc activates multiple metabolic networks to generate substrates for cell-cycle entry. *Oncogene, 28*, 2485-2491.

Mottet, D., Dumont, V., Deccache, Y., Demazy, C., Ninane, N., Raes, M., Michiels, C. (2003). Regulation of hypoxia-inducible factor-1alpha protein level during hypoxic conditions by the phosphatidylinositol 3-kinase/Akt/glycogen synthase kinase 3beta pathway in HepG2 cells. *J Biol Chem, 278*, 31277-31285.

Murray, B., Wilson, D.J. (2001). A study of metabolites as intermediate effectors in angiogenesis. *Angiogenesis, 4*, 71-77.

Naik, S., Rathnasabapathy, C., Chenthil, H., Sangal, A., Dumlao, T., Kodali, S., He, Z., Kalavar, M. (2008). LDH in solid tumors as a surrogate marker for tumor burden and response to treatment. *J Clin Oncology:26, Abstract, 22164*.

O'Hayre, M., Salanga, C.L., Handel, T.M., Allen, S.J. (2008). Chemokines and cancer: migration, intracellular signaling and intercellular communication in the microenvironment. *Biochem J, 409*, 635-649.

Pan, L.X., Xu, J.N., Isaacson, P.G. (1991). Cellular H- and M-type lactate dehydrogenase (LDH) isoenzymes and tumor diagnosis--an immunohistochemical assessment. *J Pathol, 163*, 53-60.

Piek, E., Moustakas, A., Kurisaki, A., Heldin, C.H., ten Dijke, P. (1999). TGF-(beta) type I receptor/ALK-5 and Smad proteins mediate epithelial to mesenchymal transdifferentiation in NMuMG breast epithelial cells. *J Cell Sci, 112 (Pt 24)*, 4557-4568.

Piek, E., Roberts, A.B. (2001). Suppressor and oncogenic roles of transforming growth factor-beta and its signaling pathways in tumorigenesis. *Adv Cancer Res, 83*, 1-54.

Postovit, L.M., Adams, M.A., Lash, G.E., Heaton, J.P., Graham, C.H. (2002). Oxygen-mediated regulation of tumor cell invasiveness. Involvement of a nitric oxide signaling pathway. *J Biol Chem, 277*, 35730-35737.

Pouyssegur, J., Dayan, F., Mazure, N.M. (2006). Hypoxia signaling in cancer and approaches to enforce tumor regression. *Nature, 441*, 437-443.

Pugh, C.W., O'Rourke, J.F., Nagao, M., Gleadle, J.M., Ratcliffe, P.J. (1997). Activation of hypoxia-inducible factor-1; definition of regulatory domains within the alpha subunit. *J Biol Chem, 272*, 11205-11214.

Rady, P., Arany, I., Bojan, F., Kertai, P. (1979). Activities of four glycolytic enzymes (HK, PFK, PK, and LDH) and isozymic pattern of LDH in mouse lung tumor induced by urethan. *J Cancer Res Clin Oncol, 95*, 287-289.

Ramont, L., Pasco, S., Hornebeck, W., Maquart, F.X., Monboisse, J.C. (2003). Transforming growth factor-beta1 inhibits tumor growth in a mouse melanoma model by down-regulating the plasminogen activation system. *Exp Cell Res, 291*, 1-10.

Rigg, A.S., Lemoine, N.R. (2001). Adenoviral delivery of TIMP1 or TIMP2 can modify the invasive behavior of pancreatic cancer and can have a significant antitumor effect in vivo. *Cancer Gene Ther, 8*, 869-878.

Rossignol, F., Solares, M., Balanza, E., Coudert, J., Clottes, E. (2003). Expression of lactate dehydrogenase A and B genes in different tissues of rats adapted to chronic hypobaric hypoxia. *J Cell Biochem, 89*, 67-79.

Rozhin, J., Sameni, M., Ziegler, G., Sloane, B.F. (1994). Pericellular pH affects distribution and secretion of cathepsin B in malignant cells. *Cancer Res, 54*, 6517-6525.

Schindl, M., Schoppmann, S.F., Samonigg, H., Hausmaninger, H., Kwasny, W., Gnant, M., Jakesz, R., Kubista, E., Birner, P., Oberhuber, G. (2002). Overexpression of hypoxia-inducible factor 1alpha is associated with an unfavorable prognosis in lymph node-positive breast cancer. *Clin Cancer Res, 8*, 1831-1837.

Semenza, G.L., Artemov, D., Bedi, A., Bhujwalla, Z., Chiles, K., Feldser, D., Laughner, E., Ravi, R., Simons, J., Taghavi, P., Zhong, H. (2001). 'The metabolism of tumors': 70 years later. *Novartis Found Symp, 240*, 251-260; discussion 260-254.

Semenza, G.L., Jiang, B.H., Leung, S.W., Passantino, R., Concordet, J.P., Maire, P., Giallongo, A. (1996a). Hypoxia response elements in the aldolase A, enolase 1, and lactate dehydrogenase A gene promoters contain essential binding sites for hypoxia-inducible factor 1. *J Biol Chem, 271*, 32529-32537.

Semenza, G.L., Rue, E.A., Iyer, N.V., Pang, M.G., Kearns, W.G. (1996b). Assignment of the hypoxia-inducible factor 1alpha gene to a region of conserved synteny on mouse chromosome 12 and human chromosome 14q. *Genomics, 34*, 437-439.

Shim, H., Dolde, C., Lewis, B.C., Wu, C.S., Dang, G., Jungmann, R.A., Dalla-Favera, R., Dang, C.V. (1997). c-Myc transactivation of LDH-A: implications for tumor metabolism and growth. *Proc Natl Acad Sci U S A, 94*, 6658-6663.

Shivers, S.C., Wang, X., Li, W., Joseph, E., Messina, J., Glass, L.F., DeConti, R., Cruse, C.W., Berman, C., Fenske, N.A., Lyman, G.H., Reintgen, D.S. (1998). Molecular staging of malignant melanoma: correlation with clinical outcome. *Jama, 280*, 1410-1415.

Sirott, M.N., Bajorin, D.F., Wong, G.Y., Tao, Y., Chapman, P.B., Templeton, M.A., Houghton, A.N. (1993). Prognostic factors in patients with metastatic malignant melanoma. A multivariate analysis. *Cancer, 72*, 3091-3098.

Stubbs, M., McSheehy, P.M., Griffiths, J.R., Bashford, C.L. (2000). Causes and consequences of tumor acidity and implications for treatment. *Mol Med Today, 6*, 15-19.

Suh, S.Y., Ahn, H.Y. (2007). Lactate dehydrogenase as a prognostic factor for survival time of terminally ill cancer patients: a preliminary study. *Eur J Cancer, 43*, 1051-1059.

Svastova, E., Hulikova, A., Rafajova, M., Zat'ovicova, M., Gibadulinova, A., Casini, A., Cecchi, A., Scozzafava, A., Supuran, C.T., Pastorek, J., Pastorekova, S. (2004). Hypoxia activates the capacity of tumor-associated carbonic anhydrase IX to acidify extracellular pH. *FEBS Lett, 577*, 439-445.

Thomlinson, R.H., Gray, L.H. (1955). The histological structure of some human lung cancers and the possible implications for radiotherapy. *Br J Cancer, 9*, 539-549.

Tian, M., Zhang, H., Higuchi, T., Oriuchi, N., Inoue, T., Endo, K. (2004). Effect of mitomycin C and vinblastine on FDG uptake of human nonsmall-cell lung cancer xenografts in nude mice. *Cancer Biother Radiopharm, 19*, 601-605.

Tyagi, P. (2005). Vatalanib (PTK787/ZK 222584) in combination with FOLFOX4 versus FOLFOX4 alone as first-line treatment for colorectal cancer: preliminary results from the CONFIRM-1 trial. *Clin Colorectal Cancer, 5*, 24-26.

Vaupel, P., Okunieff, P., Neuringer, L.J. (1989). Blood flow, tissue oxygenation, pH distribution, and energy metabolism of murine mammary adenocarcinomas during growth. *Adv Exp Med Biol, 248*, 835-845.

Vengellur, A., Woods, B.G., Ryan, H.E., Johnson, R.S., LaPres, J.J. (2003). Gene expression profiling of the hypoxia signaling pathway in hypoxia-inducible factor 1alpha null mouse embryonic fibroblasts. *Gene Expr, 11*, 181-197.

von Eyben, F.E. (2001). A systematic review of lactate dehydrogenase isoenzyme 1 and germ cell tumors. *Clin Biochem, 34*, 441-454.

Walenta, S., Mueller-Klieser, W.F. (2004). Lactate: mirror and motor of tumor malignancy. *Semin Radiat Oncol, 14*, 267-274.

Walenta, S., Schroeder, T., Mueller-Klieser, W. (2004). Lactate in solid malignant tumors: potential basis of a metabolic classification in clinical oncology. *Curr Med Chem, 11*, 2195-2204.

Warburg, O. (1930). The Metabolism of Tumors (London: Arnold Constable).

Wenger, R.H. (2002). Cellular adaptation to hypoxia: O2-sensing protein hydroxylases, hypoxia-inducible transcription factors, and O2-regulated gene expression. *Faseb J, 16*, 1151-1162.

Wolfgang, C.D., Chen, B.P., Martindale, J.L., Holbrook, N.J., Hai, T. (1997). gadd153/Chop10, a potential target gene of the transcriptional repressor ATF3. *Mol Cell Biol, 17*, 6700-6707.

Wu, P.K., Chen, W.M., Chen, C.F., Lee, O.K., Haung, C.K., Chen, T.H. (2009). Primary Osteogenic Sarcoma with Pulmonary Metastasis: Clinical Results and Prognostic Factors in 91 Patients. *Jpn J Clin Oncol*.

Wykoff, C.C., Beasley, N.J., Watson, P.H., Turner, K.J., Pastorek, J., Sibtain, A., Wilson, G.D., Turley, H., Talks, K.L., Maxwell, P.H., Pugh, C.W., Ratcliffe, P.J., Harris, A.L. (2000). Hypoxia-inducible expression of tumor-associated carbonic anhydrases. *Cancer Res, 60*, 7075-7083.

Yalcin, A., Telang, S., Clem, B., Chesney, J. (2009). Regulation of glucose metabolism by 6-phosphofructo-2-kinase/fructose-2,6-bisphosphatases in cancer. *Exp Mol Pathol, 86*, 174-179.

Young, S.D., Marshall, R.S., Hill, R.P. (1988). Hypoxia induces DNA overreplication and enhances metastatic potential of murine tumor cells. *Proc Natl Acad Sci U S A, 85*, 9533-9537.

Zabel, D.D., Feng, J.J., Scheuenstuhl, H., Hunt, T.K., Hussain, M.Z. (1996). Lactate stimulation of macrophage-derived angiogenic activity is associated with inhibition of Poly(ADP-ribose) synthesis. *Lab Invest, 74*, 644-649.

Zhong, H., De Marzo, A.M., Laughner, E., Lim, M., Hilton, D.A., Zagzag, D., Buechler, P., Isaacs, W.B., Semenza, G.L., Simons, J.W. (1999). Overexpression of hypoxia-inducible factor 1alpha in common human cancers and their metastases. *Cancer Res, 59*, 5830-5835.

LIST OF ORIGINAL PUBLICATIONS

Papers

I Najjar*, M., Langhammer*, S., , Hess-Stumpp, H., Kaekoenen, S.-M., Liu, N. and Thierauch, K.-H. (2009). LDH-A influences expression of the hypoxia-inducible factor 1α (HIF1α) and is critical for growth of experimental human colon carcinoma tumors in vivo. CANCER CELL, in preparation.

II Najjar, M., Langhammer, S., Thierauch, KH., Kaekoenen, SM. and Liu, N. (2009). An Old Story with New Twists: Lactate Dehydrogenase 5 (LDH-V) in Tumor Development. MOLECULAR CANCER THERAPY, in preparation.

Posters

Langhammer*, S., Najjar*, M., Berhörster, K., Hess-Stumpp, H., and Thierauch, K.-H. (2008). LDH-A is critical for tumor growth of colon carcinoma cells *in vivo*. Poster number 255, Page 160 (abstract book)

Poster presented at the KEYSTONE SYMPOSIA: Molecular Mechanisms of Angiogenesis an Development and Disease, January 15-20, Vancouver, BC.

Najjar*, M., Langhammer*, S., Berhörster, K., Hess-Stumpp, H., and Thierauch, K.-H. (2008). LDH-A is critical for tumor growth of colon carcinoma cells *in vivo*. EACR Member 11813

Poster presented at the 20th European Association of Cancer Research (EACR-20) SYMPOSIA, July 5-8, 2008, Lyon, France.

LIST OF TABLES

LIST OF FIGURES

Ehrenwörtliche Erklärung

Hiermit versichere ich, Maher Najjar, dass ich die vorliegende Arbeit selbstständig durchgeführt und verfasst habe. Dabei wurde keine anderen als die angegebenen Quellen und Hilfsmittel verwendet.

Berlin, 03.09.2009

Maher Najjar